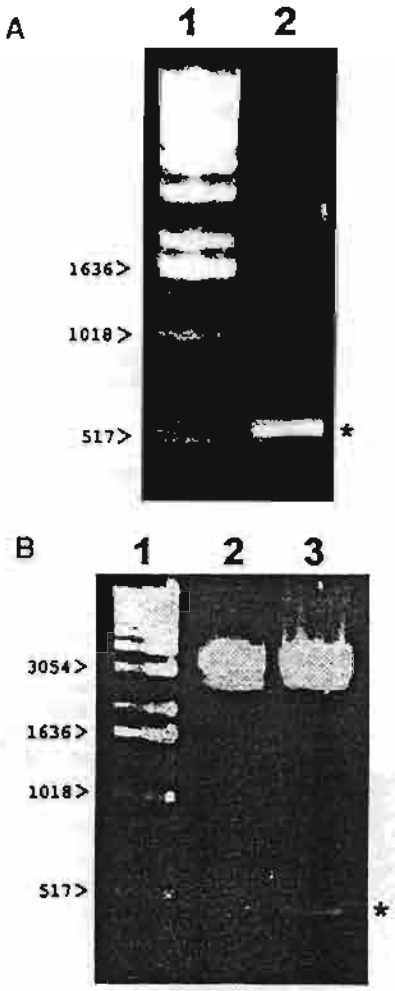

Fig. 1 a CD99 gene PCR amplification product from the pCDM 8-CD99 vector using primers CD99MatF and CD99MatR. Lanes: *1* DNA molecular weight marker (Roche), *2* 1 µl amplified product. A single band at 537 bp is depicted (*). b Restriction fragment analysis of pComb3-CD99. The constructed pComb3-CD99 was digested with *Sfi*I and electrophoresis was performed on a 1% agarose gel. Lanes: *1* DNA molecular weight marker, *2* uncut pComb3H-CD99, *3* *Sfi*I-digested pComb3H-CD99; inserted CD99 gene at 489 bp (*)

Validation of bioactive domain on CD99-ϕ by aggregation inhibition assay

The Jurkat human T-cell line was used as a target for homotypic cell aggregation. After washing three times, 75 µl Jurkat cells (2.5×10^5 cells/ml) were transferred to a 96-well flat-bottomed tissue culture plate (Costar, Cambridge, Mass.). The aggregation base line was obtained by adding 50 µl of 0.15 µg/ml MT99/1 to the well. For the aggregation inhibition assay, 50 µl of 10^{12} pfu/ml CD99-ϕ were preincubated with 50 µl of 0.15 µg/ml MT99/1 for 1 h at 37°C before adding to the Jurkat cells. VCSM13 was used in place of CD99-ϕ as a negative inhibition control system. The final volume of each well was adjusted to 175 µl with culture medium. The culture was then maintained at 37°C in a humidified atmosphere with 5% CO_2 in RPMI-1640 supplemented with 10% fetal bovine serum and antibiotics. Cell aggregation was monitored every hour for 4 h under an inverted microscope (Olympus, Tokyo, Japan).

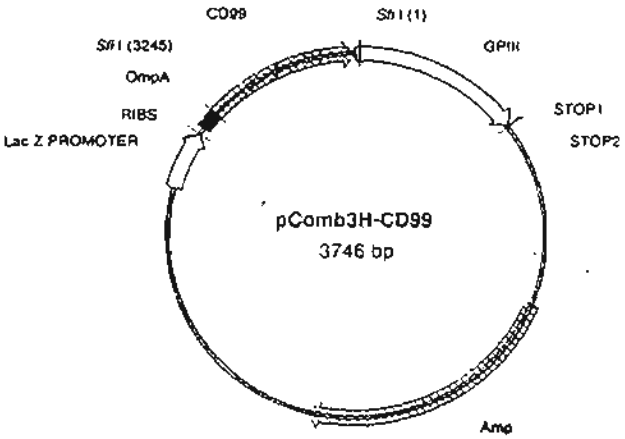

Fig. 2 Map of pComb3H-CD99. The two *Sfi*I cloning sites into which the CD99 gene was inserted are indicated. Signal sequence (*OmpA*), ribosome binding site (*RIBS*), *lac* promoter, and *gpIII* gene are also depicted

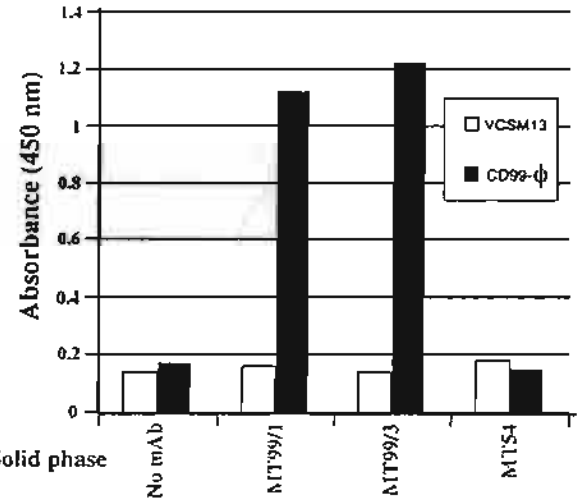

Fig. 3 Sandwich ELISA for the detection of phage bearing CD99. Solid phase was coated with either MT99/1, MT99/3, MT54 or no monoclonal antibody (mAb). VCSM13 was used as a negative control. The bound phage was traced with horseradish peroxidase (HRP)-conjugated sheep anti-M13

Results

Construction of a phagemid expressing CD99

In order to generate phage expressing CD99 molecules, a cDNA encoding CD99 protein cloned in the eukaryotic expression vector pCDM 8 (pCDM 8-CD99) (Kasinrerk et al. 2000) was used. From pCDM 8-CD99, we amplified the mature CD99 gene using primers CD99MatF and

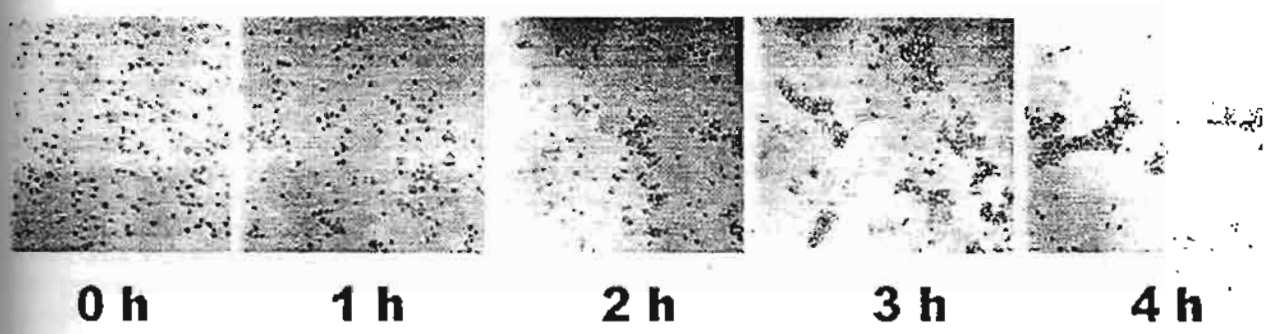

Fig. 4 Induction of Jurkat cell aggregation by MT99/1. Jurkat cells were incubated with MT99/1. Homotypic cell aggregation was monitored under an inverted microscope for 4 h

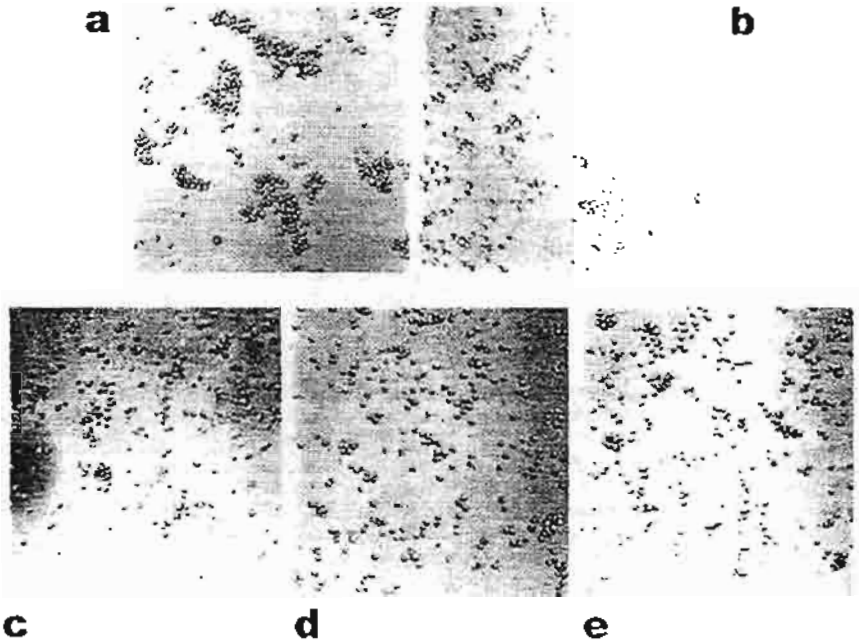

Fig. 5a–e Inhibition of MT99/1-induced Jurkat cell aggregation by CD99-ϕ. Jurkat cells were incubated with MT99/1 preincubated with VCSM13 (a) or CD99-ϕ (b). As controls, Jurkat cells were cultured with VCSM13 (c) or CD99-ϕ (d) alone. Non-induced Jurkat cells were referred as auto-aggregation base-line control (e). The degree of aggregation was observed after 4 h of cultivation

CD99MatR. The amplified product of 537 bp obtained (Fig. 1A) was then inserted into pComb3HSS phagemid in the correct reading frame by means of the *SfiI* cleavage sites on both the 5' and 3' ends. Thus, a new vector, pComb3H-CD99, harboring the CD99 gene was generated. In this vector, CD99-DNA is flanked upstream by the OmpA signal sequence and downstream by gpIII. The correct insertion of CD99 was verified by restriction analysis with *SfiI* (Fig. 1B). PCR-analysis using primers CD99MatF and CD99MatR produced a single band of 537 bp. A map of pComb3H-CD99 is shown in Fig. 2.

Generation of phage displaying the CD99 molecule

To produce phage displaying CD99 (CD99-ϕ), VCSM13 filamentous phage was used to infect pComb3H-CD99-transformed *E. coli* XL-1 Blue. Propagation of VCSM13 results in incorporation of the CD99-gpIII fusion protein during the viral packaging process. The recombinant phage particles thus produced were screened for the expression of recombinant CD99 by sandwich ELISA. As shown in Fig. 3, the generated CD99-ϕ specifically bound to both CD99 mAbs (MT99/1 and MT99/3). In contrast, VCSM13 prepared from non-transformed XL-1 Blue was not captured by either CD99 mAb. A negative result was also obtained in wells coated with CD54 mAb MT54, irrespective of the phage type added (Fig. 3). These results suggested that CD99-expressing phage particles had been successfully produced.

CD99-expressing phages carry a bioactive domain

It has been demonstrated that CD99 mAbs induce homotypic Jurkat cell aggregation (Kasinrerk et. al.

2000). In the presence of MT99/1, Jurkat cells started to show homotypic cell aggregation after 1 h incubation and reached maximum aggregation at 4 h incubation (Fig. 4). The induction of cell aggregation by MT99/1 was then used to evaluate the CD99 bioactive domain on CD99-ϕ. As shown in Fig. 5, preincubation of MT99/1 with CD99-ϕ inhibited Jurkat aggregation. In contrast, induction of cell aggregation was not altered after preincubation of MT99/1 with VCSM13. When Jurkat cells were cultured in the presence of VCSM13 or CD99-ϕ alone, very few auto-aggregation foci resulted after 4 h incubation (Fig. 5). The same degree of auto-aggregation degree also appeared in the non-induction Jurkat culture control (Fig. 5). These results indicated that the generated CD99-ϕ carry a properly folded bioactive epitope, which was recognized by MT99/1.

Discussion

The phage display technique has been described for the production of recombinant molecules such as antibodies (Hoogenboom and Chames 2000), tissue plasminogen activator (Manosroi et al. 2001), or collagen-binding protein from *Necator americanus* (Viaene et al. 2001). The conformational structure of the heterologous molecules can be vastly improved as they are delivered to the periplasmic space of *E. coli*, which has higher oxidizing conditions compared to the cytoplasm. In the present report, we genetically engineered a cell surface molecule, CD99, using phage display. The PCR-amplified CD99 cDNA was inserted into *Sfi*I-cleaved pComb3HSS phagemid. The resulting phagemid (pComb3H-CD99) was then used to generate CD99-expressing phages using helper phage VCSM13. Expression of CD99 was demonstrated by sandwich ELISA; CD99-ϕ were recognized by CD99 mAbs MT99/1 and MT99/3. Since an HRP-labeled anti-M13 phage antibody was used as the tracing antibody, the CD99 molecules were manifestly linked to phage particles.

mAbs against CD99 protein produced in our department were previously shown to induce homotypic cell aggregation of Jurkat cells (Kasinrerk et al. 2000). In the present study, the inhibition of Jurkat cell aggregation induced by MT99/1 was used to evaluate the presence of CD99 bioactive domains on CD99-ϕ. The degree of Jurkat cell aggregation was significantly reduced when MT99/1 was preincubated with CD99-ϕ. The CD99 molecule was clearly implicated as the inhibitor since preincubation of MT99/1 with VCSM13 did not obstruct cell aggregation. The inhibition of MT99/1-induced Jurkat aggregation by CD99-ϕ suggested that the generated CD99-ϕ contained a properly folded bioactive domain. This successful preservation of the bioactive domain allows further use of CD99-ϕ in the screening of specific ligands on the leukocyte surface.

Taken together, our findings demonstrate the feasibility of using the phage display technique to display the CD99 molecule. This technique has a high potential to generate phage expressing other leukocyte surface molecules, providing the corresponding cDNA is available. In practical terms, the recombinant phages produced will be useful for identification and functional analysis of the receptors of the molecules of interest. In addition, the recombinant phagemid can be easily switched from a phage display version to a secretory version without subcloning to a new vector, as demonstrated in our recent study (Manosroi et al. 2001). As the defined fermentation conditions allowed protein levels of 100 mg/ml to be obtained, an adequate quantity of soluble molecule of interest can be produced (Manosroi et al. 2002). The soluble protein produced can be used for other immunological studies, e.g., epitope characterization and immunomodulation assays.

Acknowledgements This work was supported by The Thailand Research Fund and The National Center for Genetic Engineering and Biotechnology (BIOTEC) of the National Science and Technology Development Agency, Thailand. We thank S. Moonsom and W. Silaket for expert technical assistance.

References

Appenzeller U, Blaser K, Crameri R (2001) Phage display as a tool for rapid cloning of allergenic proteins. Arch Immunol Ther Exp (Engl Trans) 49:19–25

Barbas CF III, Wagner J (1995) Synthetic human antibodies: selecting and evolving functional proteins. Methods Enzymol 8:94–103

Becker GW, Hsiung HM (1986) Expression, secretion and folding of human growth hormone in *Escherichia coli*. Purification and characterization. FEBS Lett 204:145–150

Bowen MA, Bajorath J, Siadak AW, Modrell B, Malacko AR, Marquardt H, Nadler SG, Aruffo A (1996) The amino-terminal immunoglobulin-like domain of activated leukocyte cell adhesion molecule binds specifically to the membrane-proximal scavenger receptor cysteine-rich domain of CD6 with a 1:1 stoichiometry. J Biol Chem 271:17390–17396

Crameri R, Blaser K (1996) Cloning *Aspergillus fumigatus* allergens by the pJuFo filamentous phage display system. Int Arch Allergy Immunol 110:41–45

Dracheva S, Palermo RE, Powers GD, Waugh DS (1995) Expression of soluble human interleukin-2 receptor alpha-chain in *Escherichia coli*. Protein Expr Purif 6:737–747

Gaudin Y, Moreira S, Benejean J, Blondel D, Flamand A, Tuffereau C (1999) Soluble ectodomain of rabies virus glycoprotein expressed in eukaryotic cells folds in a monomeric conformation that is antigenically distinct from the native state of the complete, membrane-anchored glycoprotein. J Gen Virol 80:1647–1656

Hoogenboom HR, Chames P (2000) Natural and designer binding sites made by phage display technology. Immunol Today 21:371–378

Kasinrerk W, Tokrasinwit N, Moonsom S, Stockinger H (2000) CD99 monoclonal antibody induce homotypic adhesion of Jurkat cells through protein tyrosine kinase and protein kinase C-dependent pathway. Immunol Lett 71:33–41

Koch C, Staffler G, Hüttinger R, Hilgert I, Prager E, Cerny J, Steinlein P, Majdic O, Horejsi V, Stockinger H (1999) T cell activation-associated epitopes of CD147 in regulation of the T cell response, and their definition by antibody affinity and antigen density. Int Immunol 11:777–786

Kurokawa MS, Ohoka S, Matsui T, Sekine T, Yamamoto K, Nishioka K, Kato T (2002) Expression of MHC class I

molecules together with antigenic peptides on filamentous phages. Immunol Lett 80:163–168

Lasters I, Van Herzeele N, Lijnen HR, Collen D, Jespers L (1997) Enzymatic properties of phage-displayed fragments of human plasminogen. Eur J Biochem 244:946–952

Manosroi J, Tayapiwatana C, Gotz F, Werner R, Manosroi A (2001) Secretion of active recombinant human tissue plasminogen activator derivatives in *Escherichia coli*. Appl Environ Microbiol 67:2657–2664

Manosroi J, Tayapiwatana C, Manosroi A, Beer J, Bergemann K, Werner RG (2002) Lekteplase – a secreted tissue plasminogen activator derivative from *Escherichia coli*. Arzneimittelforschung 52:60–66

Martinez-Pomares L, Crocker PR, Da Silva R, Holmes N, Colominas C, Rudd P, Dwek R, Gordon S (1999) Cell-specific glycoforms of sialoadhesin and CD45 are counter-receptors for the cysteine-rich domain of the mannose receptor. J Biol Chem 274:35211–35218

McCafferty J, Fitzgerald KJ, Earnshaw J, Chiswell DJ, Link J, Smith R, Kenten J (1994) Selection and rapid purification of murine antibody fragments that bind a transition-state analog by phage display. Appl Biochem Biotechnol 47:157–171

Noonsom S, Khunkeawla P, Kasinrerk W (2001) Production of polyclonal and monoclonal antibodies against CD54 molecules by intrasplenic immunization of plasmid DNA encoding CD54 protein. Immunol Lett 76:25–30

Prager E, Sunder-Plassmann R, Hansmann C, Koch C, Holter W, Knapp W, Stockinger H (1996) Interaction of CD31 with a heterophilic counterreceptor involved in downregulation of human T cell responses. J Exp Med 184:41–50

Persic L, Roberts A, Wilton J, Cattaneo A, Bradbury A, Hoogenboom HR (1997) An integrated vector system for the eukaryotic expression of antibodies or their fragments after selection from phage display libraries. Gene 187:9–18

Smith GP (1985) Filamentous fusion phage: novel expression vectors that display cloned antigens on the virion surface. Science 228:1315–1317

Viaene A, Crab A, Meiring M, Pritchard D, Deckmyn H (2001) Identification of a collagen-binding protein from *Necator americanus* by using a cDNA-expression phage display library. J Parasitol 87:619–625

Vilardell C, Juan M, Miralles A, Barcelo JJ, Esparza J, Palou E, Vilella R, Places L, Lozano F, Alberola-Ila J, Gaya A, Yague J (1998) Isolation of two CD50 (ICAM-3)-negative Jurkat T-cell clones and their application for analysis of CD50 function. Tissue Antigens 51:509–519

Wojnar P, Lechner M, Merschak P, Redl B (2001) Molecular cloning of a novel lipocalin-1 interacting human cell membrane receptor using phage display. J Biol Chem 276:20206–20212

Autosomal Recessive Distal Renal Tubular Acidosis Caused by G701D Mutation of *Anion Exchanger 1* Gene

Pa-thai Yenchitsomanus, PhD, Somkiat Vasuvattakul, MD, Sukachart Kirdpon, MD, Sirijitta Wasanawatana, MD, Wattanachai Susaengrat, MD, Suchai Sreethiphayawan, MD, Duangporn Chuawatana, BSc, Sumitra Mingkum, BSc, Nunghathai Sawasdee, BSc, Peti Thuwajit, MD, PhD, Prapon Wilairat, PhD, Prida Malasit, MD, and Sumalee Nimmannit, MD

• **Anion exchanger 1 (AE1 or band 3), encoded by the *AE1* or *SLC4A1* gene, regulates chloride-bicarbonate exchange in erythrocytes and α-intercalated cells of the distal nephron. Defects of AE1 at the basolateral membrane of α-intercalated cells may result in the failure of hydrogen ion secretion at the apical membrane, leading to distal renal tubular acidosis (dRTA). Abnormalities of the *AE1* gene were previously reported to be associated with autosomal dominant dRTA. However, recent studies of Thai dRTA families have shown that mutations in this gene result in autosomal recessive (AR) dRTA, giving rise to the postulation that *AE1* gene mutations causing AR dRTA might be found commonly in Thai pediatric patients with dRTA. We performed a study of the *AE1* gene using DNA linkage, polymerase chain reaction single-strand conformation polymorphism, restriction endonuclease *Hpa*II digestion, and DNA sequence analyses in eight families involving 12 Thai children with dRTA, shown by abnormal urinary acidification using a short acid-loading test, as well as among their family members. Seven patients with dRTA from five families had the same homozygous missense G701D mutation of the *AE1* gene. Their parents or siblings heterozygous for the *AE1* G701D mutation were clinically normal and did not have abnormal urinary acidification, although a heterozygous sibling in one family had abnormal urinary acidification. Results of this and previous studies show that a homozygous *AE1* G701D mutation causes AR dRTA and is a common molecular defect among Thai pediatric patients with dRTA.**

INDEX WORDS: Distal renal tubular acidosis (dRTA); band 3; anion exchanger 1 (AE1); *SCL4A1*; Thai.

ACID-BASE HOMEOSTASIS in the human body is critical for normal growth, development, and metabolic function. Human arterial blood pH is normally regulated at 7.4. The kidney has a major role in this regulation because of its ability to sustain bicarbonate reabsorption and acid excretion. H^+-ATPase pump located in the apical membrane of α-intercalated (or type A) cells of the distal nephron is important in the process of net acid excretion,[1] which occurs in association with bicarbonate reabsorption across the basolateral membrane of these cells, mediated by anion Cl^-/HCO_3^- exchanger 1 (kAE1 or band 3).[2-4]

Failure to either excrete acid or reabsorb bicarbonate by these cells leads to distal renal tubular acidosis (dRTA), characterized by the incapability of the kidney to acidify urine in the presence of systemic metabolic acidosis.[1,5] Autosomal dominant (AD)[6] and autosomal recessive (AR)[7,8] patterns of inheritance have been observed in kindreds with primary dRTA, with a broad spectrum of clinical severity. Patients with AR dRTA usually are severely affected in infancy with failure to thrive, growth retardation, and rickets. Many patients with AR dRTA can have sensorineural deafness,[8-10] but others have preserved hearing.[11] Patients with AD dRTA remain asymptomatic until adolescence or adulthood.

Defects in several enzymes or transporters involving transepithelial acid excretion and bicarbonate reabsorption in α-intercalated cells cause

From the Division of Medical Molecular Biology, Department of Research and Development, Renal Division, Department of Medicine, Faculty of Medicine Siriraj Hospital; Department of Biochemistry, Faculty of Science, Mahidol University, Bangkok; Departments of Pediatrics and Biochemistry, Faculty of Medicine, Khon Kaen University; Pediatrics and Medicine Units, Khon Kaen Hospital, Khon Kaen; Medical Biotechnology Unit, National Center for Biotechnology and Genetic Engineering, National Science and Technology Development Agency, Bangkok, Thailand.

Received July 3, 2001; accepted in revised form February 25, 2002.

P.Y. and S.V. contributed equally to this work.

Supported in part by Siriraj Grant for Research Development and the Thailand Research Fund (TRF). P.W. and P.M. are recipients of the Senior Research Scholar Award of the TRF.

Address reprint requests to Pa-thai Yenchitsomanus, PhD, Division of Medical Molecular Biology, Department of Research and Development, Faculty of Medicine Siriraj Hospital, Mahidol University, Bangkok 10700, Thailand. E-mail: grpye@mahidol.ac.th

0272-6386/02/4001-0004$35.00/0

doi:10.1053/ajkd.2002.33909

heritable dRTA. These include H^+-ATPase and H^+/K^+-ATPase, which mediate hydrogen ion secretion across the luminal membrane of α-intercalated cells, kAE1 or band 3 that discharges bicarbonate across the basolateral membrane of α-intercalated cells by exchanging with chloride, and cytoplasmic carbonic anhydrase II, in which activity provides both hydrogen ion for luminal secretion through the vacuolar H^+-ATPase and bicarbonate for basolateral expulsion through kAE1.[1,5]

Recently, mutations in the *anion exchanger 1* (*AE1; SLC4A1* [MIM 109270]) gene located on chromosome 17q21 were found in several kindreds with AD dRTA.[12-15] Characterization of *AE1* in AD dRTA identified multiple families[12,14,15] with missense mutations in codon 589 (R589H, R589S, R589C) located in the sixth transmembrane domain (TM6), one family[12] with an S613F mutation in TM7, and another family[15] with an 11–amino acid deletion at the carboxy terminus. However, functional analysis of R589 mutations showed only a modest reduction in AE1-mediated $^{36}Cl^-$ transport expressed in *Xenopus* oocytes, whereas the S613F mutation is associated with upregulation of anion transport. Similarly, little change was evident in AE1-mediated sulfate transport in these patients' red blood cells (RBCs). Thus, the mechanism by which mutant AE1 causes AD dRTA remains unclear.

A novel *AE1* mutation linked to recessive inheritance of dRTA and hemolytic anemia in which RBC anion transport is normal recently was reported.[16] The two affected individuals, siblings of the same family, were triply homozygous for two benign mutations, M31T and K56E, and the functionally defective mutation, G701D (band 3 Bangkok I). *AE1* G701D mutation results in inactive anion transport because of impaired protein trafficking, shown by an expression study in *Xenopus* oocytes.[16] Coexpression of *AE1* G701D with the erythroid AE1 chaperonin, glycophorin A (GPA), rescued both AE1-mediated chloride transport and AE1 surface expression in oocytes.[16] Thus, genetic and functional data from this study indicate that the homozygous *AE1* G701D mutation causes recessively transmitted dRTA with apparently normal erythroid anion transport.

Our group recently described a novel compound heterozygosity of the *AE1* gene causing AR dRTA in patients with southeast Asian ovalocytosis (SAO).[17] Two clinically affected individuals from two unrelated families had one *AE1* allele with the missense G701D mutation and the other allele with a nine–amino acid deletion (residues 400 to 408), which is specific to SAO and also produces transport-inactive protein. This observation recently has been confirmed and extended to other genotypes, including ΔV850/SAO, A858D/SAO, ΔV850/ΔV850, and ΔV850/A858D in Malaysian and Papua New Guinean patients with dRTA.[18]

Because two cases with homozygosity and two cases with compound heterozygosity of the *AE1* G701D mutation have been detected in Thai children with dRTA, this mutation might be found commonly in Thai pediatric patients with dRTA. Therefore, we performed an analysis of the *AE1* gene in 12 Thai children with dRTA and identified 7 patients from five families homozygous for the *AE1* G701D mutation.

METHODS

Patients

The study group consisted of 12 patients with dRTA, their siblings, and their parents in eight families from the northeast region of Thailand. Altogether, 29 subjects were included on the study. Criteria for inclusion of patients were the presence of systemic acidosis with serum bicarbonate levels less than 20 mEq/L, inability to reduce urine pH to less than 5.5, and low rate of ammonium excretion. A short acid-loading test (discussed next) was performed to confirm the diagnosis in all patients. Subjects who did not meet these criteria or showed normal results in the acid-loading test were excluded from the study. The test also was conducted on patients' parents and siblings. All subjects were prescribed a normal diet, and medications were terminated 1 week before the acid-loading test. During the first admission, 10 mL of blood was collected from patients, their siblings, and their parents, with informed consent, for biochemical and DNA analyses.

Short Acid-Loading Test

Renal acidification was examined using the short acid-loading test, which has been performed as a diagnostic tool as previously described by Wrong and Davies.[19] Briefly, 0.1 g/kg of NH_4Cl was administered orally to subjects. Urine was sampled at the beginning of the acid load and at hourly intervals for the subsequent 6 hours. Urinary pH, titratable acid, and ammonium excretion were measured. Urine ammonium and titratable acid and serum potassium, bicarbonate, and creatinine levels were determined as previously described.[17] Results of the acid-loading test that indicated a urinary acidification defect were the inability to decrease

urine pH to less than 5.5 with a low rate of urine ammonium excretion (<20 μEq/min) after acid loading.

D17S787 Microsatellite Analysis

Genomic DNA was prepared from peripheral leukocytes by means of the standard phenol-chloroform extraction method. To investigate the possible involvement of the *AE1* gene in causing dRTA in patients, segregation of this gene in families was studied by DNA linkage using the D17S787 microsatellite, a polymorphic marker mapped to the same region (17q21) as the *AE1* gene (National Center for Biotechnology Information [NCBI]; GeneMap'99). The microsatellite region was amplified by polymerase chain reaction (PCR) using a pair of primers with the sequences 5′-TGGGCTCAACTATATGAACC-3′ (L-primer) and 5′-TTGATACCTTTTTGAAGGGG-3′ (R-primer). The L-primer was end-labeled with phosphorus 32 (^{32}P) by using γ-^{32}P adenosine triphosphate and T4 polynucleotide kinase. The PCR mixture (25 μL) contained 125 ng of genomic DNA, 12.5 pmol of each primer, 0.5 pmol of ^{32}P-labeled primer, 0.25 U *Taq* polymerase (Promega, Madison, WI), and other standard components. PCR was performed for 37 cycles: each cycle consisted of 1 minute at 95°C, 1 minute at 62°C, and 1 minute at 72°C. The radioactive PCR product was analyzed by electrophoresis on denaturing 6% polyacrylamide gel and detected by autoradiography.

Screening for AE1 *Mutation by PCR and Single-Strand Conformation Polymorphism*

Mutations of the *AE1* gene were screened by PCR and single-strand conformation polymorphism (PCR-SSCP) as previously described.[17] Briefly, sequences in exons 4 to 20 and the kidney promoter sequence in intron 3 were amplified by PCR. PCR-amplified products were denatured by heating in buffer containing formamide and sodium hydroxide. SSCP analysis was performed by electrophoresis on nondenaturing 10% polyacrylamide gel, and bands were visualized by silver staining.

Analysis of AE1 *G701D Mutation by Restriction Endonuclease* HpaII *Digestion*

The presence of the *AE1* G701D mutation abolishes the recognition site of restriction endonuclease *HpaII*.[17] Thus, this mutation can be detected readily by digesting the amplified exon 17 fragment with *HpaII* (Promega) and examining the fragments produced by agarose gel electrophoresis. A normal allele produces two fragments of 254 and 67 bp, whereas the G701D allele results in a single fragment of 321 bp.

DNA Sequence Analysis

PCR products that showed mobility shift on the SSCP gel were reamplified for purification using QIAquick Gel Extraction Kit (Qiagen, GmbH, Germany). Purified PCR products then were sequenced using ABI-PRISM BigDye Terminator Cycle Sequencing Ready Reaction Kit (Applied Biosystems, Foster City, CA) and an automated sequencer ABI-PRISM310 (Applied Biosystems).

RESULTS

Twelve patients with dRTA from eight families examined on this study presented with failure to thrive and growth retardation. Eight of the patients had rickets, and one patient had nephrocalcinosis (Table 1). No patient had clinical hearing loss; however, audiometry tests were not conducted.

Hypokalemic and hyperchloremic metabolic acidosis, with normal serum creatinine levels accompanied by alkaline urinary pH, were observed during their admission for an acid-loading study (Table 2). Examination of patients' RBC indices and morphological characteristics showed the presence of microcytes, spherocytes, ovalocytes, and elliptocytes (Fig 1), but no feature of hemolytic anemia. All patients had previously been treated with potassium and bicarbonate replacement for varying periods.

Short acid-loading tests were performed on patients and their family members. All 12 patients showed abnormal renal acidification function (Table 1). That is, after acid loading, patients could not acidify their urinary pH to less than 6.0 and did not excrete ammonium greater than 20 μEq/min (Table 2). In all families except one, parents and other unaffected siblings could fully acidify their urine and had appropriate rates of ammonium excretion after acid loading. However, in family D, the patient's younger sister (Table 1, family D, no. II-2) had abnormal urinary acidification (data not shown) without clinical manifestations; thus, an incomplete form of dRTA was diagnosed.

Involvement of the *AE1* mutation in causing dRTA was studied in these families. The same patterns of mobility shifts were observed in the PCR-SSCP analysis of *AE1* exon 17 in seven patients from five families (A, B, C, D, and E; Fig 2, lanes 5 to 11). However, a normal mobility pattern of exon 17 was detected in five patients from three families (F, G, and H; Fig 2, lanes 12 to 16). Results of DNA linkage analysis in the five families (A through E) also supported the association of *AE1* and dRTA. In families A and B, the two affected siblings (II-1 and II-2) had the same genotypes: 142/142 (nt) in family A, and 140/138 in family B (Fig 3). In family C, a different set of genotypes in the patient (160/142) and the unaffected sibling (156/142) was

Table 1. Clinical Diagnosis, Acid-Loading Test, and *AE1* Genotypes of Patients and Members of Eight Thai Families With dRTA

Family	No.	Relationship	Age (y)	Clinical Diagnosis	ALT	*AE1* Genotype
A	I-1	Father	33	Normal	Normal	G701D/N
	I-2	Mother	36	Normal	Normal	G701D/N
	II-1	Son	12	dRTA & rickets	Abnormal	G701D/G701D
	II-2	Son	9	dRTA & rickets	Abnormal	G701D/G701D
B	I-1	Mother	46	Normal	Normal	G701D/N
	II-1	Son	17	dRTA & rickets	Abnormal	G701D/G701D
	II-2	Son	14	dRTA & rickets	Abnormal	G701D/G701D
C	I-1	Father	38	Normal	Normal	G701D/N
	I-2	Mother	31	Normal	Normal	G701D/N
	II-1	Daughter	12	dRTA & rickets	Abnormal	G701D/G701D
	II-2	Daughter	9	Normal	Normal	N/N
D	I-1	Father	30	Normal	Indeterminate*	G701D/N
	I-2	Mother	—	Normal	Normal	G701D/N
	II-1	Daughter	8	dRTA & nephrocalcinosis	Abnormal	G701D/G701D
	II-2	Daughter	—	Normal	Abnormal	G701D/N
E	I-1	Mother	40	Normal	Normal	G701D/N
	II-1	Son	7	dRTA	Abnormal	G701D/G701D
F	I-1	Father	41	Normal	Normal	N/N
	I-2	Mother	31	Normal	Normal	N/N
	II-1	Daughter	15	dRTA	Abnormal	N/N
	II-2	Daughter	5	Normal	Normal	N/N
G	I-1	Mother	35	Normal	ND	N/N
	II-1	Daughter	12	Normal	Normal	N/N
	II-2	Daughter	10	dRTA	Abnormal	N/N
H	I-1	Father	44	Normal	Normal	N/N
	I-2	Mother	45	Normal	Normal	N/N
	II-1	Son	24	dRTA & rickets	Abnormal	N/N
	II-2	Son	22	dRTA & rickets	Abnormal	N/N
	II-3	Daughter	21	dRTA & rickets	Abnormal	N/N

Abbreviations: ALT, acid-loading test; ND, not determined.
*The diagnosis could not be made because of conflicting results of repeated acid-loading tests.

detected. Similarly, in family D, differences in genotypes were observed between the patient with full-blown dRTA (152/138) and her younger sister with only an abnormal renal acidification (140/138). Family E was not informative because only the patient and his mother were available for analysis. In addition to results of PCR-SSCP mentioned previously, DNA linkage and restriction endonuclease *Hpa*II digestion studies did not support the involvement of *AE1* in dRTA of the F, G, and H families.

Results of *AE1* G701D analysis by *Hpa*II digestion in the seven patients with dRTA from families A, B, C, D, and E showed that all patients' samples had only the undigested 321-bp fragment of exon 17, indicating they were homozygous for the G701D mutation (Fig 3). Samples from parents showed both the undigested 321-bp and two digested 254- and 67-bp fragments, consistent with the presence of both normal and G701D alleles. *Hpa*II digestion analysis in the five patients from families F, G, and H showed they did not carry the G701D mutation (data not shown). DNA sequencing of exon 17 from all seven patients from the five families (A, B, C, D, and E) showed a nucleotide substitution in codon 701, C<u>G</u>G→C<u>A</u>G, in both alleles (an example of the sequencing profile is shown in Fig 3), indicating the presence of a homozygous G701D mutation, whereas exon 17 from patients' parents showed the presence of both normal and G701D codons (Fig 3). *AE1* G701D alleles in all patients were associated with the Memphis I (K56E) polymorphism, resulting from a nucleotide replacement (<u>A</u>AG→<u>G</u>AG) at codon 56 (data not shown). We previously showed that

Table 2. Results of Blood and Urine Analyses During the First Admission and After a Short Acid-Loading Study in the 12 Patients With dRTA

		During First Admission				After Acid Loading Study		
Family	No.	Serum Potassium (mmol/L)	Serum Bicarbonate (mmol/L)	Urine pH	Serum Creatinine (mg/dL)	Urine Ammonium (μEq/min)	Urine Titrable Acid (μEq/min)	Urine pH
A	II-1	2.3	10	7.5	0.7	6.3	1.6	7.2
	II-2	3.5	9	7 6	0.6	7 3	1.4	7.1
B	II-1	2.9	13	7.0	0.3	8.4	6 9	6.7
	II-2	3.8	25	7.4	0.6	10.3	4 9	6.9
C	II-1	1.5	11	7 5	0.7	6.8	1.4	7.3
D	II-1	3.6	14	7.4	0.6	4.3	3.9	7.0
E	II-1	3.4	15	7.2	0.6	14.1	4.9	6.6
F	II-1	4.1	11	6.7	1.4	6.2	3.0	6.4
G	II-2	1.9	14	7.1	0.8	10.4	4.9	6.3
H	II-1	2.9	12	7 0	1.1	18.8	6.1	6 6
	II-2	2.9	16	6.8	0 9	8.5	5.1	6.9
	II-3	2.3	11	6 5	1.0	11.5	3.8	6.6

both the *AE1* G701D and SAO mutations are linked in *cis* to the Memphis I (K56E) polymorphism,[17] as observed by others.[16,18]

DISCUSSION

The failure of acid secretion from α-intercalated cells in the distal nephron may result from a defect of the transport protein mediating hydrogen ion secretion across apical membranes or that mediating bicarbonate reabsorption through the basolateral membrane. An abnormality of kAE1 that functions in chloride-bicarbonate exchange at the basolateral membrane of α-intercalated cells leads to a failure of hydrogen ion secretion across the apical membrane, compromising cellular mechanisms regulating intracellular acid-base balance and thereby causing dRTA. Therefore, secondary to abnormal kAE1 function, the net activities of H^+-ATPase and probably also H^+/K^+-ATPase pumps are decreased. The reduction in distal hydrogen ion secretion also may result in potassium wasting[20] brought about by enhancement of potassium secretion to maintain electroneutrality, possibly leading to hypokalemia.

During the past few years, defects of the *AE1* gene in dRTA have been extensively investigated, and mutations, particularly at R589 of this gene, were found to be associated with AD dRTA,[12-15] but without supporting evidence from functional studies. A novel *AE1* (G701D) mutation, with impaired protein trafficking shown in *Xenopus* oocytes and linked to AR dRTA, was reported recently in two affected Thai siblings

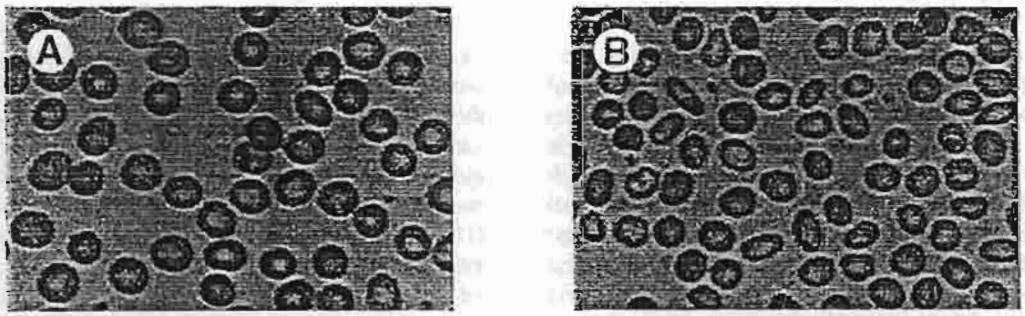

Fig 1. RBC morphological characteristics of (A) a healthy individual and (B) a representative patient with dRTA with the homozygous *AE1* G701D mutation. Note that xerocytosis-like RBCs, previously observed in patients homozygous for both the *AE1* G701D mutation and Hb E,[16] are not present in the blood smear of this homozygous *AE1* G701D patient with dRTA without Hb E.

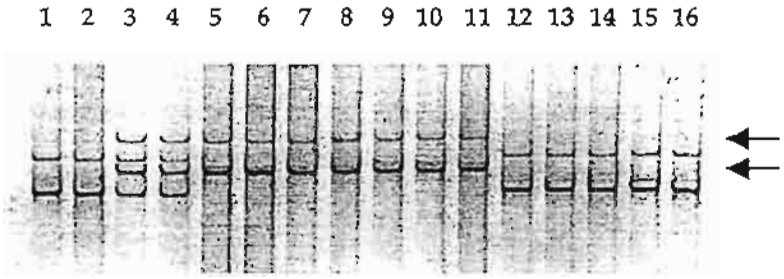

Fig 2. Results for exon 17 screening for *AE1* mutations by PCR-SSCP. Two normal samples (lanes 1 and 2), 2 samples from individuals known to be heterozygous for the *AE1* G701D mutation (lanes 3 and 4), and 12 samples from patients with dRTA (lanes 5 to 16) were examined on the gel. Samples from 7 patients with dRTA (lanes 5 to 11) had the same pattern of mobility shift. Bands indicated by arrows are located at the same positions as those observed in samples from known individuals with heterozygous *AE1* G701D mutation (lanes 3 and 4). Samples from 5 patients with dRTA (lanes 12 to 16) did not show mobility shift in this exon.

from the same family, both homozygous for the *AE1* G701D mutation.[16] Compound heterozygosity of this mutation with that of a 27-nucleotide deletion in exon 11 of the *AE1* gene commonly found in the southeast Asian population is seen in AR dRTA associated with SAO.[17,18] Thus, the presence of a homozygous *AE1* G701D mutation, first identified in two Thai pediatric patients with dRTA from northeastern Thailand,[16] and of compound heterozygosity between *AE1* G701D and SAO mutations in two affected Thai children from southern Thailand[17] and three affected Malaysian children[18] led us to suspect that the *AE1* G701D mutation might be of ancient origin that has evolved in this region and might be a common mutation causing AR dRTA in Thai pediatric patients.

We therefore investigated abnormality of the *AE1* gene in 12 other Thai pediatric patients with dRTA from eight families, giving particular attention to the *AE1* G701D mutation, as well as other *AE1* mutations reported to be associated with AD and AR dRTA, by means of DNA linkage, PCR-SSCP, restriction endonuclease *Hpa*II digestion, and DNA sequence analyses. Seven patients with dRTA from five families were found to be homozygous for the *AE1* G701D mutation; only one family (family A) had consanguinity. Parents and siblings heterozygous for the *AE1* G701D mutation did not have dRTA. These findings are consistent with those previously documented by our group[17] and others.[16,18]

However, five patients with dRTA from three families (F, G, and H) did not have the *AE1* G701D mutation. In this group of patients, PCR-SSCP analysis of other exons did not show mobility shift patterns, indicating that mutant *AE1* was not involved in causing dRTA in these patients, although the sensitivity of SSCP is not absolute. In addition, DNA linkage analysis using the D17S787 microsatellite located approximately 3 centimorgans (cM) from *AE1*, which supported the role of a homozygous *AE1* G701D mutation as the cause of dRTA in the five families mentioned previously, failed to show an involvement of *AE1* mutations in the cause of dRTA in patients from families F, G, and H, and abnormalities in other genes must be sought. Possible candidates are *ATP6B1* and *ATP6N1B*, encoding subunits of kidney vacuolar H^+-ATPase, in which mutations have been reported to cause AR dRTA with sensorineural deafness[10] and preserved hearing,[11] respectively. A small minority (13%) of patients with AR dRTA with *ATP6B1* mutations did not have hearing loss.[10]

The younger sister (II-2) of the patient in family D had abnormal renal acidification without observed clinical manifestations and was found to be heterozygous for the *AE1* G701D mutation. Using PCR-SSCP analysis, we did not observe mobility shift patterns in other exons of this gene. Furthermore, *AE1* messenger RNA isolated from blood samples from II-2 and her father (I-1) were analyzed by reverse transcriptase PCR and electrophoresis to investigate the presence of a mutation that might affect processing of messenger RNA, but that could not be detected by genomic DNA analysis of exons. However, no such abnormality in *AE1* was detected (data not shown). Possible explanations

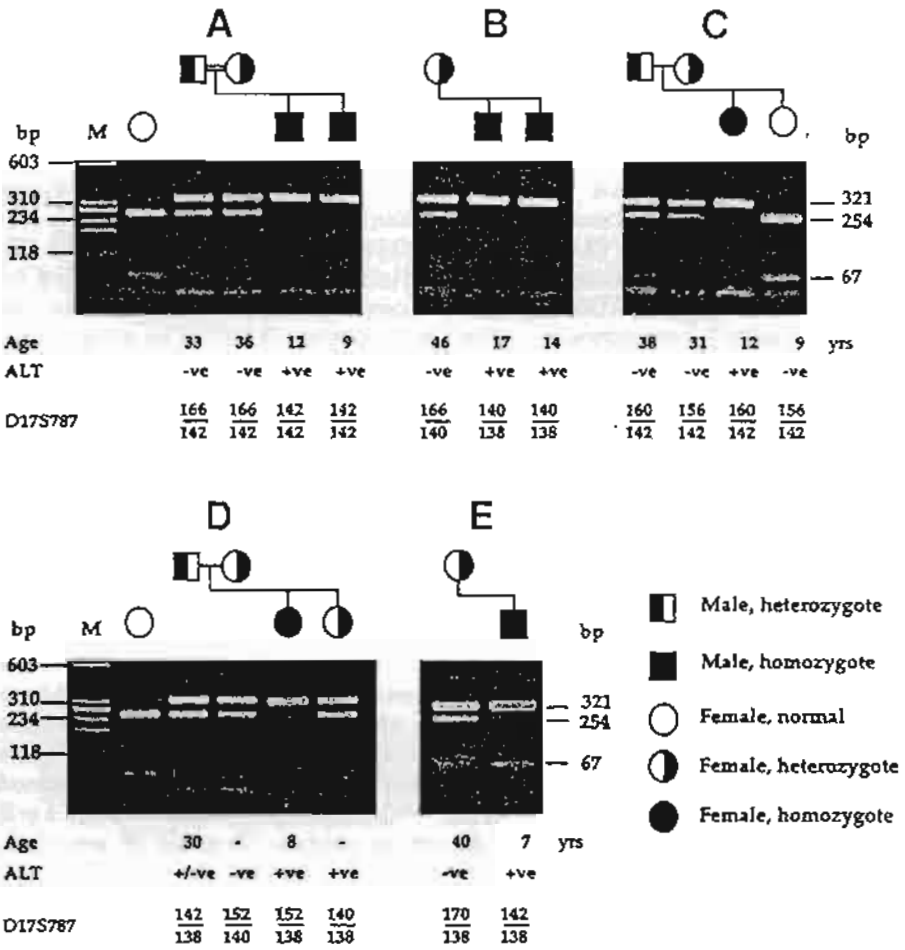

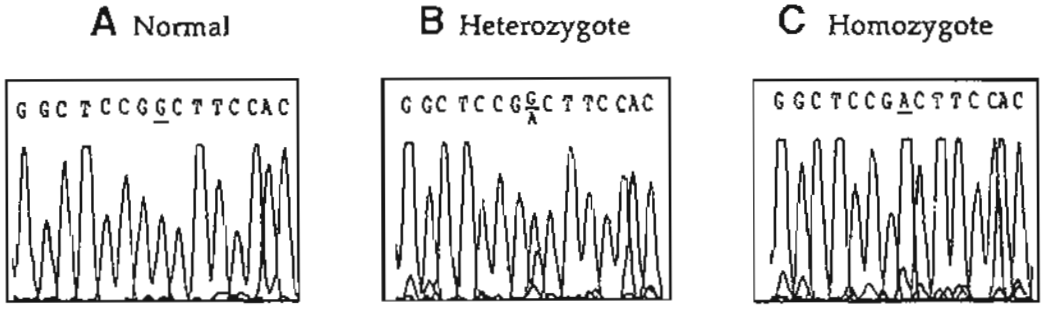

Fig 3. (Top) Analysis of the *AE1* G701D mutation by restriction endonuclease *Hpa*II digestion of amplified exon 17 DNA fragments from seven patients with dRTA, their parents, and siblings in five families (A, B, C, D, and E). The amplified DNA fragment with the *AE1* G701D mutation was not cleaved with *Hpa*II and showed a fragment size of 321 bp, whereas that without the mutation could be cleaved with this enzyme, showing fragment sizes of 254 and 67 bp. An individual with the homozygous *AE1* G701D mutation has only a 321-bp fragment, a healthy individual has 254- and 67-bp fragments, and a heterozygous individual has all three fragments. M is standard DNA size markers, PhiX174 DNA/*Hae*III. An amplified *Hpa*II-digested DNA from a healthy woman (○) also was applied as a control sample. Ages of family members, results of the short acid-loading test (ALT), genotypes in the *AE1* gene region determined by the polymorphic microsatellite D17S787, DNA marker of individuals in the family also are shown under the gel. Genotypes are indicated as nucleotide sizes of the microsatellite DNA. (Bottom) Characterization of the *AE1* G701D mutation by DNA sequence analysis. An amplified DNA fragment of exon 17 from (A) normal, (B) heterozygote, and (C) homozygote subjects shows codon 701 sequence of CGG/CGG, CGG/CAG, and CAG/CAG, respectively.

for the abnormal renal acidification in this individual encompass compound heterozygosity at two loci, phenotypic modification from polymorphisms of other gene(s), or the effect of unknown environmental factor(s).

It should be noted that all seven patients with dRTA homozygous for the *AE1* G701D mutation on this study did not have xerocytic hemolytic anemia (Fig 1), found in two patients with the homozygous *AE1* G701D mutation previously documented.[16] This difference may occur because patients on our study were not also homozygous for hemoglobin (Hb) E, as were both patients of the previous work. Four of seven patients on this study were examined for Hb types: three patients were found to have normal Hb typing, and one patient was heterozygous for Hb E. Although Hb typing was not conducted in the remaining three patients, routine hematologic and RBC morphological examination did not show evidence of hemolytic anemia. It seems most likely that the xerocytic hemolytic anemia observed in the two patients in the previous study[16] was caused by the presence of both homozygous Hb E and mutant AE1 (band 3). Hb E is a relatively unstable hemoglobin,[21,22] and in conditions of metabolic acidosis and/or other intraerythrocytic changes caused by acidosis, its presence may compromise RBC stability. Because at least one patient with dRTA on our study was heterozygous for Hb E, the presence of a single Hb E allele in dRTA is probably insufficient to cause xerocytic hemolytic anemia.

Mildly abnormal RBC morphological characteristics in our patients with dRTA with homozygous *AE1* G701D (in the absence of abnormal Hb or thalassemia) indicate that this mutation also may affect RBC shape because AE1 (band 3) is a transmembrane protein that interacts with the underlying cytoskeletal network responsible for maintaining the proper form of RBCs.

Expression and functional studies of *Xenopus* oocytes showed that the AE1 G701D-mutant protein fails to accumulate at the cell surface; however, this defect can be rescued by coexpression of the mutant protein with GPA.[16,18] Because GPA is present in RBCs, but absent in α-intercalated cells of the kidney, SO_4^{2-} anion influx studies using RBCs from *AE1* G701D homozygotes with dRTA were found to be normal[16,18] (Thuwajit et al, unpublished data). Proper placement of kAE1 into the basolateral membrane of α-intercalated kidney cells will depend on a mechanism different from that shown in erythroid cells.

Results of this study provide additional evidence to support the notion that a homozygous *AE1* G701D mutation causes AR dRTA, and this genotype is a common molecular defect of AR dRTA in Thai pediatric patients, especially from northeastern Thailand. However, in the general Thai population, the frequency of this mutation was low; one mutant of 434 alleles (0.2304%) was detected, although this may not be the case in the northeastern population. The *AE1* G701D mutation was the first identified to have a clear functional defect resulting in dRTA with an AR mode of inheritance.[16-18] Other *AE1* mutations causing AR dRTA subsequently have been identified[18] (Yenchitsomanus et al, unpublished data). The molecular mechanism of *AE1* mutation causing AD dRTA remains to be elucidated. Further studies of defects of *AE1* and its encoded protein will provide insight into the molecular mechanisms by which *AE1* mutations cause AD and AR forms of dRTA.

NOTE ADDED IN PROOF

Two recent papers (Toye et al [*Blood* 99:342-347, 2002] and Quilty et al [*Am J Physiol* 282: F810-F820, 2002]) reported that band 3 Walton (a C-terminal deletion) and AE1 R589H (as well as R589C and R589S) protein had impaired trafficking to cell surface in the expression studies using Madin-Darby canine kidney (MDCK) and human embryonic kidney (HEK293) cell lines, respectively. Dominant dRTA associated with these two mutations probably results from a dominant-negative effect due to the formation of heterodimer between mutant and normal proteins.

ACKNOWLEDGMENT

The authors thank staff members of Khon Kaen Hospital for their generous assistance and patients and their families for participation in this project.

REFERENCES

1. Rodriguez-Soriano J: New insights into the pathogenesis of renal tubular acidosis—From functional to molecular studies. Pediatr Nephrol 14:1121-1136, 2000

2. Wagner S, Vogel R, Lietzke R, Koob R, Drenckhahn D: Immunochemical characterization of a band 3-like anion

exchanger in collecting duct of human kidney. Am J Physiol 253:F213-F221, 1987

3. Alper SL, Natale L, Gluck S, Lodish HF, Brown D: Sub-types of intercalated cells in rat kidney collecting duct defined by antibodies against erythroid band 3 and renal vacuolar H^+-ATPase. Proc Natl Acad Sci U S A 86:5429-5433, 1989

4. Tanner MJ: The structure and function of band 3 (AE1): Recent developments. Mol Membr Biol 14:155-165, 1997

5. Bastani B, Gluck SL: New insights into the pathogenesis of distal renal tubular acidosis. Miner Electrolyte Metab 22:396-409, 1996

6. Chaabani H, Hadj-Khlil A, Ben-Dhia N, Braham H: The primary hereditary form of distal renal tubular acidosis: Clinical and genetic studies in 60-member kindred. Clin Genet 45:194-199, 1994

7. Brown MT, Cunningham MJ, Ingelfinger JR, Becker AN: Progressive sensorineural hearing loss in association with distal renal tubular acidosis. Arch Otolaryngol Head Neck Surg 119:458-460, 1993

8. Bajaj G, Quan A: Renal tubular acidosis and deafness: Report of a large family. Am J Kidney Dis 27:880-882, 1996

9. Bentur L, Alon U, Mandel H, Pery M, Berant M: Familial distal renal tubular acidosis with neurosensory deafness: Early nephrocalcinosis. Am J Nephrol 9:470-474, 1989

10. Karet FE, Finberg KE, Nelson RD, et al: Mutations in the gene encoding B1 subunit of H^+-ATPase cause renal tubular acidosis with sensorineural deafness. Nat Genet 21:84-90, 1999

11. Smith AN, Skaug J, Choate KA, et al: Mutations in *ATP6N1B*, encoding a new kidney vacuolar proton pump 116-kD subunit, cause recessive distal renal tubular acidosis with preserved hearing. Nat Genet 26:71-75, 2000

12. Bruce LJ, Cope DL, Jones GK, et al: Familial distal renal tubular acidosis is associated with mutations in the red cell anion exchanger (band 3, AE1) gene. J Clin Invest 100:1693-1707, 1997

13. Bruce LJ, Unwin RJ, Wrong O, Tanner MJ: The association between familial distal renal tubular acidosis and mutations in the red cell anion exchanger (band 3, AE1) gene. Biochem Cell Biol 76:723-728, 1998

14. Jarolim P, Shayakul C, Prabakaran D, et al: Autosomal dominant distal renal tubular acidosis is associated in three families with heterozygosity for the R589H mutation in the AE1 (band 3) $Cl^-/HCO3^-$ exchanger. J Biol Chem 273:6380-6388, 1998

15. Karet FE, Gainza FJ, Gyory AZ, et al: Mutations in the chloride-bicarbonate exchanger gene AE1 cause autosomal dominant but not autosomal recessive distal renal tubular acidosis. Proc Natl Acad Sci U S A 95:6337-6342, 1998

16. Tanphaichitr VS, Sumboonnanonda A, Ideguchi H, Shayakul C, Brugnara C, Takao M, Veerakul G, Alper SL: Novel AE1 mutations in recessive distal renal tubular acidosis. Loss-of-function is rescued by glycophorin A. J Clin Invest 102:2173-2179, 1998

17. Vasuvattakul S, Yenchitsomanus PT, Vachuanichsanong P, et al: Autosomal recessive distal renal tubular acidosis associated with Southeast Asian ovalocytosis. Kidney Int 56:1674-1682, 1999

18. Bruce LJ, Wrong O, Toye AM, et al: Band 3 mutations, renal tubular acidosis and South-East Asian ovalocytosis in Malaysia and Papua New Guinea: Loss of up to 95% band 3 transport in red cells. Biochem J 350:41-51, 2000

19. Wrong O, Davies H: The excretion of acid in renal disease. Q J Med 28:259-313, 1959

20. Sebastian A, McSherry E, Morris RCJ: Renal potassium wasting in renal tubular acidosis (RTA): Its occurrence in types 1 and 2 RTA despite sustained correction of systemic acidosis. J Clin Invest 50:667-678, 1971

21. Frischer H, Bowman J: Hemoglobin E, an oxidatively unstable mutation. J Lab Clin Med 85:531-539, 1975

22. Rees DC, Styles L, Vichinsky EP, Clegg JB, Weatherall DJ: The hemoglobin E syndromes. Ann N Y Acad Sci 850:334-343, 1998

ARTICLE IN PRESS

Available online at www.sciencedirect.com

SCIENCE DIRECT®

ELSEVIER

Immunology Letters 00 (2003) 1–6

Immunology Letters

www.elsevier.com/locate/

A flow cytometric method for enumeration of lymphocyte sub-populations in sample containing lysis-resistant red blood cells

Watchara Kasinrerk [a,b,*]

[a] Department of Clinical Immunology, Faculty of Associated Medical Sciences, Chiang Mai University, Chiang Mai 50200, Thailand
[b] Medical Biotechnology Unit, The National Center for Genetic Engineering and Biotechnology of the National Science and Technology Development Agency at the Faculty of Associated Medical Sciences, Chiang Mai University, Chiang Mai 50200, Thailand

Received 16 December 2002; accepted 18 February 2003

Abstract

Determination of lymphocyte sub-populations is usually carried out by flow cytometry using two-color immunophenotyping reagent. By this technique, however, the combination of FSC and SSC with CD45-FITC/CD14-PE is unable to identify the lymphocyte population in a sample containing lysis-resistant red blood cells (RBC). The actual values of lymphocyte sub-populations, therefore, cannot be determined in these RBC contaminated samples. To overcome this problem, we describe here the use of 7-aminoactinomycin D (7-AAD) to exclude lysis-resistant RBC from white blood cells (WBC). By adding 7-AAD, lymphocytes of samples containing RBC could be identified by using FL3/SSC, therefore, the actual number of lymphocyte sub-populations of the stained cells was obtained. We have proved that 7-AAD can be used to exclude contaminated RBC and has no effect on the measurement of lymphocyte sub-populations by using two-color immunophenotyping reagent. In routine blood samples that contain lysis-resistant RBC, 7-AAD markedly increased the purity of lymphocytes in the lymphocyte gate to >95% and the lymphocyte sub-populations therefore could be correctly determined. The described method is inexpensive, simple and gives successful analysis of lymphocyte sub-populations in a sample containing lysis-resistant RBC.

Keywords: Flow cytometry; 7-AAD; Lymphocyte sub-populations; Lysis-resistant RBC; Two-color staining

1. Introduction

Human immunodeficiency virus (HIV) is a retrovirus that infects cells those possess the CD4 receptor [1–3]. This infection causes the depletion of CD4+ lymphocytes, which is a major clinical finding in progressive infection [2–5]. In HIV infection, the absolute number of CD4+ lymphocytes is an important marker for prognosis, classification of the state of disease, treatment decision and monitoring of therapy [5–9]. Immunophenotyping using lysed whole blood stained with monoclonal antibody panels and analyzed by flow cytometry (FCM) is the current standard method [10,11]. The two-color immunophenotyping is a common method for determining CD4+ lymphocytes in routine laboratory. This technique includes the use of monoclonal antibody panels that contain appropriate monoclonal antibody combinations to enumerate CD3+, CD4+ and CD8+ lymphocytes. The two-color antibodies contain CD3-FITC/CD4-PE for quantitation of T and CD4+ lymphocytes and CD3-FITC/CD8-PE for T and CD8+ lymphocytes. The reagent also includes CD45-FITC/CD14-PE to establish and verify light scatter gating of lymphocytes. The fluorescein labeled isotype matched control mAbs for autofluorescence and non-specific binding are also included in this two-color reagent. By using this two-color reagent, blood cells are stained with the panels of mAbs and RBC are lysed by RBC lysing solution. The remaining WBC is then analyzed by FCM. The lymphocyte population is initially identified based on light scatter characteristics. The quality of the lymphocyte gate is validated by CD45 and CD14 markers. The CD3+, CD4+ and CD8+ lymphocytes in the gated lymphocyte population are then determined using FL1 and FL2

* Tel./fax: +66-53-946-043.
E-mail address: watchara@chiangmai.ac.th (W. Kasinrerk).

0165-2478/03/$ - see front matter © 2003 Published by Elsevier Science B.V.
doi:10.1016/S0165-2478(03)00047-6

channels. The advantages of the two-color reagent are that it can provide number of all T lymphocyte sub-populations that can be used for quality control of the measurement [10–13]. However, a potential problem with this method is that in some samples, particularly in blood samples obtained from AIDS patients on therapy, there may be considerable RBC contamination in the lymphocyte light scatter gate due to the presence of lysis-resistant RBC that scatter light like lymphocytes. If significant numbers of contaminated RBC are present in the acquisition lymphocyte gate, the obtained CD4+ and CD8− lymphocytes number will be erroneously decreased.

To overcome this problem, in the present report, a fluorescein dye 7-AAD [14,15] was used to discriminate RBC and WBC. 7-AAD intercalates between cytosine and guanine bases and is easily excited at 488 nm. The fluorescence emission of the dye has a peak at 670 nm and can be detected with FL3. In this study, 7-AAD was added to the samples that contained lysis-resistant RBC and analyzed by FCM. 7-AAD therefore stained WBC but not RBC and lymphocytes could be separated from the contaminated RBC and gated for the enumeration of CD3+, CD4+ and CD8+ lymphocytes. By adding 7-AAD, the actual percentages of CD3+, CD4+ and CD8−lymphocytes could be obtained. We demonstrated here that the 7-AAD can be used for determination of lymphocyte sub-populations in the sample presence of lysis-resistant RBC.

2. Materials and methods

2.1. Blood samples

Normal and HIV infected blood samples were obtained from the Medical Technology Service Center, Faculty of Associated Medical Sciences, Chiang Mai University, Chiang Mai, Thailand. Peripheral blood specimens were collected by venipuncture into K3EDTA-containing tubes (Becton Dickinson, San Jose, CA).

2.2. Antibodies and reagents

The two-color direct immunofluorescence reagent (Simultest) for enumeration of lymphocyte sub-populations was purchased from Becton Dickinson Immunocytometry System (San Jose, CA). This reagent contains four dual-fluorochrom conjugated monoclonal antibody pairs including CD45-FITC/CD14-PE, IgG1-FITC/IgG2b-PE (isotype matched control), CD3-FITC/CD4-PE and CD3-FITC/CD8-PE. 7-AAD was purchased from Sigma (St. Louis, MO) and dissolved in DMSO at a concentration of 10 mg/ml.

2.3. Immunofluorescence staining

Twenty microliters of each monoclonal antibody reagent pairs was added to 100 μl of whole blood in separated 12 × 75 mm test tubes. All tubes were gently mixed and incubated at room temperature for 15–30 min in the dark. Following the incubation period, 2 ml of RBC lysing solution (Becton Dickinson) was added and incubated for another 10 min. After centrifugation at 500 × *g* for 5 min and subsequent washing with 2 ml PBS containing 0.1% sodium azide, the cell pellets were resuspended in 0.5 ml of 1% paraformaldehyde in PBS. The stained cells were analyzed by a flow cytometer (FACScalibur, Becton Dickinson) using the Simulset software analysis program (Becton Dickinson).

To study the use of 7-AAD for exclusion of RBC, blood samples were stained using two-color reagent, as described above. Before flow cytometric analysis, 100 μl of 1% autologous RBC was added into all staining tubes. Five microliters of 12.5 μg/ml 7-AAD in PBS were then added into each tube and incubated at room temperature in the dark for 30 min. Then, the cells were analyzed by FCM using CellQuest software program (Becton Dickinson).

For enumeration of lymphocyte sub-populations in blood samples containing lysis-resistant RBC, blood specimens were stained using two-color reagent, as described above. Five microliters of 12.5 μg/ml 7-AAD in PBS was added into each tube and incubated at room temperature in dark for 30 min. Cells were analyzed by FCM using CellQuest software program (Becton Dickinson).

2.4. Flow cytometric analysis

Samples stained in two-color immunofluorescence were analyzed using Simulset software. A minimum of 2000 lymphocytes was initially acquired using CD45/CD14 tube. By this software, lymphocyte population was identified automatically based on the intensity of the CD45/CD14 immunofluorescence and a corresponding forward and side light scatter (FSC/SSC). The lymphocyte gate (lymphogate) was drawn. The purity of lymphocytes in the lymphogate is defined as the proportion of events within the gate that are lymphocytes. At least 2000 lymphocytes were acquired for other tubes after the CD45/CD14 tube. The isotype control tube determined non-specific binding and set marker for distinguishing fluorescence-negative and -positive cell populations. The CD3/CD4 and CD3/CD8 tubes were analyzed for the number of CD3+ and CD4+ lymphocytes and CD3+ and CD8+ lymphocytes, respectively, base on their FITC and PE fluorescence using FL1 and FL2, respectively. By this flow cytometric analysis, results were reported as the percentages of the lymphocyte sub-populations in total lymphocytes.

For CellQuest software, a minimum of 10,000 cells was measured for each 7-AAD added tube. By monitoring FL3 and SSC, RBC were gated out from the 7-AAD stained WBC having bright red fluorescence by the FL3 threshold. The remaining WBC was analyzed using FSC/SSC and lymphocyte population was gated according to their size and granularity. The percentages of CD3+, CD4+ and CD8+ lymphocytes were determined from the CD3/CD4 and CD3/CD8 tubes using FL1 and FL2.

3. Results

For measurement of CD4+ and CD8+lymphocytes by two-color immunophenotyping method, whole blood were stained with panels of monoclonal antibodies as described in Section 2. The lymphocyte population was gated according to their size and granularity using light scatter detectors (FSC/SSC). In general, RBC are removed by RBC lysing solution before flow cytometric analysis, thus very low number of non-lymphocytes will be observed in the lymphocyte gate (Fig. 1A). By the proper gating, the purity of lymphocytes in the gate will be >95%, as determined by the use of CD45-FITC and CD14-PE (Fig. 1B). Percentage of CD3+, CD4+ and CD8+ lymphocytes in the gate can then be determined using CD3-FITC/CD4-PE and CD3-FITC/CD8-PE (Fig. 1C, D).

However, in some blood samples, particularly in AIDS patients on treatment, there is RBC contamination in the lymphocyte light scatter gate (Fig. 2) due to the presence of lysis-resistant RBC that scatters light, similar to lymphocytes. By this contamination, the purity of lymphocytes in the gate will be reduced and therefore the percentage of lymphocyte sub-populations will be erroneously decreased.

In order to eliminate contaminated RBC in the lymphogate, in the present study, 7-AAD was used to discriminate nucleus containing WBC from non-nucleus containing RBC. To validate this approach, whole blood from ten donors were separated into two tubes. Both tubes were stained with CD45-FITC/CD14 PE reagent and RBC were lysed by lysing solution after staining. The first tube was analyzed after RBC lysis. For the second tube, RBC was re-added before analysis. As predicted, the purity of lymphocytes in the lymphocyte light scatter gate of the second tube was very low ($3.3 \pm 1.3\%$; mean $\pm$ S.D.) (Fig. 3B) compared to the first tube ($95 \pm 1.5\%$; mean $\pm$ S.D.) (Fig. 3A). Then, 7-AAD solution was added into the second tube and re-analyzed. For flow cytometric analysis after adding of 7-ADD, cells were acquired by CellQuest software using FL3/SSC. As WBC contains nucleus, but red blood cells do not, WBC were stained with 7-AAD. After excitation, WBC therefore emitted the fluorescence light that was detected by the FL3 detector. By using the appropriate FL3 threshold cut off, the non-7-AAD stained RBC were excluded (Fig. 3C). After acquisition, the acquired cells were analyzed using FSC and SSC. As shown in Fig. 3(D), the lymphocyte population could be easily gated with high purity ($97 \pm 1.1\%$; mean $\pm$ S.D.) as those obtained from the first tube (Fig. 3A). These results indicated that the 7-AAD could be used to eliminate RBC which were contaminated in the lymphocyte gate.

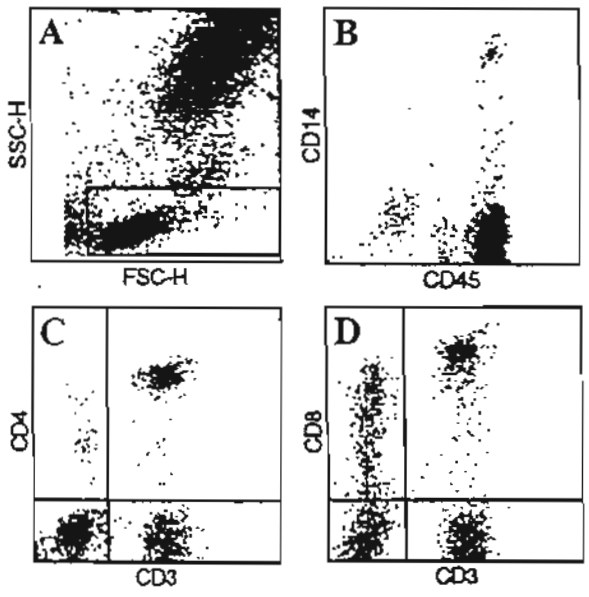

Fig. 1. Representative of two-parameter dot plot analysis of lysed whole blood stained with two-color immunophenotyping reagent (Simultest). Lymphocyte gate was established from FSC/SSC data acquisition (A), which corresponded to the bright CD45+/CD14− (B) using the SimulSet software. The CD3+, CD4+ and CD8+ lymphocytes were identified from CD3-FITC/CD4-PE (C) and CD3-FITC/CD8-PE tube (D).

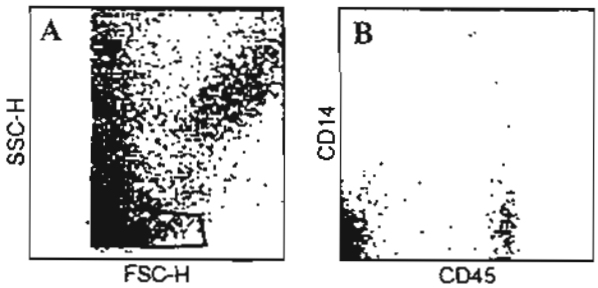

Fig. 2. Representative of two-parameter dot plot analysis of lysed whole blood of an AIDS patient stained with two-color immunophenotyping reagent (Simultest). The FSC/SSC dot plot shows the lymphocyte gate that contains a high proportion of lysis-resistant RBC (A). The CD45-FITC/CD14-PE dot plot indicated that the purity of lymphocytes in the lymphogate was very low (B).

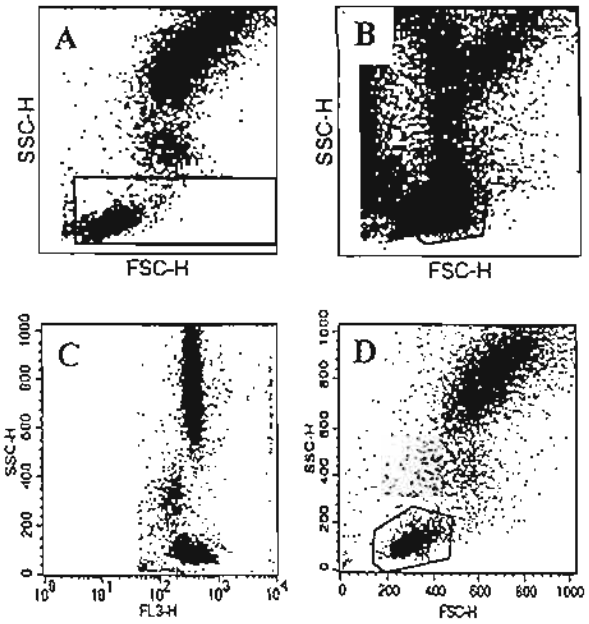

Fig. 3. Two-parameter dot plot analysis showing lysed whole blood before (A) and after adding RBC (B). After adding 7-AAD, the contaminated RBC could be eliminated using data acquisition from FL3/SSC (C) and lymphocytes could be identified from FSC/SSC detector (D).

To verify that the 7-AAD solution can be used to measure lymphocyte sub-populations in samples containing RBC, ten healthy and ten HIV infected blood samples were separated into three sets. In the first set, blood samples were stained with two-color reagent (Simultest) and RBC were lysed as standard method. The second set, cells were stained and RBC were lysed as the first set. Afterwards, RBC were re-added in to the tubes. The third set, cells were stained and RBC were lysed and RBC were re-added, as was carried out in the second tube and 7-AAD was subsequently added. All samples were acquired by flow cytometer and the percentage of CD3+, CD4+ and CD8+ lymphocytes in lymphogate was determined. In the second set, the purity of lymphocytes in lymphogate of all samples was very lower (> 10%), the percentages of CD3+, CD4+ and CD8+ lymphocytes therefore could not be determined. However, after adding 7-AAD (in the third set), the purity of lymphocytes in the lymphocyte gate recovered to the same level observed in the first set (> 95%). As predicted, the percentages of CD3+, CD4− and CD8− lymphocytes were comparable between the first and third sets, with the correlation coefficient of 0.998, 0.997 and 0.991, respectively (Fig. 4). The results demonstrated that the addition of 7-AAD could be used to eliminate RBC in the lymphogate and had no effect on the determination of lymphocyte sub-populations. After adding 7-AAD, the stained cells could be kept at 4 °C for up to 24 h before flow cytometric analysis (data not showed).

7-AAD solution was then used for the determination of CD3+, CD4+ and CD8+ lymphocytes in samples containing lysis-resistant red blood cells in routine laboratory ($n = 10$). Fig. 5 shows flow cytometric analysis of a blood sample before and after adding 7-AAD. Without 7-AAD, the lymphocytes could not be gated due to the contamination of RBC (% purity of lymphocytes = 28; Fig. 5A). The percentage of lymphocyte sub-populations, therefore, could not be precisely obtained from this sample. However, after adding of 7-AAD, the lymphocytes could be gated with 98% purity (Fig. 5B) and the percentages of CD3+, CD4+ and CD8− lymphocytes could be obtained (Fig. 5C, D). Our results demonstrate that the 7-AAD can be used for the determination of lymphocyte sub-populations in the sample presence of lysis-resistant RBC.

4. Discussion

The use of CD4+ lymphocyte measurements has had a significant impact on the diagnosis, monitoring and therapeutic control of HIV infection [5–9]. Immunophenotyping using lysed whole blood stained with two-color monoclonal antibody panels and analyzed by FCM is the current standard method for determination of CD4+ lymphocytes [10,11]. By this two-color immunophenotyping, the lymphocyte population are initially identified and gated according to their forward and side scatter characteristics [16]. The purity of the lymphocytes in the gate is validated by mAbs CD45-FITC and CD14-PE, which separates lymphocytes from granulocytes and monocytes based on the fluorescence patterns [17]. Then, CD4+ and CD8+ lymphocytes in the lymphocyte population are determined, using mAbs CD3-FITC/CD4-PE and CD3-FITC/CD8-PE according to their fluorescent staining patterns. By this analysis strategy, several guidelines addressing quality control for enumeration of lymphocyte sub-populations have been developed [10–13]. These include the use of monoclonal antibody panels that contain appropriate mAb combinations to determine CD4+ and CD8+ lymphocytes. In order to ensure the quality of the results, CD4+ and CD8+ lymphocytes must be identified as being positive for CD3/CD4 and CD3/CD8, respectively [12]. The isotype matched control mAbs have to be included for controlling autofluorescence and non-specific binding. In addition, mAbs CD45 and CD14 are included to establish and verify light scatter gating of lymphocyte populations. The purity of lymphocytes in the lymphocyte light scatter gate is important. A significant number of non-lymphocytes presented in the lymphocyte gate can lead to an erroneous decrease of CD4+ and CD8+ lymphocyte

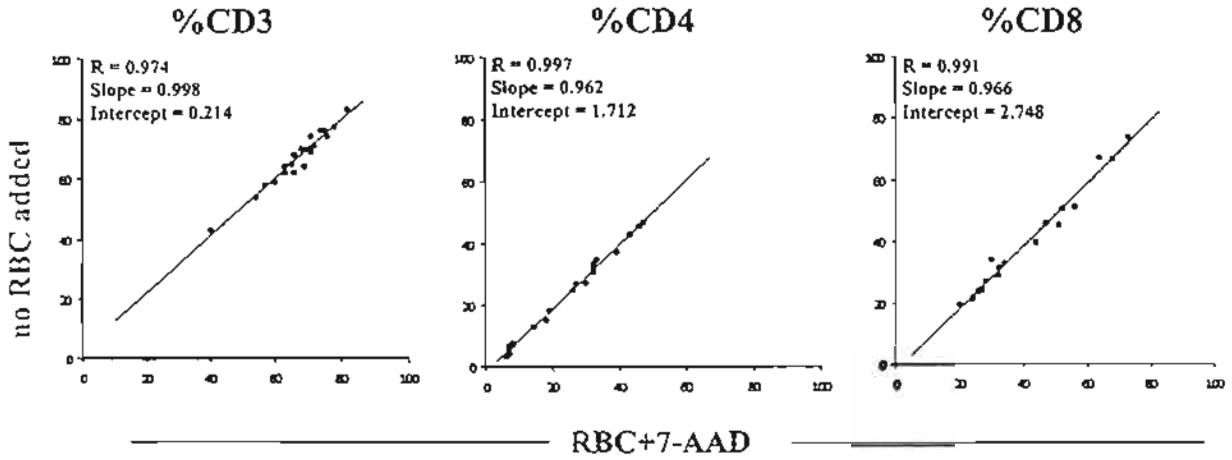

Fig. 4. Correlation of % CD3−, CD4+ and CD8+ lymphocytes obtained from lysed whole blood stained with two-color reagent (Simultest) between two experiments, without (no RBC) and with RBC plus 7-AAD (RBC+7-AAD). The correlation coefficient, slope and intercept of each comparison are depicted on the top left corner.

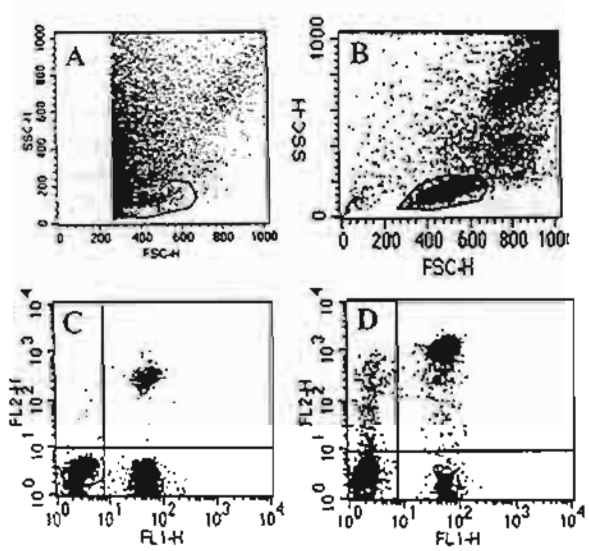

Fig. 5. Two-parameter dot plot analysis of lysed whole blood of an AIDS patient stained with two-color reagent (Simultest). The scattering of cells using FSC/SSC before (A) and after 7-AAD adding (B) is demonstrated. The CD3−, CD4− and CD8+ lymphocytes were identified from CD3-FITC/CD4-PE (C) and CD3-FITC/CD8-PE tube (D) after the addition of 7-AAD.

numbers. The obtained CD4+ and CD8+ lymphocyte values are, therefore, rejected if the purity of lymphocytes in the lymphogate in $<90\%$ [10,11]. Routinely, in some samples, particularly in AIDS patients on therapy, non-lymphocyte contamination in the lymphocyte gate may occur due to the presence of lysis-resistant RBC. The actual value of CD4+ lymphocyte, therefore, cannot be obtained from these samples.

7-AAD [14,15], a DNA binding fluorescein dye, is efficiently excited by the 488 nm laser line commonly used in FCM. After excitation, it yields fluorescence emission into the far red spectrum (≈ 650 nm) which can be detected by FL3. 7-AAD is excluded by viable cells but can penetrate cell membranes of dying or dead cells. As 7-AAD intercalates into double-stranded nucleic acid, therefore, this reagent is widely used for dead cell discrimination [14,15]. In this article, we have used 7-AAD to discriminate lysis-resistant RBC from WBC in the lymphocyte gate in the measurement of lymphocyte sub-populations. In our described method, whole blood was firstly stained with two-color monoclonal antibody panels and RBC was lysed by lysing solution that contain fixative. Then, 7-AAD was added into the stained cell suspension. By the RBC lysing solution, blood cell membrane was permeabilized and allowed 7-AAD to penetrate. As WBC, but not for RBC, contain nucleic acid, WBC were therefore stained with 7-AAD. On flow cytometric analysis, after excitation with 488 nm, WBC emitted 670 nm that could be detected by FL3. Thus, WBC could be separated from RBC according to their FL3 fluorescence patterns.

In our experiments, we first verified whether 7-AAD could be used for the exclusion of RBC contamination in the lymphocyte gate. Blood samples were separated into two tubes and stained with mAbs CD45-FITC/CD14-PE and RBC were lysed by lysing solution. The first tube was carried out as standard procedure, whereas in the second tube, RBC was re-filled into the tube. In the RBC re-filled tube, lymphocyte populations could not be identified because of the contamination of the added RBC. However, after adding 7-AAD, by using FL3/SSC, the lymphocyte populations could be distinguished and the FCS/SSC pattern of the lymphocyte after gating is similar to those obtained from the first set. These results indicated that 7-AAD can enter permeable fixed blood cells and stained WBC. There-

fore. WBC could be separated from RBC by their fluorescence emission spectrum.

7-AAD was used in the immunophenotyping of CD3+, CD4+ and CD8+ lymphocytes in blood samples containing RBC and compared to the same blood sample but no RBC contamination. The actual percentages of CD3+, CD4+ and CD8+ lymphocytes could be obtained from the RBC contaminated samples. These results imply that 7-AAD can be used to exclude of contaminated RBC and has no effect on the measurement of lymphocyte sub-populations. We have applied 7-ADD in the routine blood samples containing lysis-resistant RBC, which the lymphocyte sub-populations were unable to be determined. We demonstrated here that after adding 7-AAD, the number of lymphocyte sub-populations of these blood samples could be determined. In the same context, CD45 mAb conjugated with peridinin chlorophyll protein (PerCP) have been reported to exclude lysis-resistant RBC from lymphocyte population [11,12,18–20]. However, CD45-PerCP is more expensive than 7-AAD. The described technique in this article is very useful in routine laboratory. When using the standard method for determination of lymphocyte sub-populations, in any samples those containing lysis-resistant RBC and actual number of lymphocytes cannot be determined. By the addition of 7-AAD into the stained cells, the sample can be re-analyzed and then the lymphocyte sub-populations can be measured.

In conclusion, we have demonstrated here a flow cytometric analysis of lymphocyte sub-populations in blood samples containing lysis-resistant RBC. This technique is inexpensive and simple in the determination of lymphocyte sub-populations of samples that contain lysis-resistant RBC and cannot be analyzed with the existing standard two-color assay.

Acknowledgements

This work was supported by The Thailand Research Fund and The National Center for Genetic Engineering and Biotechnology (BIOTEC) of the National Science and Technology Development Agency. The author would like to thanks Waraporn Silakate for skilful technical assistance.

References

[1] F. De Wolf, M. Roos, J.M Lange, J.T. Houweling, R.A. Coutinho, J. van der Noordaa, et al., AIDS Res. Hum. Retrovir 4 () 433–440.
[2] J.V. Giorgi, P.G. Nishanian, I. Schmid, L.E. Hultin, H.L. Cheng, R. Detels, J. Clin. Immunol. 7 () 140–150
[3] W. Lang, H. Perkins, R.E. Anderson, R. Royce, N. Jewell, W Winkelstein, Jr. J. Acquir. Immune Defic. Syndr. 2 () 63–69.
[4] H. Masur, F.P. Ognibene, R. Yarchoan, J.H. Shelhamer, B.F Baird, W. Travis, et al., Ann. Intern. Med. 111 () 223–231.
[5] J.L. Fahey, J.M Taylor, R. Detels, B. Hofmann, R Melmed, P Nishanian, et al., New Engl. J. Med. 322 () 166–172.
[6] National Institutes of Health, Am. J. Med. 89 () 335–344.
[7] Centers for Disease Control, Guidelines for the performance of CD4+ T-cell determinations in persons with human immunodeficiency virus infection, MMWR Recomm. Rep. 41 (RR-8) (1992) 1–17.
[8] P.A. Volberding, S.W. Lagakos, M.A. Koch, et al., New Engl. J. Med. 322 () 941–949.
[9] S. Vella, M. Giuliano, L.G Dally, et al., J. Acquir. Immune Defic. Syndr. 7 () 31–38.
[10] National Committee for Clinical Laboratory Standards, Clinical applications of flow cytometry, quality assurance and immunophenotyping of peripheral blood lymphocytes, Tentative Guideline, NCCLS publication H42-T, Villanova, PA, 1992.
[11] J.K. Nicholson, Cytometry 18 () 55–59.
[12] Centers for Disease Control, Revised guidelines for performing CD4+ T-cell determinations in persons infected with human immunodeficiency virus (HIV), Centers for Disease Control and Prevention, MMWR Recomm Rep. 46 (RR-2) (1997) 1–29
[13] T. Calvelli, T.N. Denny, H. Paxton, R. Gelman, J. Kagan, Cytometry 14 () 702–715.
[14] T.J. Fetterhoff, S.P Holland, K.J. Wile, Cytometry 14 () 27–30.
[15] I. Schmid, W.J. Krall, C.H. Uittenbogaart, J. Braun, J.V. Giorgi, Cytometry 13 () 204–208.
[16] J.M. Thompson, J.R. Gralow, R. Levy, R.A. Miller, Cytometry 6 () 401–406.
[17] M.R. Loken, J.M. Brosnan, B.A. Bach, K.A. Ault, Cytometry 11 () 453–459.
[18] C.T. Schnizlein-Bick, F.F. Mandy, M.R. O'Gorman, H. Paxton J.K. Nicholson, L.E. Hultin, R.S. Gelman, C.L. Wilkening, D Levnat, Cytometry 50 () 46–52.
[19] K. Pattanapanyasat, V. Pengruangrojanachai, C. Thepthai, S. Suwanagool, C. Wasi, Asian Pac. J. Allergy Immunol. 12 () 105–109
[20] K. Pattanapanyasat, D.E. Kyle, P. Tongtawe, K. Yongvanitchit, S. Fucharoen, Cytometry 18 () 199–208.

nature
medicine

Original antigenic sin and apoptosis in the pathogenesis of dengue hemorrhagic fever

Juthathip Mongkolsapaya[1,2,7], Wanwisa Dejnirattisai[2,7], Xiao-ning Xu[1], Sirijitt Vasanawathana[3], Nattaya Tangthawornchaikul[4], Aroonrung Chairunsri[2], Siraporn Sawasdivorn[6], Thaneeya Duangchinda[1], Tao Dong[1], Sarah Rowland-Jones[1,5], Pa-thai Yenchitsomanus[2], Andrew McMichael[1], Prida Malasit[2,4] & Gavin Screaton[1,5]

Dengue virus presents a growing threat to public health in the developing world. Four major serotypes of dengue virus have been characterized, and epidemiological evidence shows that dengue hemorrhagic fever (DHF), the more serious manifestation of the disease, occurs more frequently upon reinfection with a second serotype. We have studied dengue virus–specific T-cell responses in Thai children. During acute infection, few dengue-responsive CD8⁺ T cells were recovered; most of those present showed an activated phenotype and were undergoing programmed cell death. Many dengue-specific T cells were of low affinity for the infecting virus and showed higher affinity for other, probably previously encountered strains. Profound T-cell activation and death may contribute to the systemic disturbances leading to DHF, and original antigenic sin in the T-cell responses may suppress or delay viral elimination, leading to higher viral loads and increased immunopathology.

Dengue is an arthropod-borne flavivirus that can be subdivided into four major serotypes (Den-1, Den-2, Den-3 and Den-4). Symptoms begin 5–7 d after a bite from an infected mosquito. Patients develop a high fever for 2–7 d, which corresponds to a period of high viremia[1]. When the fever remits on the defervescent day, defined as day 0, patients can get worse and in severe cases can develop shock. After defervescence the viral load falls to undetectable levels by 48 h, at which time the patient will generally begin to improve. The majority of infections are asymptomatic or cause a self-limiting febrile illness known as dengue fever. The more severe form of dengue infection, DHF, is characterized by high fever, hemorrhagic phenomena and plasma leakage, and may be life threatening. DHF is classified into four grades, the more severe of which (grades III and IV) are associated with dengue shock syndrome[2]. There are hundreds of thousands of cases of DHF each year, and without appropriate treatment mortality can be over 20%. With hospitalization and supportive care, mainly careful fluid management, this can be reduced below 1%.

The pathogenesis of DHF is not well characterized, but key epidemiological studies indicate that it often occurs when a dengue-immune person becomes secondarily infected with a virus of a different serotype[3,4], although severe disease on primary infection has been reported, particularly in neonates[5]. Halstead proposed a model of antibody-dependent enhancement whereby, upon secondary infection, pre-existing non-neutralizing antibodies may opsonize the virus and enhance its uptake and replication in macrophages. This has been shown to lead to higher viral loads both *in vitro* and in an *in vivo* primate model[6,7]. As was pointed out by the author of the *in vivo* study, however, an important challenge is to establish a connection between an infection of mononuclear cells and pathophysiologic changes[6].

To this end, others have suggested that the disease may be caused by T-cell activation; the levels of several cytokines such as tumor necrosis factor-α, as well as the magnitude of T-cell responses, have been correlated with disease severity[8,9]. So far, only a few peptide epitopes have been isolated for CD8⁺ cytotoxic T lymphocytes (CTLs). The latter have often been from Western volunteers who do not possess the common Asian human leukocyte antigen (HLA) types. To date, no well-defined epitopes have been defined for HLA-A*11, which is found in around 30% of the population in southeast Asia, or for the other common Asian HLA alleles A*24 (20%) or A*33 (15%)[10]. The lack of understanding of such epitopes has meant that dengue virus–specific CD8⁺ T-cell responses have not been studied over the time course of acute dengue.

RESULTS

Identification of a new HLA-A*11–restricted T-cell epitope

Because of the relatively small volume of blood samples available from acutely infected children, we decided to search for dengue CTL epitopes in healthy Thai adults, the majority of whom have been infected with dengue on one or more occasions. Previous studies have

[1]MRC Human Immunology Unit, Weatherall Institute of Molecular Medicine, John Radcliffe Hospital, Oxford, OX3 9DS, UK. [2]Medical Molecular Biology Unit, Faculty of Medicine, Siriraj Hospital, Mahidol University, Bangkok noi, Bangkok 10700, Thailand. [3]Pediatric Department, Khon Kaen Hospital, Ministry of Public Health, Khonkaen 40000, Thailand. [4]Medical Biotechnology Unit, National Center for Genetic Engineering and Biotechnology (BIOTEC), National Science and Technology Development Agency (NSTDA) Patumthani 12120, Thailand. [5]Nuffield Department of Medicine, John Radcliffe Hospital, Headington, Oxford, OX3 9DU, UK. [6]Queen Sirikit National Institute of Child Health, Bangkok 10400, Thailand. [7]These authors contributed equally to this work. Correspondence should be addressed to G.S. (screaton@molbiol.ox.ac.uk) or P.M. (sipml@mahidol.ac.th).

suggested that the envelope and NS3 proteins are frequent targets of immune responses in flavivirus infections, including dengue[11,12]. Peripheral blood mononuclear cells (PBMCs) from 20 healthy donors were screened with a panel of 210 overlapping peptides (15-mers overlapping by ten amino acids) spanning the envelope and NS3 proteins of dengue serotype 2 strain 16681. Pools of peptides were screened against PBMCs using an interferon (IFN)-γ Elispot assay. We found a T-cell response to peptide FSPGTSGSPIIDKKG (FSP), which covers NS3 residues 130–144, in two of the donors. Using a set of truncated peptides, the highest responses were found to the 11-mer peptide GTSGSPIIDKK (11GTS), although there were also responses to the 10-mer peptide GTSGSPIIDK (10GTS), truncated by one amino acid at the C terminus (Table 1a). Both of the donors expressed HLA-A*11 and the epitope conformed to the A11 consensus, which predicts peptides with a positively charged C-terminal anchor, frequently lysine, that are 10 or 11 residues in length. An FSP-specific CTL line was generated from one of the donors by stimulation with the FSP 15-mer peptide. This line was used to confirm the HLA restriction (Fig. 1a).

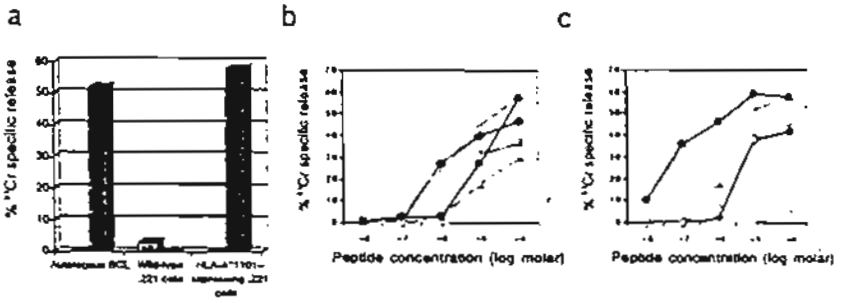

Figure 1 Defining a new HLA-A*11–restricted T-cell epitope. (a) HLA-A*1101 restriction of the GTSGSPIIDKK-specific response shown by a 4-h chromium-release assay using a GTS-specific CTL line from donor 1 (effector/target ratio = 10:1). Targets were an EBV-transformed autologous B-cell line (BCL), wild-type .221 cells and HLA-A*1101–expressing .221 cells pulsed with GTSGSPIIDKK (D2.1: ■) or no peptide (▣). (b,c) The FSP-specific CTL line was cocultured with a ^{51}Cr-labeled B-cell line (E/T ratio = 20:1) pulsed with 11-mers (b: D1.1 ( ), D2.1 (◆), D2.2 (▽), D2.3 (▲), D2.4 ( ) D3.1 (●) and D4.1(+)) and 10-mers (c: D1.1 ( ), D2.1 (◆), D2.2 (▽), D2.3 (▲), D2.4 ( ) or D3.1/D4.1(●)).

Variants of the HLA-A*11–restricted GTS epitope

In general there is a 30–40% difference in amino acid sequences between dengue serotypes, so we searched for variants of the GTS epitope among the published dengue NS3 sequences. Six variants were identified: three from Den-2 (D2.2, D2.3 and D2.4) and one each from the other serotypes (D1.1, D3.1 and D4.1; Table 1b). All of these variants were synthesized as 10- and 11-mers and tested on the FSP-specific T-cell line that had been generated by stimulation with the D2.1 epitope (Fig. 1b,c). All variants, apart from D2.4, stimulated T-cell responses at high concentrations, but there were marked differences in the titration curves, where the lower concentrations of peptide were probably more representative of the concentrations achieved *in vivo*. D2.4, which did not stimulate the cell line, has a relatively conservative alanine substitution at position 8. D1.1, D2.3 and D3.1 worked better as 10-mers than 11-mers (extra C-terminal amino acid), suggesting they were using the arginine at position 10 as the C-terminal anchor.

Different patterns of response during acute infection

Next, we studied responses in hospitalized children suffering an acute or current dengue virus infection. Samples were collected during the acute hospitalization phase and at the 2-week and 2-month follow-ups. Acute dengue infection was diagnosed by detection of the dengue viral genome from acute sera by RT-PCR or serological testing[13–16]. All but 2 of 73 patients were shown by serology to be suffering a secondary or sequential infection. The 19 patients expressing HLA-A*11 were included in this study; all had secondary infections, and 12 were infected with Den-1, 6 had Den-2 and 1 had Den-3 (Table 1c). The disease severity was classified according to World Health Organization guidelines[17].

PBMCs were screened with all dengue variant epitopes by IFN-γ Elispot assays. Unexpectedly, we found low or absent Elispot responses in samples taken during acute hospital admission. In contrast, all the follow-up samples taken at 2 weeks and 2 months gave responses (Fig. 2a,b and Supplementary Fig. 1 online). A similar pattern is seen in hepatitis C virus infection: antigen-specific T cells, although relatively prevalent, do not produce IFN-γ during an acute infection and the response returns 10 weeks later, after viral clearance[18]. Similarly, antigen-specific CD8$^+$ T cells in mice exposed to lymphocytic choriomeningitis virus (LCMV) proliferate rapidly at first and produce IFN-γ, but the cells later become 'stunned' and cease producing IFN-γ. Production of this cytokine is eventually regained, however[19,20].

The magnitude, timing, pattern of response and peptide titration curves to the variant peptides varied between patients. These results suggest that there is some cross-reactivity between the different epitopes but that the cross-reactivity is only partial. To gain further insight into this cross-reactivity, we did peptide titrations of fresh *ex vivo* PBMCs with the variant peptides. As expected, there were differences in the peptide titration curves, suggesting differences in functional avidity in dengue-specific T cells (Fig. 2c,d and Supplementary Fig. 2 online).

Using MHC class I tetramers to study the acute response

To study dengue-specific responses in more detail, we made class I major histocompatibility complex (MHC) peptide tetrameric complexes containing the following dengue variant peptide sequences: D2.2 10-mer, D1.1 11-mer and D3.1 10-mer (10-mers derived from D3.1 and D4.1 sequences are the same). FACS analysis showed that all tetramers stained the FSP CTL line (data not shown). Based on this and the Elispot results, the D3.1 10-mer was selected for further studies. Its specificity was confirmed by staining PBMCs taken from individuals that were HLA-A*11–positive and dengue-immune, HLA-A*11–positive and dengue-nonimmune, or HLA-A*11–negative and dengue-immune (Fig. 3a).

Acute and follow-up PBMCs from dengue-infected patients were then stained with the tetramers. The average of the relative frequencies of GTS-specific CD8$^+$ T cells is shown in Figure 3b. The responses peaked at 2 weeks and mirrored the results of the IFN-γ Elispot assay. Unlike the Elispot results, however, almost all of the patients had low but detectable levels (0.02–2.5%) of GTS-specific CD8$^+$ T cells during the acute phase. When we compared disease severity to the magnitude of the GTS-specific CD8$^+$ T-cell response at 14 d, we found that dengue-infected patients had higher circulating GTS-specific CD8$^+$ T cells than normal dengue-immune individuals (Fig. 3c). The three patients with dengue shock syndrome (DHF grade III) all had peak responses greater than 2% (mean ± s.d. was 4.26 ± 2.03; n = 3) com-

pared with patients with DHF grades I or II (mean ± s.d. was 0.84 ± 0.82; $n = 11$).

During the acute phase, the GTS-specific T cells showed an activated effector phenotype, with almost all of them expressing CD45RO, CD27, CD38 and HLA-DR, but not CCR7 (Supplementary Fig. 3 online). They also stained with Ki67, indicating that the cells were proliferating. As expected, the activation markers were reduced in the follow-up samples, which also showed a reduction in CD28 and some re-expression of CD45RA (Supplementary Fig. 3 online).

Massive apoptosis in dengue T cells

We were interested to determine why, in the early stages of the illness, the frequencies of antigen-specific T cells were so low in contrast to other virus infections such as HIV or Epstein-Barr virus[21]. Three possibilities exist: the cells may not have had time to proliferate fully, they may have been sequestered in peripheral tissues or lymphoid organs, or they may have been dying at an increased rate. PBMCs taken from eight patients were stained with tetramer followed by TUNEL (a marker for DNA fragmentation). During acute infection, the majority of GTS-specific T cells were TUNEL-positive (Fig. 4b). In contrast, fewer than 20% of tetramer-negative $CD8^+$ T cells were apoptotic. In the follow-up samples, a minority of $CD8^+$ T cells, both tetramer-positive and tetramer-negative, were positive for TUNEL staining. Costaining experiments showed that the GTS-specific T cells expressed little or no tumor necrosis factor receptor-1, death receptor-4 or death receptor-5 (data not shown). However, most of the GTS-specific T cells expressed the death receptor Fas and had low levels of the antiapoptotic protein Bcl-2 (Fig. 4c). It is usually difficult to detect circulating apoptotic cells, as they are very rapidly removed from the circulation. It is possible that there is a deficiency in the clearance of apoptotic cells in acute dengue virus infection.

The very high percentage of apoptotic cells detected here, combined with the expression of the proliferation marker Ki67 by 75–100% of cells (Fig. 4c and Supplementary Fig. 3 online), suggests that there is huge proliferation balanced by massive apoptosis in the acute setting. Apoptosis is reduced upon viral clearance, allowing a rebound in CTL numbers at 2 weeks, which reduces by 2 months as memory is established.

Table 1 Dengue NS3 peptides and patient details

a

Peptide sequence	SFCs per million PBMCs
FSPGTSGSPIIDKKG	92
GTSGSPIID	12
TSGSPIIDK	0
GTSGSPIIDKK	148
TSGSPIIDKK	4
PGTSGSPIIDK	0
GTSGSPIIDK	84

b

Variant	Dengue serotype	Sequence	Number of sequences found[a] per total[b]
D2.1	2	GTSGSPIIDKK	29/39
D2.2	2	GTSGSPIVDRK	6/39
D2.3	2	GTSGSPIVDKK	3/39
D2.4	2	GTSGSPIADKK	1/39
D1.1	1	GTSGSPIVNRE	5/5
D3.1	3	GTSGSPIINRE	2/2
D4.1	4	GTSGSPIINRK	2/2

c

Patient	Diagnosis	Serology	Dengue serotype	HLA class I type		
				A	B	C
K05	Dengue fever (DF)	Secondary	Den-1	11/33	44/58	3/7
K14	DF	Secondary	Den-1	11/24	13/40	3/7
K17	DF	Secondary	Den-1	11/02	46/–	1/1
K21	DF	Secondary	Den-1	11/30	15/35	4/4
K237	DF	Secondary	Den-1	11/02	15/55	7/8
K01	DHF grade I	Secondary	Den-1	11/29	7/18	7/15
K19	DHF grade I	Secondary	Den-2	11/02	13/15	4/8
K203	DHF grade I	Secondary	Den-1	11/24	27/40	7/15
K221	DHF grade I	Secondary	Den-1	11/02	27/40	3/7
K239	DHF grade I	Secondary	Den-2	11/02	40/40	3/7
K24	DHF grade II	Secondary	Den-2	11/24	27/51	3/14
K201	DHF grade II	Secondary	Den-1	11/24	15/46	1/8
K206	DHF grade II	Secondary	Den-1	11/68	27/40	8/8
K213	DHF grade II	Secondary	Den-2	11/24	27/40	3/15
K214	DHF grade II	Secondary	Den-3	11/24	46/51	1/14
K234	DHF grade II	Secondary	Den-1	11/24	35/46	1/4
K10	DHF grade III	Secondary	Den-2	11/2	15/15	8/8
K22	DHF grade III	Secondary	Den-1	11/2	27/46	1/12
K27	DHF grade III	Secondary	Den-2	11/2	18/46	1/7

(a) Truncated Den-2 peptides were used to define the optimum peptide. SFCs, spot-forming cells. (b) The sequence of D2.1 was used to search for variant dengue sequences published in GenBank. [a]Number of sequences found in GenBank. [b]Total number of GenBank-published NS3 sequences for each dengue serotype. (c) Summary of dengue-infected patients.

T-cell original antigenic sin during secondary infection

To search for serotype-specific and serotype–cross-reactive responses, we stained samples with pairs of variant tetramers (Fig. 5a and Supplementary Fig. 4 online) Although this double staining assay is more a measure of relative avidity than of absolute specificity, it clearly shows the existence of multiple dengue-specific T-cell populations in a single individual. The 10GTS-D3.1 tetramer was the most cross-reactive, confirming the Elispot data. Staining with either the D1.1 or D2.2 tetramers showed the existence of dual populations with high and low staining.

Particularly relevant is the finding that in secondary infection with Den-1, many of the T cells showed a preference for Den-3 tetramers, and in Den-2 infection, many of the cells reacted better with the Den-1 and Den-3 tetramers. The measurable tetramer response was low in the early acute samples and increased in the later samples, so these cells had clearly been stimulated to proliferate by the currently infecting

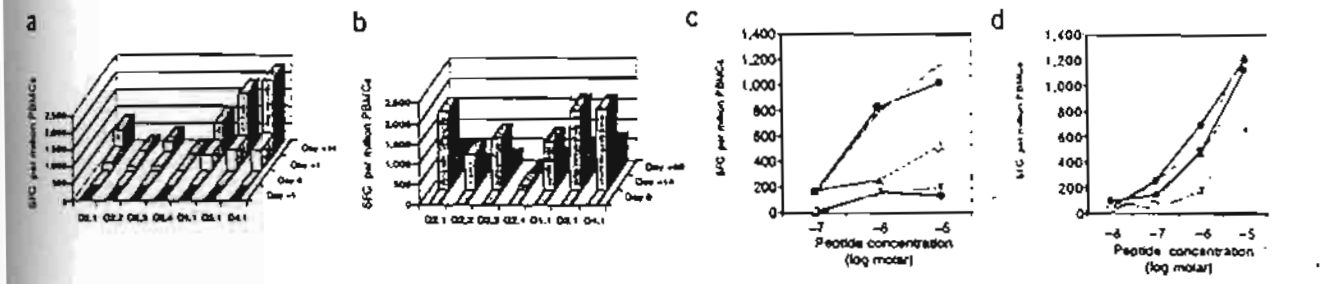

Figure 2 T-cell responses in dengue-infected patients. (a,b) PBMCs taken from dengue-infected patients K22 (a, Den-1 infection) and K10 (b, Den-2 infection) were stimulated with seven variant 11GTS epitope peptides (D2.1, D2.2, D2.3, D2.4, D1.1, D3.1 and D4.1). Samples were taken at the indicated time points. (c,d) PBMCs taken from dengue-infected patients K237 (c, Den-1 infection) and K27 (d, Den-2 infection) were stimulated with the indicated concentrations of variant 11GTS epitope peptides D1.1 ( ), D2.1 (◆), D2.2 (✕), D2.3 (▲), D3.1 (●) and D4.1 (+). Responses were measured as spot-forming cells (SFCs) per million PBMCs by IFN-γ Elispot assay.

virus. In other words, a single virus can stimulate the proliferation from memory of a spectrum of clones with different affinities and cross-reactivities. The finding that secondary infection with a virus carrying a similar but distinct epitope can stimulate the proliferation of cross-reacting, low-affinity clones is consistent with the phenomenon of original antigenic sin. We believe this is the first direct demonstration of this phenomenon in T cells for a human pathogen.

It would be interesting to know which viruses were responsible for the infections preceding the acute infection examined in this study. Unfortunately, the current methods to define this are not optimal and in many cases it is impossible to extract more information, above using PCR to identify the currently infecting virus and using serology to establish that the infection is secondary. Original antigenic sin has been reported for dengue antibody responses, and cross-reactivity in virus neutralization tests can sometimes allow deconvolution of a person's previous dengue exposure[22]. In an attempt to gain more information, we did virus serotype neutralization assays in which patient serum is used to inhibit infection by the four dengue serotypes of a monolayer on an LLC-MK2 cell line. The results of this analysis must be interpreted with caution, but they indicate that the patient with Den-1 infection (Fig. 5a and Supplementary Table 1 online) may have been exposed to at least Den-3, and the patient with Den-2 infection may have been exposed to Den-1, Den-3 or both.

Finally, to further show differences in structural avidity between dengue-specific T cells, we performed tetramer dissociation assays. In these assays, cells were incubated with saturating concentrations of phycoerythrin-labeled variant tetramers at 4 °C. The cells were then washed and incubated with an excess of unlabeled tetramer, and the rate of tetramer dissociation was assayed by fluorescence-activated cell sorting (FACS). Three representative examples of CTL lines are shown in Figure 5b. The assays show a spectrum of responses ranging from almost complete cross-reactivity to much lower cross-reactivity. The Den-2 tetramer dissociated faster than the Den-1 and Den-3 tetramers from cells derived (and cloned in the absence of peptide stimulation) from a patient with a current Den-2 infection. Scatchard analysis confirmed this finding, as the Den-2 tetramer showed a K_d of 10.6 μM, whereas Den-1 and Den-3 had K_d values of 1.6 and 1.2 μM, respectively (data not shown).

DISCUSSION

Dengue virus infections are now one of the biggest threats to public health in a number of developing countries. Over 2.5 billion people are at risk, and there are up to 50 million people infected per year. Epidemics are common in southeast Asia, South America and the western Pacific[2]. In addition to the mortality and morbidity associated with infection, dengue also imposes a considerable burden on the

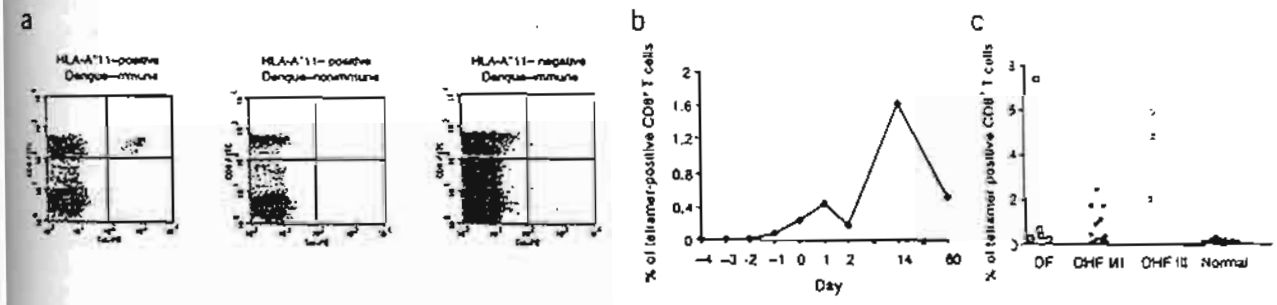

Figure 3 Analysis of responses using an HLA-A*11 tetramer. (a) Specificity of the GTS A11 tetramer. PBMCs were double-stained with phycoerythrin-conjugated GTS A11 tetramer (Tet-PE) and FITC-conjugated monoclonal antibody to CD8 (CD8-FITC). PBMCs were obtained from an HLA-A*11–positive, dengue-immune individual (left), an HLA-A*11–positive, dengue-nonimmune individual (center) or an HLA-A*11–negative, dengue-immune individual (right). (b) Mean frequency of GTS-specific CD8+ T cells during the course of acute dengue infection and follow-up. (c) Frequency of dengue GTS-specific CD8+ T cells at 14 d, from patients with different severities of disease (dengue fever (DF), DHF grades I and II, and DHF grade III) compared with the frequencies in 15 normal healthy individuals (mean ± s.d. of 1.18 ± 0.19 in patients versus 0.12 ± 0.1 in healthy individuals; Fisher's exact test P value = 0.0014).

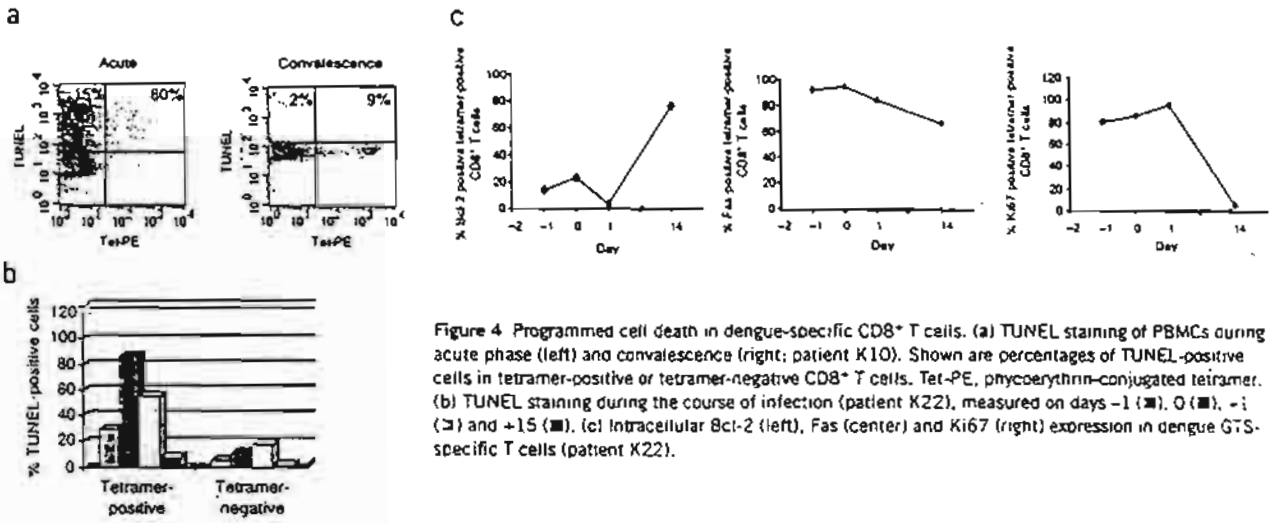

Figure 4 Programmed cell death in dengue-specific CD8+ T cells. (a) TUNEL staining of PBMCs during acute phase (left) and convalescence (right; patient K10). Shown are percentages of TUNEL-positive cells in tetramer-positive or tetramer-negative CD8+ T cells. Tet-PE, phycoerythrin-conjugated tetramer. (b) TUNEL staining during the course of infection (patient K22), measured on days −1 (■), 0 (■), +1 (□) and +15 (■). (c) Intracellular Bcl-2 (left), Fas (center) and Ki67 (right) expression in dengue GTS-specific T cells (patient K22).

finances and infrastructure of the health-care systems in these countries. Because of the scale of the problem, there is currently much interest in the generation of a dengue vaccine. These efforts have been hampered by two major factors: first, the lack of an animal model for severe dengue infection, and second, the epidemiological evidence for secondary infection in severe dengue. A better understanding of the pathogenesis of DHF would enhance our ability to develop safe vaccines, and would also expedite clinical trials by reducing their perceived risks.

In this study, we carried out a detailed analysis of a CTL response during acute dengue, and our results suggest an immunopathogenic role for T cells in DHF. Up to 7% of circulating CD8+ T cells react with the A11-restricted GTS epitope, and there is an association between the magnitude of the T-cell response and disease. The three patients with dengue shock syndrome (DHF grade III) all had peak responses of greater than 2% compared with 1 of 11 patients with DHF grades I and II, and 1 of 5 patients with dengue fever (Fisher's exact P value of 0.01 for dengue shock syndrome versus dengue fever and DHF grades I and II). These results are in agreement with a recent report showing a correlation between disease severity and T-cell responses to an HLA-B*07–restricted NS3 epitope[9].

A number of investigators have studied the potential for T cells to cause damage in animal models. Much of this work has been done in the mouse LCMV model. LCMV is a noncytopathic virus, but when an infection leads to a high antigen load combined with a large CTL response, immune damage to infected tissues can ensue[23]. There are a number of factors that can modify disease in this model, including viral dose and strain, previous infection, site of immunization or inoculation, age of the mice and presence of circulating antibodies[24].

Original antigenic sin was first shown for antibody responses, and implies that the response to a secondary challenge is dominated by the proliferation of cross-reacting memory cells induced by the primary infection, which may be of lower affinity for the secondary challenging antigen[25]. In this report we chose to use the term 'original antigenic sin' to denote the resurrection from memory of a response, without prejudice as to whether this will be to the benefit or the detriment of the host. Antigenic sin has the advantage that it can lead to the rapid

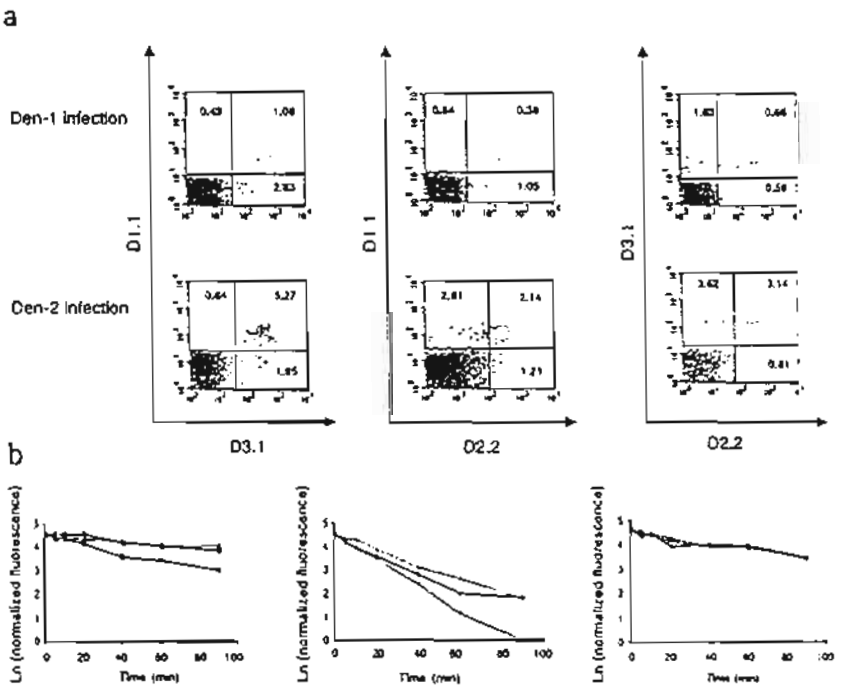

Figure 5 Differential avidities of T cells for dengue serotypes. (a) Double tetramer staining of three pairs of tetramers (D1.1/D2.2, D1.1/D3.1 and D2.2/D3.1) used to stain PBMCs from patients with acute Den-1 (K22) and Den-2 infection (K10). Plots represent double tetramer staining gated on CD8+ T cells. Percentage of cells is indicated in the three tetramer-positive quadrants. (b) Dissociation kinetics of the interaction between A1101-GTS D1.1 (◆), D2.2 (▼) or D3.1 (▲) tetramers with a GTS-specific CTL line derived from healthy donors 20 (left) and 12 (right) and a dengue-specific CTL line from patient K213 (center; Den-2 infection) cultured in the absence of peptide.

mobilization of a memory response, which in many instances may be advantageous. Memory cells have a much lower threshold for activation compared with naive cells[26], however, so there is a risk that clones activated by original antigenic sin may have lower affinity and be less effective at clearing the secondary challenge[27], and indeed may promote immunopathology.

Recently, original antigenic sin has been shown to occur in T cells upon infection of mice with related strains of LCMV[28]. In these experiments, reinfection with certain viral strains recalled the less-effective primary response to the detriment of a *de novo* response to secondary antigen, leading to impaired viral clearance[28]. In addition, infection with heterologous virus may recall a memory response to a different primary virus challenge. This may also alter immunopathology such as the fat necrosis, necrotizing bronchiolitis and bronchiolitis obliterans seen in LCMV-immune mice upon infection with vaccinia virus, although in this instance heterologous immunity enhanced viral control[29,30]. In dengue there is also the possibility of cross-reaction with other flaviviruses, as dengue cocirculates with Japanese encephalitis virus in southeast Asia and yellow fever virus in South America.

In dengue virus infection, there is a correlation between viral load and disease severity[1], and the high viral load has been attributed to antibody-dependent enhancement[4–7]. In this study, we saw expansion of T cells with relatively lower affinity for the currently infecting virus and higher affinity for serotypes presumed to be previously encountered. This skewing of the response could result from the detrimental effects of original antigenic sin. An alternative explanation would be that the high antigenic load associated with a second dengue infection, when immune enhancement occurs, may preferentially drive high-affinity T cells into apoptosis, which would increase the frequency of lower-affinity cells.

Dengue can also infect macrophages and dendritic cells, where it can proliferate and activate the dendritic cells[31,32]. The effects of antibody-dependent enhancement leading to high viral loads, together with enhanced antigen presentation, result in extensive T-cell activation. Acutely, the CTLs are stunned with low IFN-γ expression and, for the reasons described above, a relatively high proportion of the activated clones may be of lower affinity and may not be very effective at clearing virus, especially in the absence of IFN-γ [27,33], yet they may contribute to damage. A dynamic equilibrium is established between T-cell activation and proliferation and cell death. The activation and death of these cells leads to cytokine release and immune-mediated tissue damage, which has been shown to occur by provoking massive activation-induced cell death of $CD4^+$ and $CD8^+$ T cells in several mouse models[23,34].

In this study we have identified and studied a CTL response restricted by one of the major southeast Asian MHC class I subtypes. Larger studies will identify more CD8 epitopes, and it is reasonable to expect that some of these will be serotype-specific. If we can identify enough of these, it may be possible to incorporate them into a dengue vaccine that would improve safety by avoiding potential antibody enhancement or cross-reactivity in T-cell responses.

METHODS

Samples. Blood samples were taken after patient consent and approval from the ethical committee of Khonkaen hospital, Thailand, and normal healthy subjects from Bangkok. Acute dengue infection was identified by RT-PCR–based dengue gene identification or dengue-specific IgM capture ELISA and hemagglutination inhibition test against all four dengue serotypes[13–17]. Secondary dengue infection (an acute infection in a patient who had previously encountered dengue on one or more occasions) was defined as a dengue-specific IgM/IgG ratio < 1.8, by IgM and IgG capture ELISA, or a ≥4-fold rise in hemagglutination inhibition antibody titer against any dengue serotype in paired acute and convalescent sera[14–17]. Plaque-reduction neutralization tests were done as previously described[35]. Percent reduction of plaques was plotted against serum dilutions. The dilution giving 50% plaque reduction was reported as the neutralizing titer.

Disease severity was classified according to World Health Organization criteria[17]. Day of defervescence was defined as day 0, the day before defervescence as day −1, the day after defervescence as day +1, and so forth.

PBMCs were isolated from whole blood by Ficoll-Hypaque density gradient centrifugation and cryopreserved until tested. HLA typing was performed by sequence-specific primer PCR[36].

FACS analysis. PBMCs were stained with phycoerythrin-labeled tetramer at 37 °C for 20 min and then for surface markers at 4 °C for 20 min by addition of a panel of conjugated antibodies. CCR7 staining was indirect. For intracellular staining, tetramer-stained cells were fixed and permeabilized in FACS permeabilization buffer (BD Pharmingen). Apoptosis was assessed using the TUNEL assay according to the manufacturer's protocol (Roche).

Elispot assay and T-cell culture. Briefly, PBMCs were added to polyvinylidene difluoride–backed plates (Millipore) precoated with a monoclonal antibody to IFN-γ (1-DIK; MABTECH). Peptides were then added at a final concentration of 10 μM and the PBMCs were cultured overnight. Cells were discarded and spots were revealed by incubation with biotinylated monoclonal antibody to IFN-γ (MABTECH) followed by streptavidin-conjugated alkaline phosphatase and substrate. The spots were counted using an AID-Elispot Reader (Autoimmun Diagnostika). The number of specific T-cell responders was calculated after subtracting negative control values.

To generate the T-cell line, PBMCs were incubated with 100 μM of peptide for 1 h, after which IL-7 (Peprotech) was added at 25 ng/ml. After 3 d, IL-2 was added at 50 U/ml. Cells were tested for function after 1 week and restimulated every 2 weeks using autologous Epstein-Barr virus–transformed B-cell lines pulsed with peptide as targets. Chromium-release assays were done and specific ^{51}Cr release was calculated as [(experimental release − spontaneous release) ÷ (maximum release − spontaneous release)] × 100.

MHC tetrameric complexes. Tetramers were prepared as previously described[37]. Briefly, the extracellular domain of HLA-A*1101 (heavy chain) containing the BirA biotinylation enzyme recognition site at the C terminus and β2-microglobulin was expressed in *E. coli* as inclusion bodies. Monomeric complexes of peptide, heavy chain and β2-microglobulin (referred to here as 'monomers') were formed by refolding *in vitro* and then biotinylated using BirA (Avidity). Monomers were purified by fast-performance liquid chromatography, and tetramers were formed by mixing biotinylated monomer with fluorochrome-conjugated streptavidin at a 4:1 molar ratio. The tetramer dissociation assay was done as previously described[38,39]. Dengue-specific CTL lines were stained for 30 min at 4 °C with saturating concentrations of phycoerythrin-labeled tetramer. CTL lines were then washed three times and an aliquot of cells was removed for FACS analysis. The remaining PBMCs were incubated with a 100-fold excess of unlabeled tetramer at 4 °C to block the binding and rebinding of phycoerythrin-labeled tetramer. Further aliquots of cells were removed and analyzed by FACS at appropriate time points. The total fluorescence within the phycoerythrin-positive gate was plotted against time to give the dissociation curve. The total fluorescence is the sum of the fluorescence intensity of tetramer-positive cells normalized per lymphocyte. This was then normalized to the percentage of the total fluorescence at the initial time point and plotted on a logarithmic scale.

Scatchard analysis. The assay to estimate the apparent K_d values for the interaction between tetramer and peptide-specific CTL lines was done as previously described[38,39]. Dengue-specific CTL lines were stained for 3 h at ambient temperature (22 °C) with a range of subsaturating concentrations of phycoerythrin-labeled tetramer. CTL lines were then washed three times and analyzed by FACS. Tetramer concentration (μM) was plotted against bound tetramer (total fluorescence). In addition, Scatchard plots of bound tetramer (total fluorescence) versus bound tetramer/free tetramer (fluorescence units per μM) were plotted. Apparent K_d values were derived from the negative reciprocal of the slope of the line fit to Scatchard plots of bound tetramer versus bound tetramer/free tetramer.

Note: Supplementary information is available on the Nature Medicine website.

ACKNOWLEDGMENTS

We thank S. Chunharas at the National Health Foundation, Thailand; M. Mammen and A Nisalak at the Armed Forces Research Institute of Medical Science, Thailand; T. Roston and K. Digleria at the Medical Research Council Human Immunology Unit, UK; P. Pecpirin, O. Keawsrikaow, S. Jintasongthai, M. Mitchai, C. Ratchatane and S. Sima at Khonkhaen Hospital, Thailand; Sasithorn Bejrachandra Siriraj Hospital, Thailand; and M. Callan and P. Klenerman for useful discussion. This work was supported by the Medical Research Council UK (J.M., X.X., T.D., S.R.J., A.M and G.S.), the Senior Research Scholar Program of the Thailand Research Fund (P.M.), a Royal Golden Jubilee Award from the Thailand Research Fund (W.D.) and the Royal Thai Government Doctoral Scholarship (T.D.).

COMPETING INTERESTS STATEMENT

The authors declare that they have no competing financial interests.

Received 24 January; accepted 15 May 2003
Published online 15 June 2003; doi:10.1038/nm887

1. Vaughn, D.W. *et al.* Dengue viremia titer, antibody response pattern, and virus serotype correlate with disease severity. *J. Infect. Dis.* 181, 2–9 (2000).
2. Fact sheet no. 117: Dengue and dengue haemorrhagic fever (World Health Organization, Geneva, 2002).
3. Sangkawibha, N. *et al.* Risk factors in dengue shock syndrome: a prospective epidemiologic study in Rayong, Thailand. I. The 1980 outbreak. *Am. J. Epidemiol.* 120, 653–669 (1984).
4. Guzman, M.G. *et al.* Epidemiologic studies on dengue in Santiago de Cuba, 1997. *Am. J. Epidemiol.* 152, 793–799 (2000).
5. Halstead, S.B. *et al.* Dengue hemorrhagic fever in infants: research opportunities ignored. *Emerg. Infect. Dis.* 8, 1474–1479 (2002).
6. Halstead, S.B. *In vivo* enhancement of dengue virus infection in rhesus monkeys by passively transferred antibody. *J. Infect. Dis.* 140, 527–533 (1979).
7. Halstead, S. & O'Rourke, E. Antibody-enhanced dengue virus infection in primate leukocytes. *Nature* 265, 739–741 (1977).
8. Rothman, A.L. & Ennis, F.A. Immunopathogenesis of dengue hemorrhagic fever. *Virology* 257, 1–6 (1999).
9. Zivna, I. *et al.* T cell responses to an HLA-B*07-restricted epitope on the dengue NS3 protein correlate with disease severity. *J. Immunol.* 168, 5959–5965 (2002).
10. Chandanayingyong, D. *et al.* HLA-A, -B, -DRB1, -DQA1, and -DQB1 polymorphism in Thais. *Hum. Immunol.* 53, 174–182 (1997).
11. Kurane, I. & Ennis, F.A. Cytotoxic T lymphocytes in dengue virus infection. *Curr. Top. Microbiol. Immunol.* 189, 93–108 (1994).
12. Mathew, A. *et al.* Dominant recognition by human CD8+ cytotoxic T lymphocytes of dengue virus nonstructural proteins NS3 and NS1.2a. *J. Clin. Invest.* 98, 1684–1691 (1996).
13. Yenchitsomanus, P.T. *et al.* Rapid detection and identification of dengue viruses by polymerase chain reaction (PCR). *Southeast Asian J. Trop. Med. Public Health* 27, 228–236 (1996).
14. Vorndam, V., & Kuno, G. Laboratory diagnosis of dengue virus infections. in *Dengue and Dengue Hemorrhagic Fever* (eds. Gubler, D.J., & Kuno, G.) 313–333 (Cabi Publishers, Wallingford, UK, 1997).
15. Innis, B.L. *et al.* An enzyme-linked immunosorbent assay to characterize dengue infections where dengue and Japanese encephalitis co-circulate. *Am. J. Trop. Med. Hyg.* 40, 418–427 (1989).
16. Clarke, D.H. & Casals, J. Techniques for hemaggutination and hemagglutination inhibition with arthropod-borne viruses. *Am. J. Trop. Med. Hyg.* 7, 561–573 (1958).
17. Dengue haemorrhagic fever: diagnostic, treatment, prevention and control (World Health Organization, Geneva, 1997).
18. Lechner, F. *et al.* Analysis of successful immune responses in persons infected with hepatitis C virus. *J. Exp. Med.* 191, 1499–1512 (2000).
19. Zajac, A.J. *et al.* Viral immune evasion due to persistence of activated T cells without effector function. *J. Exp. Med.* 188, 2205–2213 (1998).
20. Gallimore, A. *et al.* Induction and exhaustion of lymphocytic choriomeningitis virus-specific cytotoxic T lymphocytes visualized using soluble tetrameric major histocompatibility complex class I-peptide complexes. *J. Exp. Med.* 187, 1383–1393 (1998).
21. Appay, V. *et al.* Memory CD8+ T cells vary in differentiation phenotype in different persistent virus infections. *Nat. Med.* 8, 379–385 (2002).
22. Halstead, S.B., Rojanasuphot, S. & Sangkawibha, N. Original antigenic sin in dengue. *Am. J. Trop. Med. Hyg.* 32, 154–156 (1983).
23. Aichele, P. *et al.* Peptide antigen treatment of naive and virus-immune mice: antigen-specific tolerance versus immunopathology. *Immunity* 6, 519–529 (1997).
24. Klenerman, P. & Zinkernagel, R.M. What can we learn about human immunodeficiency virus infection from a study of lymphocytic choriomeningitis virus? *Immunol. Rev.* 159, 5–16 (1997).
25. Fazekas de St. G. & Webster, R.G. Disquisitions of original antigenic sin. I. Evidence in man. *J. Exp. Med.* 124, 331–345 (1966).
26. Veiga-Fernandes, H., Walter, U., Bourgeois, C., McLean, A. & Rocha, B. Response of naive and memory CD8+ T cells to antigen stimulation *in vivo*. *Nat. Immunol.* 1, 47–53 (2000).
27. Alexander-Miller, M., Leggatt, G. & Berzofsky, J. Selective expansion of high- or low-avidity cytotoxic T lymphocytes and efficacy for adoptive immunotherapy. *Proc. Natl. Acad. Sci. USA* 93, 4102–4107 (1996).
28. Klenerman, P. & Zinkernagel, R.M. Original antigenic sin impairs cytotoxic T lymphocyte responses to viruses bearing variant epitopes. *Nature* 394, 482–485 (1998).
29. Chen, H.D. *et al.* Memory CD8+ T cells in heterologous antiviral immunity and immunopathology in the lung. *Nat. Immunol.* 2, 1067–1076 (2001).
30. Selin, L.K., Varga, S.M., Wong, I.C. & Welsh, R.M. Protective heterologous antiviral immunity and enhanced immunopathogenesis mediated by memory T cell populations. *J. Exp. Med.* 188, 1705–1715 (1998).
31. Wu, S.J. *et al.* Human skin Langerhans cells are targets of dengue virus infection. *Nat. Med.* 6, 816–820 (2000).
32. Libraty, D.H., Pichyangkul, S., Ajariyakhajorn, C., Endy, T.P. & Ennis, F.A. Human dendritic cells are activated by dengue virus infection: enhancement by gamma interferon and implications for disease pathogenesis. *J. Virol.* 75, 3501–3508 (2001).
33. Von Herrath, M., Coon, B. & Oldstone, M. Low-affinity cytotoxic T-lymphocytes require IFN-gamma to clear an acute viral infection. *Virology* 229, 349–349 (1997).
34. Combadiere, B., Sousa, C.R., Germain, R.N. & Lenardo, M.J. Selective induction of apoptosis in mature T lymphocytes by variant T cell receptor ligands. *J. Exp. Med.* 187, 349–355 (1998).
35. Russell, P.K., Nisalak, A., Sukhavachana, P. & Vivona, S. A plaque reduction test for dengue virus neutralizing antibodies. *J. Immunol.* 99, 285–290 (1967).
36. Krausa, P., Barouch, D., Bodmer, J.G. & Browning, M.J. Rapid characterization of HLA class I alleles by gene mapping using ARMS PCR. *Eur. J. Immunogenet.* 22, 283–287 (1995).
37. Altman, J.D. *et al.* Phenotypic analysis of antigen-specific T lymphocytes. *Science* 274, 94–96 (1996).
38. Savage, P., Boniface, J. & Davis, M. A kinetic basis for T cell receptor repertoire selection during an immune response. *Immunity* 10, 485–492 (1999).
39. Davenport, M., Fazou, C., McMichael, A. & Callan, M. Clonal selection, clonal senescence, and clonal succession: the evolution of the T cell response to infection with a persistent virus. *J. Immunol.* 168, 3309–3317 (2002).

ELSEVIER

Journal of Virological Methods 109 (2003) 55–61

Journal of Virological Methods

www.elsevier.com/locate/jviromet

Production of anti-dengue NS1 monoclonal antibodies by DNA immunization

Chunya Puttikhunt [a], Watchara Kasinrerk [a,b], Supa Srisa-ad [a], Thaneeya Duangchinda [a], Waraporn Silakate [b], Seangdeun Moonsom [b], Nopporn Sittisombut [a,c], Prida Malasit [a,d,*]

[a] *Medical Biotechnology Unit, National Center for Genetic Engineering and Biotechnology (BIOTEC), National Science and Technology Development Agency, Bangkok 10700, Thailand*

[b] *Department of Clinical Immunology, Faculty of Associated Medical Sciences, Chiang Mai University, Chiang Mai 50200, Thailand*

[c] *Department of Microbiology, Faculty of Medicine, Chiang Mai University, Chiang Mai 50200, Thailand*

[d] *Division of Medical Molecular Biology, Office for Research and Development, Faculty of Medicine, Siriraj Hospital, 12th floor Adulyadej-Vikrom building, Mahidol University, Bangkok 10700, Thailand*

Received 11 April 2002; received in revised form 7 January 2003; accepted 8 January 2003

Abstract

Monoclonal antibodies against dengue NS1 protein were generated following immunization of mice with plasmid DNA encoding the transmembrane form of NS1 from dengue serotype 2 virus. A mammalian expression vector, pDisplay, was engineered to direct cell surface expression of dengue NS1 and tested for transient expression in COS cells. Two mice were immunized intramuscularly with six doses of 100 μg of plasmid at 2-week intervals; one mouse received a booster of live virus prior to the last plasmid injection. Both mice showed antibody responses against dengue antigens in dot enzyme immunoassay. Following fusion, hybridomas were screened with dot enzyme immunoassay against all four dengue serotypes. Specificity to the NS1 protein was confirmed by western blot analysis. Among five anti-dengue NS1 monoclonal antibodies generated, two clones were serotype 2 specific, two clones reacted with all four serotypes and the last also reacted with Japanese encephalitis virus. Reactivity against native or denatured forms of NS1 revealed three clones with reactivity to linear epitopes and two clones recognizing conformational epitopes. Such diverse specificity of anti-dengue NS1 monoclonal antibodies indicates that DNA immunization, especially with the combination of virus boosting, is an efficient way of producing monoclonal antibodies against viral protein. This has opened up a possibility of producing monoclonal antibodies to rare viral proteins that are difficult to isolate or purify.

Keywords: NS1 protein; DNA immunization; Monoclonal antibody; Dengue virus

1. Introduction

Dengue virus contains a positive polarity, single-stranded RNA genome of approximately 11 kb in length. A single polyprotein was co-translationally processed by viral and cellular proteases into three structural proteins: capsid, prM, and envelope (E), and seven non-structural proteins; NS1, NS2a, NS2b, NS3, NS4a, NS4b and NS5 (Chang, 1997). Existing monoclonal antibodies against the dengue proteins available worldwide are mainly those directed against E, NS1 and prM proteins. These clones were obtained by immunization with either dengue virus or dengue recombinant proteins (Falconar and Young, 1991; Gentry et al., 1982; Henchal et al., 1987; Kaufman et al., 1989, 1987; Pupo_Antunez et al., 2001; Roehrig et al., 1998). Antibodies against other dengue proteins are rare, partly due to the difficulties in preparing adequate quantity of antigens for immunization.

During the 1990s, in vivo expression of genes encoding exogenous proteins in mice and its efficiency in inducing specific antibody responses following naked DNA injection were reported (Tang et al., 1992; Wolff et al., 1990). As an alternative approach to the genera-

* Corresponding author. Tel./fax: +66-2418-4793.
E-mail address: sipml@mahidol.ac.th (P. Malasit).

0166-0934/03/$ - see front matter
doi:10.1016/S0166-0934(03)00045-4

tion of immune response. DNA immunization has been shown to elicit both cellular and humoral immunity against several infectious pathogens as well as allergens and cancers (Hasan et al., 1999). Its advantages and proposed mechanisms of enhancing immunity have been extensively reviewed (Hasan et al., 1999; Hassett and Whitton, 1996; Whitton et al., 1999). When compared with conventional vaccines, DNA vaccine is safer (from lacking a replicative agent), relatively cheap to produce, heat stable, amenable to genetic manipulation and capable of inducing long-term cellular immunity (Gurunathan et al., 2000). In flaviviruses, DNA vaccines against Dengue 2 virus (Porter et al., 1998), Murray Valley encephalitis virus (Colombage et al., 1998), St Louis encephalitis virus (Phillpotts et al., 1996) and Japanese encephalitis virus (Konishi et al., 1998) were shown to be efficient in inducing antibody responses and induced full or partial protection in mice against virus challenge.

Besides vaccine application, DNA immunization strategy can be another efficient method for the purpose of production of polyclonal and monoclonal antibodies (Barry et al., 1994; Kasinrerk and Tokrasinwit, 1999; Kasinrerk et al., 1997, 1996; Moonsom et al., 2001; Ulivieri et al., 1996). In the present study, we attempted to use DNA immunization for the generation of monoclonal antibodies against a dengue non-structural protein and we demonstrated that plasmid DNA containing gene encoding dengue viral NS1 protein could be efficiently used to produce anti-NS1 monoclonal antibodies. The antibodies are reactive to different epitopes similar to those produced by conventional immunization using viral or purified antigens.

2. Materials and methods

2.1. Cell lines and hybridomas

COS seven cells were maintained in Minimum Essential Medium (MEM; Gibco-BRL, Grand Island, NY) supplemented with 10% fetal bovine serum (FBS) (Gibco-BRL) and 40 μg/ml gentamicin and 2.5 μg/ml amphotericin B in a humidified atmosphere of 5% CO_2 at 37 °C. PS clone D cells were maintained in L-15 media (Gibco-BRL) containing 10% FBS, 10% tryptose phosphate broth (Gibco-BRL) and 1.2% streptomycin and penicillin antibiotics (Sigma, St.Louis, MO, USA) at 37 °C. C6/36 cells were maintained in the same media as PS clone D but were incubated at 28 °C. During dengue virus infection of C6/36 and PS clone D cells, FBS content in L-15 media was reduced to 1%.

Hybridoma clones 1B2 (specific for dengue NS1), 4G2 and 3H5 (specific for dengue E) and 2H2 (specific for dengue prM) were grown in RPMI 1640 media (Gibco-BRL) containing 10% FBS and 1.2% streptomycin and penicillin antibiotics (Sigma) at 37 °C in 5% CO_2.

2.2. Viruses

Dengue viruses serotype 1 (strain Hawaii), serotype 2 (strain 16681), serotype 3 (strain H87) and serotype 4 (strain H241) were propagated in C6/36 mosquito cell line. Culture supernatant containing dengue virions as well as secreted NS1 protein was harvested 4–5 days after infection. Japanese encephalitis virus (strain Nakayama) was obtained from Dr Ananda Nisalak, Armed Forces Research Institute of Medical Sciences, Bangkok, Thailand and propagated in C6/36 cells.

2.3. Construction of recombinant plasmid

A 1056-bp NS1 gene segment was obtained by *Bam*HI/*Sal*I double digestion from a pMal/NS1 plasmid, which has been constructed from reverse transcriptase–polymerase chain reaction product of dengue type two virus NGC strain (S. Pattanakitsakul, unpublished data), ligated into the *Bgl*II/*Sal*I site of a mammalian expression vector pDisplay (Invitrogen, Carlsbad, CA) and transformed into DH5αF′. Selection of *E. coli* colonies containing the recombinant plasmid, pDisplay/sNS1tm, was performed by colony polymerase chain reaction and restriction enzyme digestion. The pDisplay/sNS1tm plasmid was extracted and purified by Qiagen plasmid purification kit (Qiagen, Hilden, Germany).

2.4. DEAE–dextran mediated transfection

COS cells were plated in a 60-mm tissue culture dish (Nunc, Roskilde, Denmark) at 7.5×10^5 cells/dish and incubated in 5% CO_2 at 37 °C for 24 h culture media was removed and cells were transfected with 2 ml of MEM containing 250 μg/ml DEAE-dextran (Sigma), 400 μM chloroquine diphosphate (Sigma) and 5 μg plasmid DNA for 3 h at 37 °C in 5% CO_2. Supernatant was removed and cells were treated with 10% dimethyl sulfoxide in phosphate buffered saline (PBS) for 2 min at room temperature. Cells were then washed once with MEM, replaced with MEM containing 10% FBS and incubated in a 5% CO_2 incubator at 37 °C. The culture media was changed on the next day. Transfected cells were harvested at 62 h after transfection and assayed for the expression of dengue NS1 by indirect immunofluorescence.

2.5. Indirect immunofluorescence assay

Transfected COS cells were detached from culture dish using PBS containing 0.5 mM EDTA and washed twice with PBS containing 1% bovine serum albumin

and 0.02% sodium azide. Cells were then incubated with known anti-dengue NS1 monoclonal antibody for 30 min on ice. After washing, cells were incubated with rabbit anti-mouse immunoglobulin-FITC conjugate (Dako, Glostrup, Denmark) for 30 min. Membrane fluorescence was detected using a fluorescence microscopy (Olympus, Tokyo, Japan).

2.6. Western blot analysis

Transfected COS cells were harvested and resuspended in PBS. Cells were lysed in 4 × reducing sample buffer and heated at 95 °C for 5 min. Cell lysate was then separated with 10% SDS-PAGE and blotted onto nitrocellulose membrane. The membrane was blocked with 5% skimmed milk in PBS and reacted successively with 1B2 monoclonal antibody and horse radish peroxidase-conjugated rabbit anti-mouse immunoglobulins (Dako). The antigen–antibody complex was visualized with H_2O_2 and diaminobenzidine.

Reactivity of hybridoma culture supernatants against different forms of NS1 was determined by western blot analysis. Dengue serotype 2-infected C6/36 cells were lysed with 1% Triton X-100 in PBS. Prior to electrophoretic separation, cell lysate was either not treated or subjected to 2-mercaptoethanol treatment at room temperature or at 95 °C for 5 min. Subsequent steps in electrophoresis, blotting and immunological reactions were as described above.

2.7. DNA immunization and hybridoma generation

Two 6-week-old, female Balb/c mice were injected with 50 μl of 1 mg/ml pDisplay/sNS1tm into each hind leg for five times with 2-week interval. One mouse was given the last inoculation with the same dose of plasmid DNA whereas the other received 100 μl of live dengue two virus (5×10^5 pfu/ml) and then followed by plasmid DNA as the last immunization dose 2 weeks later. Blood samples were collected just prior to the first immunization and at 2 weeks after each injection by tail bleeding. Mouse sera were separated and stored at −20 °C. Seven days after the last immunization, mice were sacrificed and spleen cells were fused with P3-X63Ag8.653 myeloma cells using 50% polyethylene glycol (Sigma). After HAT medium selection, culture supernatants were analyzed for antibody reactivity against viral protein using cell-ELISA and dot enzyme immunoassay. Hybridomas were cloned by limiting dilution and their isotypes determined by using mouse monoclonal ELISA isotyping kit (Sigma).

2.8. Cell-ELISA

PS clone D cells (5×10^4 cells in 100 μl) were plated into a 96-well tissue culture plate, infected with dengue serotype 2 virus at the multiplicity of infection of 1.0. After 24 h of incubation at 37 °C, cells were washed with PBS, fixed with 3.7% formaldehyde for 10 min, and permeabilized with 1% Triton X-100. Anti-dengue antibodies in mouse sera or hybridoma supernatants were detected by adding 50 μl of diluted mouse sera or neat supernatant into permeabilized PS monolayer in both infected wells and mock-infected wells and incubated for 1 h at room temperature. Cells were washed three times with PBS containing 0.05% Tween-20 and reacted with rabbit anti-mouse immunoglobulins-horse radish peroxidase conjugate (Dako). Following additional washing steps, H_2O_2 and OPD were added and the reaction was stopped with 4 N H_2SO_4. Optical density was spectrophotometrically determined at 492 nm. Reactivity of all tested samples was subtracted with mean optical density value of mock-infected wells and the corrected value of 0.100 or greater was considered positive. Known monoclonal antibodies against dengue E protein (4G2 and 3H5), NS1 protein (1B2) as well as prM protein (2H2) was included in every cell-ELISA plate.

2.9. Dot enzyme immunoassay

For hybridoma screening assay, a mixture of culture supernatants of C6/36 cells infected with each of the four dengue serotypes and mock-infected supernatant were dotted onto nitrocellulose membrane, blocked with 5% skimmed milk in PBS and reacted with mouse sera (1:50 dilution) or hybridoma supernatants (1:5 dilution) and incubated for 1 h at 37 °C. After washing with PBS, bound antibody was detected with rabbit anti-mouse immunoglobulins-horse radish peroxidase conjugate (Dako) and H_2O_2–diaminobenzidine–0.04% $NiCl_2$ mixture. Positive reaction appeared as dark brown dot on the membrane was graded from 0, 1+, 2+, 3+ and 4+. For determining the cross reactivity of the anti-NS1 monoclonal antibodies, the antibodies were tested against a nitrocellulose membrane that contained six dots of dengue virus serotype 1–4, Japanese encephalitis virus and mock infected C6/36 cell culture supernatants.

3. Results

3.1. Expression and immunogenicity of dengue NS1 fusion plasmid

A 1.056-kb NS1 fragment, containing nt 2422–3477 from dengue serotype 2 genome, was ligated into pDisplay to create a fusion gene containing a leader peptide sequence derived from the murine Igκ light chain, an extracellular portion of NS1 and a transmembrane anchor sequence from platelet-derived growth factor receptor. Expression of this fusion gene in

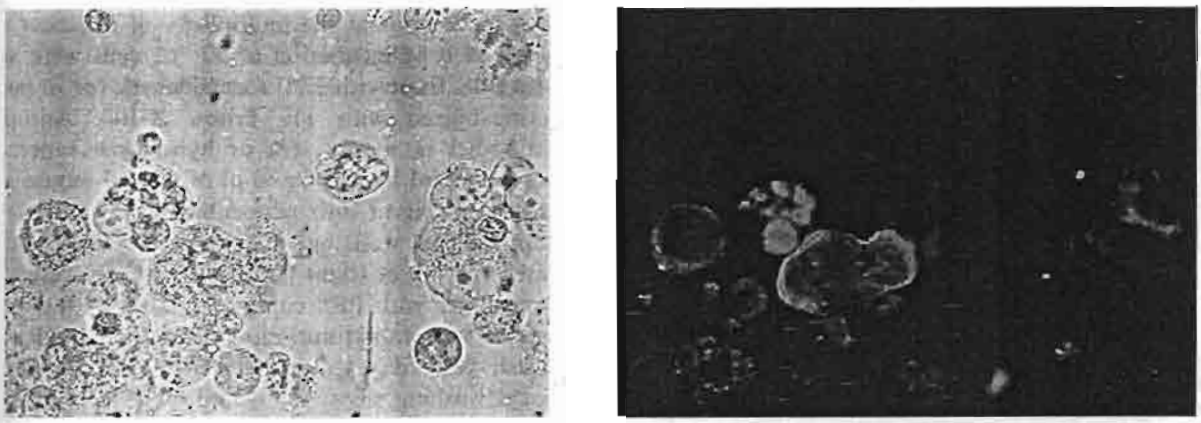

(A) (B)

Fig. 1. Photomicrograph of pDisplay/sNS1tm-transfected COS cells. COS cells were transfected with pDisplay/sNS1tm for 62 h and stained with anti-NS1 clone 1B2 and rabbit anti-mouse immunoglobulins-FITC conjugate. Cells were observed under light microscope (A) or fluorescence microscope (B).

mammalian cell was tested by transfecting recombinant plasmid into COS cells and identifying cell surface NS1 with an anti-dengue NS1 monoclonal antibody, 1B2. Within 62 h after transfection, 1B2 epitope was clearly detected by an indirect immunofluorescence method on the cell surface in about 5% of cells (Fig. 1). Under the same conditions, mock-infected COS cells did not react with 1B2. When transfected COS cell lysate was treated with 12% sodium dodecyl sulfate in the presence of reducing agent and subjected to western blot analysis, a protein band of approximately 57 kDa was identified in plasmid-transfected COS lysate, but not mock-infected lysate (Fig. 2). As expected, NS1 fusion protein expressed in transfected COS cells was slightly larger than 48-kDa native NS1 found in dengue-infected mosquito cells (Fig. 3A, lane 4). These results indicate that the NS1 fusion protein can be expressed on mammalian cell surface.

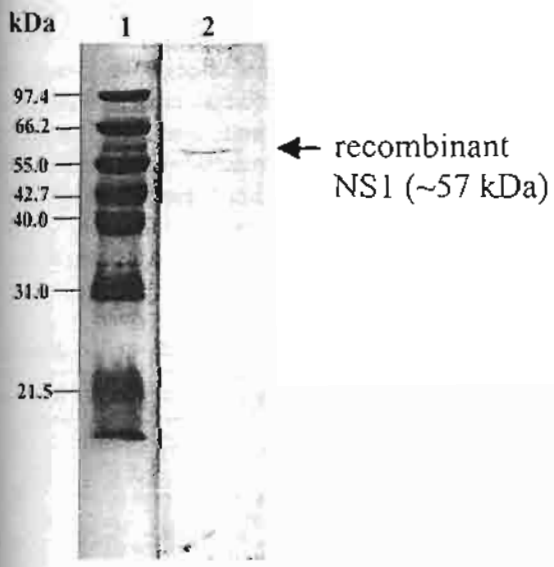

Fig. 2. Western blot analysis of pDisplay/sNS1tm-transfected COS cell lysate. Lane 1, protein markers with indicated molecular weight in kDa on the left side; lane 2, COS cells were transfected with pDisplay/sNS1tm for 62 h, and subjected to western blot analysis employing anti-NS1 clone 1B2. Cells were treated with reducing agent and heated prior to electrophoresis.

When two Balb/c mice were immunized with NS1 fusion plasmid at 2-week intervals and anti-dengue antibody response was monitored by dot enzyme immunoassay. Significant level of anti-dengue antibodies was detected equally in both mice (dot 1+ in a scale of 4, with no background in the control dot) after the third plasmid injection and continued up to the end of immunization schedules. Comparison of the antibody responses between both mice just before fusion revealed that the mouse that had been additionally boosted by live virus injection had higher antibody level (dot 2+) than the one boosted by plasmid only (dot 1+). Thus, immunization of plasmid DNA encoding dengue NS1 fusion protein can induce antibody response in mice.

3.2. Generation and characterization of anti-NS1 monoclonal antibodies

Following fusion of spleen cells from plasmid-immunized mice and selection using standard hybridoma technique, 17 out of 218 hybridoma clones (7.8%) from DNA immunized mouse and 11 out of 71 hybridoma clones (15.5%) from virus-boosted mouse were reactive to dengue antigens either by dot enzyme immunoassay or cell-ELISA. After cloning by limiting dilution, five hybridoma clones, designated NS1-1F, NS1-2F, NS1-3F, NS1-4F and NS1-2S, were selected based on their reactivity against dengue NS1 protein by western blot analysis (Table 1). The first four clones were derived from mouse immunized with DNA plus virus boost whereas NS1-2S was from DNA-immunized

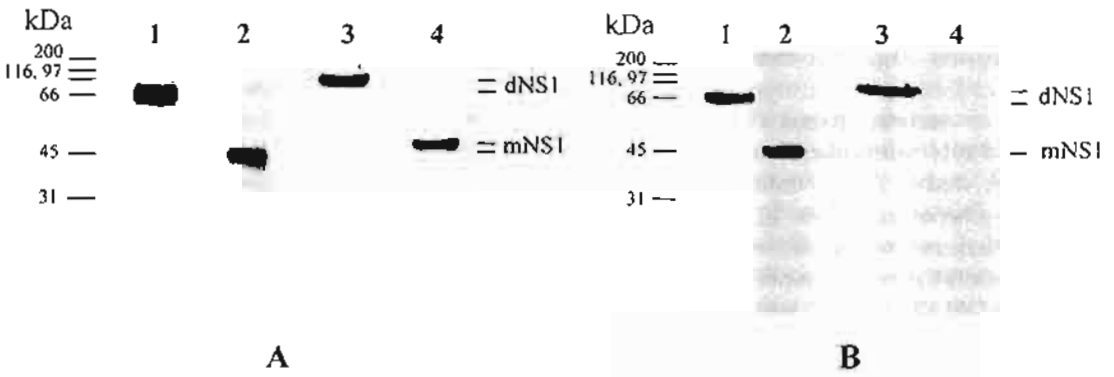

Fig. 3. Reactivity of anti-NS1 monoclonal antibodies against various forms of dengue NS1. Prior to electrophoresis and blotting, dengue-infected C6/36 cell lysate was subjected to the following treatment: lane 1, no treatment; lane 2, heat treatment; lane 3, 2-mercaptoethanol treatment; lane 4, heat and 2-mercaptoethanol treatment. Panel A, reactivity pattern of clones NS1-1F, NS1-3F and NS1-4F; panel B, reactivity pattern of clones NS1-2F and NS1-2S. Monomeric and dimeric forms of NS1 are indicated on the right side. Protein markers with indicated molecular weight in kDa are on the left side.

mouse. All clones were reactive to dengue antigen by dot enzyme immunoassay but only three of them reacted in cell-ELISA (NS1-1F, NS1-2F and NS1-3F). Three clones were of IgM class (Table 1).

Within dengue-infected cells, NS1 associates non-covalently into homodimeric form approximately 20–40 min after its synthesis (Winkler et al., 1988). With heat treatment, dimeric NS1 readily dissociates into monomeric form (Winkler et al., 1988). To investigate the reactivity of monoclonal antibodies against the two forms of dengue NS1, dengue-infected cell lysate was employed in western blot analysis either without any additional treatment, with heat treatment, with 2-mercaptoethanol treatment, or with heat and 2-mercaptoethanol treatment. Clones NS1-1F, NS1-3F and NS1-4F reacted with dimeric NS1 of approximately 66 kDa under non-reducing condition (Fig. 3A, lane 1) and 90 kDa under reducing condition (Fig. 3A, lane 3). They also reacted with the monomeric form of 45 and 48 kDa under non-reducing and reducing conditions, respectively (Fig. 3A, lanes 2 and 4). This reactivity pattern was similar to that of 1B2, indicating that NS1-1F, NS1-3F and NS1-4F recognize a linear epitope on NS1. In contrast, clones NS1-2F and NS1-2S did not bind NS1 after heat and 2-mercaptoethanol treatment (Fig. 3B, lane 4); both of them are, therefore, specific for conformational epitopes that are absent in the reduced monomeric form of NS1.

To determine cross reactivity of the five anti-NS1 clones to other dengue serotypes and Japanese encephalitis virus, dot enzyme immunoassay utilizing supernatants obtained from C6/36 cells infected with each serotype of dengue and Japanese encephalitis viruses was performed. As shown in Table 1, these anti-NS1 antibodies were classified into three groups depending on their reactivity with tested viruses. The first group, NS1-1F, appeared to be flavivirus cross-reactive as it bound all four serotypes of dengue as well as Japanese encephalitis virus. The second group, NS1-3F and NS1-4F, reacted with the four dengue serotypes but not Japanese encephalitis virus whereas the last group, NS1-2F and NS1-2S, appeared to be dengue serotype 2 specific.

Table 1
Characteristics of anti-dengue NS1 monoclonal antibodies

Designation	Immunogen	Isotype	Epitope type	Virus specificity
NS1-1F	DNA + virus	IgM	Linear	Flavivirus
NS1-2F	DNA + virus	IgM	Conformation	Dengue serotype 2
NS1-3F	DNA + virus	IgG2a	Linear	Dengue sero-complex
NS1-4F	DNA + virus	IgG1	Linear	Dengue sero-complex
NS1-2S	DNA	IgM	Conformation	Dengue serotype 2

4. Discussion

In several laboratory animals, DNA immunization has been shown to be an efficient mean for induction of both humoral and cell-mediated immune responses. In this report, we employed a recombinant plasmid encoding dengue NS1 fusion protein to aid in the generation of monoclonal antibodies to NS1 protein. A mammalian expression vector, pDisplay, was used as this vector contains a high-level expression promotor derived from cytomegalovirus; it has been used previously in DNA vaccine development against many infectious pathogens (Hasan et al., 1999). An advantage to the use of

pDisplay is the expression of target protein on cell surface. Several reports suggested that antigens presented on the cell surface are often more immunogenic than intracellular or secreted forms (Haddad et al., 1995; Men et al., 1991; Srinivasan et al., 1995). In a direct comparison study, DNA immunization with pDisplay containing hepatitis C virus E2 protein, which the expressed E2 targeted to the cell surface, induced much stronger humoral immune response in mice and macaques than pcDNA3.1 vector carrying the same gene but expressed E2 protein intracellularly (Forns et al., 1999). Interestingly, while immunization with plasmid DNA alone is adequate for the generation of anti-dengue NS1 monoclonal antibody, an additional boost with live virus injection appears to increase the number of clones obtained. Although the number of NS1-specific clones generated with the two immunization schedules are obviously small for comparison, our finding agrees well with previous reports showing enhancement of specific immune responses after antigen boost following DNA immunization (Schmolke et al., 1998; Tearina_Chu et al., 2001).

The monoclonal antibodies against dengue NS1 generated by DNA immunization in this study are quite diverse with regards to isotype, the nature of epitope recognized and cross-reactivity to NS1 from other viruses. These results suggest that the NS1 fusion protein expressed in murine cells following injection of plasmid DNA closely resembles those of native NS1 protein despite the facts that mouse is not a natural host for dengue virus and NS1 localized on the surface of dengue-infected human cells is in the glycosyl-phosphatidylinositol-linked form (Jacobs et al., 2000). Possible differences in the post-translational modifications of NS1 within murine cells as compared with infected human cells appear not to affect the immunogenicity of fusion NS1 protein generated in mice. However, we are also aware of the fact that the diversity of the antibodies obtained from the mouse that had been boosted by natural virus might also be generated by the exposure to the virus itself.

In conclusion, we have demonstrated that it is possible to produce monoclonal antibodies against the dengue NS1 protein by using DNA immunization strategy. The monoclonal antibodies are shown to be reactive to different natural epitopes of the NS1. This has opened a possibility of producing additional clones against other proteins that, in natural conditions, are expressed in small amount and/or difficult to purify or prepare. Using this similar technique, we have successfully produced antibodies to prM protein of dengue virus (manuscript in preparation). The monoclonal antibodies obtained from this report will be useful for further development of dengue NS1 diagnosis as well as functional study of dengue NS1 protein.

Acknowledgements

We thank Punjaporn Puttatesk for supervising the antibody screening using the dengue-infected cell-based ELISA. We thank Dr Sa-nga Pattanakitsakul for supplying the pMal/NS1 plasmid. We also thank Dr Ananda Nisalak for providing hybridoma clones and viruses. This work was supported by the National Center for Genetic Engineering and Biotechnology (BIOTEC), Bangkok, Thailand (grant number BT-13-06-MG-B4-4506). P. Malasit is a recipient of the senior research grant of the Thailand research fund.

References

Barry, M.A., Barry, M.E. Johnston, S.A., 1994. Production of monoclonal antibodies by genetic immunization. Biotechniques. 16: 616–618, 620.

Chang, G.-J., 1997. Molecular biology of dengue viruses. In: Gubler, D.J., Kuno, G. (Eds.), Dengue and Dengue Hemorrhagic Fever. CAB International, Wallingford, Oxon, UK, New York, p. 175.

Colombage, G., Hall, R., Pavy, M., Lobigs, M., 1998. DNA-based and alphavirus-vectored immunisation with prM and E proteins elicits long-lived and protective immunity against the flavivirus, Murray Valley encephalitis virus. Virology 250, 151–163.

Falconar, A.K., Young, P.R., 1991. Production of dimer-specific and dengue virus group cross-reactive mouse monoclonal antibodies to the dengue 2 virus non-structural glycoprotein NS1. J. Gen. Virol. 72, 961–965.

Forns, X., Emerson, S.U., Tobin, G.J., Mushahwar, I.K., Purcell, R.H., Bukh, J., 1999. DNA immunization of mice and macaques with plasmids encoding hepatitis C virus envelope E2 protein expressed intracellularly and on the cell surface. Vaccine 17, 1992–2002.

Gentry, M.K., Henchal, E.A., McCown, J.M., Brandt, W.E., Dalrymple, J.M., 1982. Identification of distinct antigenic determinants on dengue-2 virus using monoclonal antibodies. Am. J. Trop. Med. Hyg. 31, 548–555.

Gurunathan, S., Wu, C.Y., Freidag, B.L., Seder, R.A., 2000. DNA vaccines: a key for inducing long-term cellular immunity. Curr. Opin. Immunol. 12, 442–447.

Haddad, D., Liljeqvist, S., Kumar, S., Hansson, M., Stahl, S., Perlmann, H., Perlmann, P., Berzins, K., 1995. Surface display compared to periplasmic expression of a malarial antigen in *Salmonella typhimurium* and its implications for immunogenicity. FEMS Immunol. Med. Microbiol. 12, 175–186.

Hasan, U.A., Abai, A.M., Harper, D.R., Wren, B.W., Morrow, W.J., 1999. Nucleic acid immunization: concepts and techniques associated with third generation vaccines. J. Immunol. Methods 229, 1–22.

Hassett, D.E., Whitton, J.L., 1996. DNA immunization. Trends Microbiol. 4, 307–312.

Henchal, E.A., Henchal, L.S., Thaisomboonsuk, B.K., 1987. Topological mapping of unique epitopes on the dengue-2 virus NS1 protein using monoclonal antibodies. J. Gen. Virol. 68, 845–851.

Jacobs, M.G., Robinson, P.J., Bletchly, C., Mackenzie, J.M., Young, P.R., 2000. Dengue virus nonstructural protein 1 is expressed in a glycosyl-phosphatidylinositol-linked form that is capable of signal transduction. FASEB J. 14, 1603–1610.

Kasinrerk, W., Tokrasinwit, N., 1999. Inhibition of PHA-induced cell proliferation by polyclonal CD4 antibodies generated by DNA immunization. Immunol. Lett. 67, 237–242.

Kasinrerk, W., Tokrasinwit, N., Piluk, Y., 1996. Production of mouse anti-CD4 antibodies by DNA-based immunization. Asian Pac. J. Allergy Immunol. 14, 99–105.

Kasinrerk, W., Tokrasinwit, N., Changtumroung, K., 1997. Production of anti-CD4 antibodies in rabbits by DNA Immunization. Asian Pac. J. Mol. Biol. Biotech. 5, 123–129.

Kaufman, B.M., Summers, P.L., Dubois, D.R., Eckels, K.H., 1987. Monoclonal antibodies against dengue 2 virus E-glycoprotein protect mice against lethal dengue infection. Am. J. Trop. Med. Hyg. 36, 427–434.

Kaufman, B.M., Summers, P.L., Dubois, D.R., Cohen, W.H., Gentry, M.K., Timchak, R.L., Burke, D.S., Eckels, K.H., 1989. Monoclonal antibodies for dengue virus prM glycoprotein protect mice against lethal dengue infection. Am. J. Trop. Med. Hyg. 41, 576–580.

Konishi, E., Yamaoka, M., Khin Sane, W., Kurane, I., Mason, P.W., 1998. Induction of protective immunity against Japanese encephalitis in mice by immunization with a plasmid encoding Japanese encephalitis virus premembrane and envelope genes. J. Virol. 72, 4925–4930.

Men, R.H., Bray, M., Lai, C.J., 1991. Carboxy-terminally truncated dengue virus envelope glycoproteins expressed on the cell surface and secreted extracellularly exhibit increased immunogenicity in mice. J. Virol. 65, 1400–1407.

Moonsom, S., Khunkeawla, P., Kasinrerk, W., 2001. Production of polyclonal and monoclonal antibodies against CD54 molecules by intrasplenic immunization of plasmid DNA encoding CD54 protein. Immunol. Lett. 76, 25–30.

Phillpotts, R.J., Venugopal, K., Brooks, T., 1996. Immunization with DNA polynucleotides protects mice against lethal challenge with St. Louis encephalitis virus. Arch. Virol. 141, 743–749.

Porter, K.R., Kochel, T.J., Wu, S.J., Raviprakash, K., Phillips, I., Hayes, C.G., 1998. Protective efficacy of a dengue 2 DNA vaccine in mice and the effect of CpG immuno-stimulatory motifs on antibody responses. Arch. Virol. 143, 997–1003.

Pupo_Antunez, M., Rodriguez, R., Alvarez, M., Amin, N., Rodriguez, H., Otero, A., Guzman, G., 2001. Development of a monoclonal antibody specific to a recombinant envelope protein from dengue virus type 4 expressed in Pichia pastoris. Hybridoma 20, 35–41.

Roehrig, J.T., Bolin, R.A., Kelly, R.G., 1998. Monoclonal antibody mapping of the envelope glycoprotein of the dengue 2 virus, Jamaica [In Process Citation]. Virology 246, 317–328.

Schmolke, S., Tacke, M., Schmitt, U., Engel, A.M., Ofenloch-Haehnle, B., 1998. Identification of hepatitis G virus particles in human serum by E2- specific monoclonal antibodies generated by DNA immunization. J. Virol. 72, 4541–4545.

Srinivasan, J., Singh, O., Chakrabarti, S., Talwar, G.P., 1995. Targeting vaccinia virus-expressed secretory beta subunit of human chorionic gonadotropin to the cell surface induces antibodies. Infect Immun. 63, 4907–4911.

Tang, D.C., DeVit, M., Johnston, S.A., 1992. Genetic immunization is a simple method for eliciting an immune response. Nature 356, 152–154.

Tearina_Chu, T.H., Halverson, G.R., Yazdanbakhsh, K., Oyen, R., Reid, M.E., 2001. A DNA-based immunization protocol to produce monoclonal antibodies to blood group antigens. Br. J. Haematol. 113, 32–36.

Olivieri, C., Burroni, D., Telford, J.L., Baldari, C.T., 1996. Generation of a monoclonal antibody to a defined portion of the *Helicobacter pylori* vacuolating cytotoxin by DNA immunization. J. Biotechnol. 51, 191–194.

Whitton, J.L., Rodriguez, F., Zhang, J., Hassett, D.E., 1999. DNA immunization: mechanistic studies. Vaccine 17, 1612–1619.

Winkler, G., Randolph, V.B., Cleaves, G.R., Ryan, T.E., Stollar, V., 1988. Evidence that the mature form of the flavivirus nonstructural protein NS1 is a dimer. Virology 162, 187–196.

Wolff, J.A., Malone, R.W., Williams, P., Chong, W., Acsadi, G., Jani, A., Felgner, P.L., 1990. Direct gene transfer into mouse muscle in vivo. Science 247, 1465–1468.

Pediatr Nephrol (2003) 18:644–648
DOI 10.1007/s00467-003-1112-6

ORIGINAL ARTICLE

Suchai Sritippayawan · Sukachart Kirdpon
Somkiat Vasuvattakul · Sirijitta Wasanawatana
Watanachai Susaengrat · Worawee Waiyawuth
Sumalee Nimmannit · Prida Malasit
Pa-thai Yenchitsomanus

A de novo R589C mutation of *anion exchanger 1* causing distal renal tubular acidosis

Received: 22 August 2002 / Revised: 11 December 2002 / Accepted: 17 December 2002 / Published online: 16 May 2003

Abstract *Anion exchanger 1 (AE1 or SLC4A1)* mutations have been reported to cause distal renal tubular acidosis (dRTA), a disease characterized by impaired acid excretion in the distal nephron. We have recently demonstrated homozygous *AE1* G701D mutation as a common molecular defect of autosomal recessive (AR) dRTA in a group of Thai pediatric patients. In the present work, we discovered a de novo heterozygous *AE1* R589C mutation, previously documented in inherited autosomal dominant (AD) dRTA. Arginine at this position is conserved in all vertebrate AE proteins indicating its functional importance. Three different mutations at this position (R589C, R589H, and R589S) were all found in AD dRTA and a de novo R589H mutation has previously been recorded. Our report is the second de novo mutation but with a different substituted amino acid. A high prevalence of *AE1* R589 mutations and the presence of at least two de novo mutations at this position lead us to propose that codon 589 (CGC) is a "mutational hotspot" of *AE1*. The mechanism of recurrent mutations probably involves methylation and deamination altering cytosine (C) to thymine (T) in the CpG dinucleotides.

Keywords dRTA · Autosomal dominant · Band 3 · *AE1* gene · De novo mutation · Mutational hotspot · CpG dinucleotides

S. Sritippayawan · S. Vasuvattakul · S. Nimmannit
Renal Division, Department of Medicine,
Faculty of Medicine Siriraj Hospital, Mahidol University,
Bangkok 10700, Thailand

S. Kirdpon
Department of Pediatrics, Faculty of Medicine,
Khon Kaen University, Thailand

S. Wasanawatana
Pediatrics Unit, Khon Kaen Hospital, Thailand

W. Susaengrat
Medicine Unit, Khon Kaen Hospital, Thailand

W. Waiyawuth
Department of Forensic Medicine,
Faculty of Medicine Siriraj Hospital,
Mahidol University,
Bangkok, Thailand

P. Malasit · P.-t. Yenchitsomanus
Division of Medical Molecular Biology,
Faculty of Medicine Siriraj Hospital, Mahidol University,
Bangkok, Thailand

P. Malasit · P.-t. Yenchitsomanus
Medical Biotechnology Unit,
National Center for Biotechnology and Genetic Engineering (BIOTEC),
National Science and Technology Development Agency (NSTDA),
Thailand

P.-t. Yenchitsomanus (✉)
Division of Medical Molecular Biology,
Department of Research and Development,
Faculty of Medicine Siriraj Hospital, Mahidol University,
Bangkok 10700, Thailand
e-mail: grpye@mahidol.ac.th
Tel.: +662-4198940-86 ext. 6666-70, Fax: +662-4184793

Introduction

Distal renal tubular acidosis (dRTA) is a disease characterized by an incapability of the distal nephron to secrete hydrogen ion into urine in the presence of systemic metabolic acidosis. The patient with dRTA has hyperchloremic metabolic acidosis, usually accompanied by hypokalemia, metabolic bone disease, and nephrocalcinosis and/or nephrolithiasis [1, 2, 3]. The hydrogen ion secretion at the apical membrane of α-intercalated cells of the distal nephron is importantly mediated by the H^+-ATPase pump, which occurs in association with bicarbonate reabsorption across the basolateral membrane of these cells mediated by kidney anion exchanger 1 (kAE1). The defect of kAE1 at the basolateral membrane will result in intracellular bicarbonate retention, which may in turn affect intracellular carbonic acid dissociation and hydrogen ion secretion at the apical membrane.

Mutations of *AE1* or *SLC4A1* (MIM 109270), which is located on chromosome 17q21–22 and encodes both erythroid (eAE1) and kidney AE1 (kAE1) isoforms, have been found to result in dRTA [4, 5, 6, 7, 8, 9, 10, 11, 12]. The mutations of this gene were reported in both autosomal dominant (AD) [4, 5, 6, 7] and recessive (AR) [8, 9, 10, 11, 12] types of dRTA. Missense mutations in codon 589 of the *AE1* gene, resulting in substitutions of arginine by either histidine (R589H), cysteine (R589C) or serine (R589S), were identified in multiple families with AD dRTA [4, 5, 6, 7]. Two additional mutations, S613F and a truncated 11 amino acids at the carboxyl terminus of AE1 (R901X or band 3 Walton), were also associated with AD dRTA [4, 6]. Our group [9, 12] and others [8, 10, 11] have recently described *AE1* mutations associated with AR dRTA. Homozygous *AE1* G701D mutation was the first reported genotype resulting in AR dRTA [8]. Compound heterozygosity of *AE1* G701D or other mutations (such as ΔV850 and A858D) and an in-frame nine-amino-acid deletion (residues 400–408) were found to result in AR dRTA associated with Southeast Asian ovalocytosis (SAO) [9, 10]. Our recent study has shown that homozygous *AE1* G701D mutation is a common molecular defect among the studied group of Thai pediatric patients with dRTA [12]. However, in analysis of *AE1* in a Thai pediatric patient with dRTA presenting with severe clinical manifestations and in his parents, we unexpectedly identified a de novo R589C mutation, representing the first of this type. Based on the presence of this de novo mutation as well as a previously reported de novo R589H mutation [6] and also a high prevalence of R589 mutations [4, 5, 6, 7], we therefore propose that codon 589 is a "mutational hotspot" of the *AE1* gene.

Case report

A 7-year-old Thai male, a native of northeastern Thailand, was diagnosed with rickets without mental retardation 4 years ago. The presenting symptoms were dyspnea and muscle weakness. The physical examination revealed rachitic rosary, kyphoscoliosis, and growth retardation. His body weight and height were 9.6 kg and 84 cm, respectively, which were lower than the third percentile of those of the age-matched normal Thai male children. X-ray examination demonstrated typical features of osteomalacia and bilateral nephrocalcinosis. Hypokalemic and hyperchloremic metabolic acidosis with a very low urine citrate were detected, while his urine pH was 7.5 and serum creatinine 0.3 mg/dl. The urine anion gap was positive as shown in Table 1. His parents had no metabolic acidosis with normal urine citrate and renal function. The morning urine pH of the father and mother were 6.0 and 5.4, respectively (Table 1). The father was able to lower the urine pH to below 5.5 after a short acid loading test [13].

Materials and methods

Genomic DNA prepared from the patient's and his parents' blood samples were screened for *AE1* mutation by the polymerase chain reaction and the single-strand conformation polymorphism (PCR-SSCP) technique as described in our previous work [9]. The PCR product with a mobility shift on the SSCP gel was subsequently subjected to nucleotide sequencing using an ABI-PRISM Big Dye Terminator Cycle Sequencing Reaction Kit (Applied Biosystems) and an ABI-PRISM 310 automated sequencer (Applied Biosystems). The PCR products of the same region of *AE1* from the parents' and normal DNA samples were also sequenced and compared. Segregation of mutation in the family was analyzed by PCR-restriction endonuclease digestion (PCR-RED) and agarose-gel electrophoresis. Biological paternity was verified by DNA fingerprinting. Nine short tandem repeat (STR) loci in the human genome were simultaneously amplified in a single PCR by using a Profiler Plus I kit (Applied Biosystems). After amplification, PCR products of the nine STR loci were separated and detected by an ABI-PRISM 310 automated sequencer (Applied Biosystems). The digital output data were collected and analyzed by computer software (Applied Biosystem).

Table 1 Serum and urine biochemical and electrolyte values in the patient and his parents

	Father	Mother	Patient
Serum			
Creatinine (mg/dl)	0.9	0.6	0.3
Na^+ (mM)	144.0	137.5	146.0
K^+ (mM)	4.24	3.62	1.90
HCO_3^- (mM)	33.4	21.8	5.0
Cl^- (mM)	108	103	125
Urine			
pH	6.0	5.4	7.5
Citrate (mM)	0.30	1.39	0.01
Na^+ (mM)	174.5	164	70.5
K^+ (mM)	50.5	61	43.5
Cl^- (mM)	181	256	62

Results

The results of clinical and laboratory investigations showed that the patient had dRTA with severe clinical manifestations while his parents were normal. The promoter region and exons 4–20 of *AE1* in all three members of this family were screened for mutation by the PCR-SSCP method, and compared with normal controls. The patient had a pattern of mobility shifts of single-stranded DNAs from exon 14 of *AE1* (Fig. 1a), while all other exons were normal. Surprisingly, his parents had normal SSCP patterns for this fragment (Fig. 1a) and for all other exons.

The amplified DNAs of exon 14 from the patient and the parents were then analyzed by direct sequencing. A heterozygous nucleotide substitution, cytosine to thymine, at the position 1765 (C1765T) in codon 589 (CGC to TGC) was identified in the patient while the parents had normal sequencing profiles (Fig. 1b). This substitution resulted in the replacement of arginine by cysteine (R589C) in the AE1 protein. The C to T substitution would also abolish a normal *Hha*I recognition site (GCGC) in the exon 14 sequence. Thus, PCR-RED using *Hha*I could readily detect the presence of this substitution. The size of undigested PCR product of this exon was 224 base pairs (bp). In the normal individual with a homozygous wild-type sequence, the PCR product from both alleles could be digested with *Hha*I, resulting in

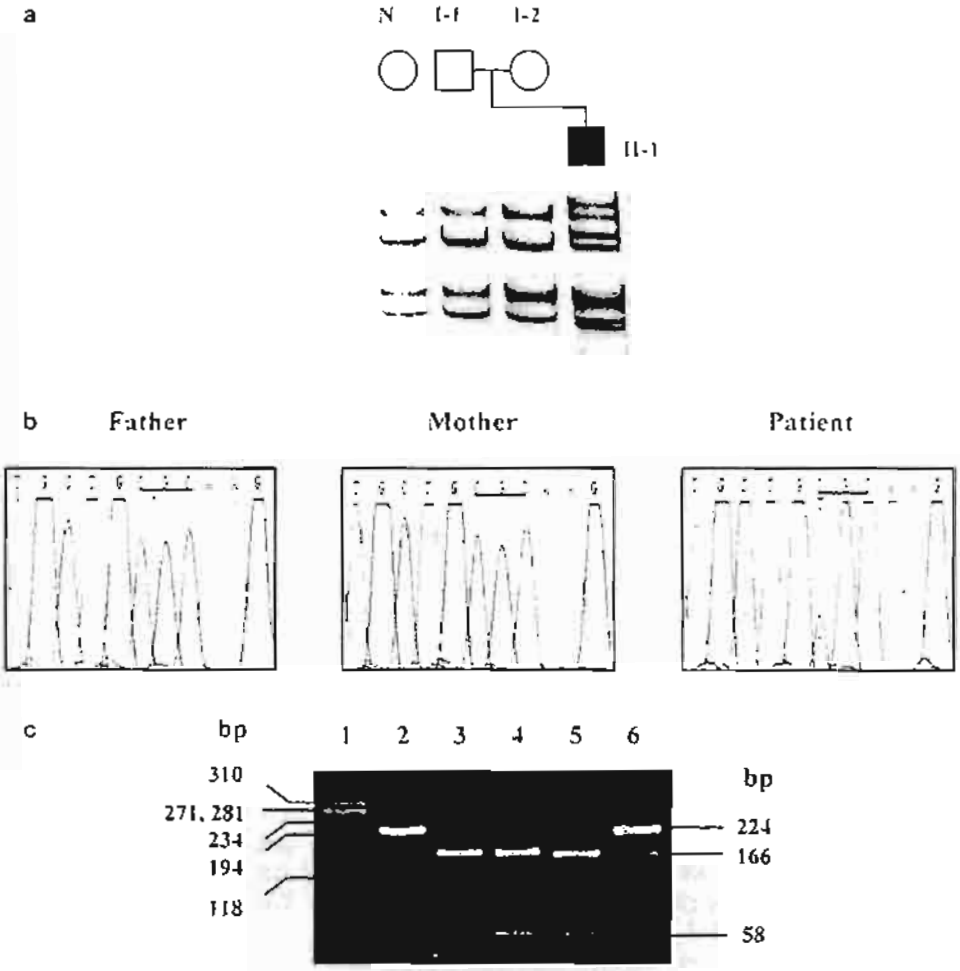

Fig. 1 a Screening of *AE1* mutation by the PCR-SSCP method, showing mobility shifts of single-stranded DNAs of exon 14 in the patient (*II-1*), while they were not observed in the parents (*I-1, I-2*) (*N* normal control sample). b Nucleotide sequencing of *AE1* exon 14 from the patient and his parents. The patient's father and mother had a homozygous normal sequence at condon 589 (CGC/CGC), while the patient had a heterozygous nucleotide substitution at codon 589 (CGC/TGC). c Analysis of R589C mutation in *AE1* exon 14 by the PCR-RED method using *Hha*I enzyme in the patient and his parents. *Lane 1* is a part of standard DNA size markers, PhiX174DNA/*Hae*III. *Lane 2* is an undigested PCR product of a normal control, showing a fragment size of 224 bp. *Lane 3* is a digested PCR product of a normal control, showing fragment sizes of 166 and 58 bp. *Lanes 4 and 5* are digested PCR products of the patient's father and mother, respectively, showing the same fragment sizes as that found in *lane 3*. *Lane 6* is a digested PCR product of the patient, showing fragments of 224, 166, and 58 bp, indicating the presence of heterozygous *AE1* codon 589 mutation

two fragments, of 166 and 58 bp. In the heterozygous individual, one undigested (244 bp) and two digested fragments (166 and 58 bp) would be observed. The result of this analysis showed that while the parents and normal control had two fragments (166 and 58 bp), the patient had three fragments (244, 166 and 58 bp), typical of the heterozygous mutation (Fig. 1c).

The presence of *AE1* R589C mutation in only the patient might occur from a false paternity. To investigate their biological relationship, DNA fingerprinting was performed by using nine STR polymorphic DNA markers. The results (Table 2) showed that for all the loci tested the patient always shared one allele at each locus with both parents, strongly indicating their biological relationship.

Table 2 Paternity testing by DNA fingerprinting using nine short tandem repeat (STR) polymorphic DNA markers, showing a biological relationship between the patient and his parents since in every locus one STR allele from the parents is present in the patient

Markers	Member		
	Father	Mother	Patient
D8S1179	14/15	13/11	14/11
D21S11	29/31.2	31.2/31.2	31.2/31.2
D18S51	14/14	16/15	14/15
D3S1358	17/15	17/16	17/16
VWA	17/15	18/20	17/20
FGA	20/21	24/22	20/22
D5S818	13/15	11/12	13/12
D13S317	10/11	8/11	11/11
D7S820	10/11	11/11	11/11

Discussion

Mutations of *AE1* have been reported in many kindreds with AD dRTA [4, 5, 6, 7]. However, analyses of *AE1* in the families with dRTA by our group [9, 12] and others [8, 10, 11] have also shown that some mutations of this gene were associated with AR dRTA, present in homozygous or compound heterozygous conditions. Since homozygous *AE1* G701D mutation was commonly found to be associated with AR dRTA in Thai pediatric patients, especially in those from northeast Thailand [12], we initially suspected that this abnormal genotype would

also be found in the child with severe clinical manifestations of dRTA reported in this study. However, instead of detecting homozygous *AE1* G701D mutation, we identified a heterozygous nucleotide (C1765T) substitution at codon 589 (from CGC to TGC), resulting in an amino acid alteration, arginine to cysteine (R589C), in the AE1 protein. This mutation was found only in the patient while his parents had normal *AE1*, despite paternity confirmation by DNA fingerprinting. Thus, it is most likely to be a de novo R589C mutation, the known *AE1* mutation associated with inherited AD dRTA. It also represents the first *AE1* mutation associated with AD dRTA identified in Thai patients.

AE1 R589 mutations have been reported in multiple families with AD dRTA [4, 5, 6, 7]. R589 could change to histidine (R589H) [4, 5, 6], serine (R589S) [6], or cysteine (R589C) [4, 7]. Altogether, *AE1* R589 mutations have been identified in 10 of 12 families with AD dRTA, including one in the present study. The R589H mutation is most common, and has been found in six families. The high prevalence of mutations at this position is unlikely to result from the founder effect because of its occurrence in different populations with the existence of allelic heterogeneity. The presence of de novo mutations strongly indicates recurrent mutations. Previously, a de novo R589H mutation has been observed in a sporadic AD dRTA case [6]. However, the de novo R589C mutation has never previously been reported; thus, the one described in this report is the first instance of this de novo change. Because of a likely high mutation rate and the presence of at least two de novo mutations, we propose that codon 589 is a "mutational hotspot" of the *AE1* gene.

The normal triplet-nucleotides for arginine at the codon 589 are CGC. Thus, the first two nucleotides are in CpG dinucleotides. The R589C mutation occurred from CGC to TGC alteration [4, 7, and this report]. The R589H mutation resulted from CGC to CAC [4, 5, 6] and its complementary change was from GCG to CTC, which are also in the CpG dinucleotides. Therefore, these two mutations (CGC to TGC and GCG to CTG) are cytosine (C) to thymine (T), on either the sense or anti-sense strand, which is most likely to occur from the same mutation mechanism.

Methylation followed by deamination is the well-known mechanism causing the alteration of cytosine to thymine [14]. The CpG dinucleotide is a known "mutational hotspot" of many genes [15, 16, 17] in the human genome as a result of the modification of 5' cytosine by cellular DNA methyltransferases and the consequent high frequency of spontaneous deamination of 5-methyl cytosine (5mC) to thymine. The high prevalence of inherited R589C and R589H mutations and the occurrence of de novo R589C and R589H mutations support the operation of this mechanism. Unlike the mutations that caused nucleotide mis-incorporation occurring during DNA replication, the mutation that resulted from methylation and deamination will not be corrected by the cellular mismatch repairing system. This may explain why the R589C (CGC to TGC) and R589H (CGC to CAC) mutations were more prevalent than such mutations as R589S (CGC to AGC), which was identified in only one family in this group. In addition, the other two possible mutations, R589P (CGC to CCC) and R589L (CGC to CTC), have not been identified. These three mutations did not occur from C to T substitutions, but they are likely to be due to the nucleotide misincorporations.

It is possible that there might also be other "mutational hotspots" in *AE1*. Diego blood group (band 3 Memphis II) polymorphism (P854L) [18] may be another example. The wild-type Di(b) antigen contains proline at position 854 while the variant Di(a) antigen has leucine at the same position. The nucleotide alteration of this polymorphism is from CCG to CTG, which is also a C to T change in the CpG dinucleotides. This polymorphism is common in different ethnic groups, and is likely to occur from recurrent mutations. Thus, codon 854 is possibly another "mutational hotspot" in *AE1*, without the disease state association. In contrast, band 3 Memphis I (K56E), which occurred from the AAG to GAG alteration and is a widespread polymorphism [19], might result from a different mechanism, which is still unclear.

R589 lies in the third intracellular loop between the sixth and seventh transmembrane domains (TM6 and TM7) of AE1. Six conserved basic amino-acid residues (R589, K590, K592, K600, R602, and R603), which may be important in its function, are present within this loop. Analysis of AE1 R589H transport function in *Xenopus* oocytes showed a significant chloride transport activity [3, 4]. Thus, the disease and its autosomal dominant inheritance are not related simply to the anion transport activity of the mutant proteins [4]. Recently, impaired trafficking of kAE1 R589H (as well as R589C and R589S), but not eAE1 R589H, was demonstrated in transfected human embryonic kidney (HEK 293) cells, indicating that this conserved arginine residue is important for proper protein trafficking to the cell membrane [20]. Coexpression of kAE1 R589H reduced cell surface expression of wild-type kAE1 due to heterodimer formation. Thus, a dominant-negative effect would account for the autosomal dominant inheritance pattern of dRTA caused by these AE1 R589H and related mutations [20]. The absence or reduction of the mutant as well as wild-type kAE1 at the basolateral membrane of α-intercalated cells in the distal nephron would affect chloride/bicarbonate exchange, leading to impaired hydrogen ion secretion at the apical membrane, which would thus result in dRTA.

Acknowledgements We thank Thitima Keskanokwong, Nunghathai Sawasdee, Atchara Paemanee, Duangporn Chuawatana, Sumitra Mingkum, and Wilaiwan Keerativutisest for their technical and other assistance. This work was financially supported by grants from the Siriraj Grant for Research Development, the National Center for Biotechnology and Genetic Engineering (BIOTEC), and the Thailand Research Fund (TRF). P.M. is a recipient of the Senior Research Scholar Award of TRF.

References

1. Rodriguez-Soriano J (2000) New insights into the pathogenesis of renal tubular acidosis—from functional to molecular studies. Pediatr Nephrol 14:1121–1136
2. Batlle D, Ghanekar H, Jain S, Mitra A (2001) Hereditary distal renal tubular acidosis: new understandings. Annu Rev Med 52:471–484
3. Chan JCM, Scheinman JI, Roth KS (2001) Renal tubular acidosis. Pediatr Rev 22:277–287
4. Bruce LJ, Cope DL, Jones GK, Schofield AE, Burley M, Povey S, Unwin RJ, Wrong O, Tanner MJA (1997) Familial distal renal tubular acidosis is associated with mutations in the red cell anion exchanger (band 3, *AE1*) gene. J Clin Invest 100:1693–1701
5. Jarolim P, Shayakul C, Prabakaran D, Jiang L, Stuart-Tilley A, Rubin HL, Simova S, Zavadil J, Herrin JT, Brouillette J, Somers MJG, Seemanova E, Brugnara C, Guay-Woodford LM, Alper SL (1998) Autosomal dominant distal renal tubular acidosis is associated in three families with heterozygosity for the R589H mutation in the AE1 (band 3) Cl^-/HCO_3^- exchanger. J Biol Chem 273:6380–6388
6. Karet FE, Gainza FJ, Gyory AZ, Unwin RJ, Wrong O, Tanner MJ, Nayir A, Alpay H, Santos F, Hulton SA, Bakkaloglu A, Ozen S, Cunningham MJ, Di Pietro A, Walker WG, Lifton RP (1998) Mutations in the chloride-bicarbonate exchanger gene AE1 cause autosomal dominant but not autosomal recessive distal renal acidosis. Proc Natl Acad Sci U S A 95:6337–6342
7. Weber S, Soergel M, Jeck N, Konrad M (2000) Atypical distal renal tubular acidosis confirmed by mutation analysis. Pediatr Nephrol 15:201–204
8. Tanphaichitr VS, Sumboonnaonda A, Ideguchi JH, Shayakul C, Brugnara C, Takao M, Veerakul G, Alper SL (1998) Novel AE1 mutations in recessive distal renal tubular acidosis: loss-of-function is rescued by glycophorin A. J Clin Invest 102:2173–2179
9. Vasuvattakul S, Yenchitsomanus P, Vachuanichsanong P, Thuwajit P, Kaitwatcharachai C, Laosombat V, Malasit P, Wilairat P, Nimmannit S (1999) Autosomal recessive distal renal tubular acidosis associated with Southeast Asian ovalocytosis. Kidney Int 56:1674–1682
10. Bruce LJ, Wrong O, Toye AM, Young MT, Ogle G, Ismail Z, Sinha AK, McMaster P, Hwaihwanje I, Nash GB, Hart S, Lavu E, Palmer R, Othman A, Unwin RJ, Tanner MJ (2000) Band 3 mutations, renal tubular acidosis and South-East Asian ovalocytosis in Malaysia and Papua New Guinea: loss of up to 95% band 3 transport in red cells. Biochem J 350:41–51
11. Ribeiro ML, Alloisio N, Almeida H, Gomes C, Texier P, Lemos C, Mimoso G, Morle L, Bey-Cabet F, Rudigoz RC, Delaunay J, Tamagnini G (2000) Severe hereditary spherocytosis and distal renal tubular acidosis associated with the total absence of band 3. Blood 96:1602–1604
12. Yenchitsomanus P, Vasuvattakul S, Kirdpon S, Wasanawatana S, Susaengrat W, Sreethiphayawan S, Chuawatana D, Mingkum S, Sawasdee N, Thuwajit P, Wilairat P, Malasit P, Nimmannit S (2002) Autosomal recessive distal renal tubular acidosis caused by G701D mutation of *anion exchanger 1* gene. Am J Kidney Dis 40:21–29
13. Wrong O, Davies H (1959) The excretion of acid in renal disease. Q J Med 28:259–313
14. Duncan BK, Miller JH (1980) Mutagenic deamination of cytosine residues in DNA. Nature 287:560–561
15. Perry DJ, Carrell RW (1989) CpG dinucleotides are "hotspots" for mutation in the antithrombin III gene. Twelve variants identified using the polymerase chain reaction. Mol Biol Med 6:239–243
16. Bottema CD, Ketterling RP, Vielhaber E, Yoon HS, Gostout B, Jacobson DP, Shapiro A, Sommer SS (1993) The pattern of spontaneous germ-line mutation: relative rates of mutation at or near CpG dinucleotides in the factor IX gene. Hum Genet 91:496–503
17. Pfeifer GP (2000) p53 mutational spectra and the role of methylated CpG sequences. Mutat Res 450:155–166
18. Bruce LJ, Anstee DJ, Spring FA, Tanner MJA (1994) Band 3 Memphis variant. II. Altered stilbene disulfonate binding and the Diego (Di(a)) blood group antigen are associated with the human erythrocyte band 3 mutation pro854-to-leu. J Biol Chem 269:16155–16158
19. Jarolim P, Rubin HL, Zhai S, Sahr KE, Liu SC, Mueller TJ, Palek J (1992) Band 3 Memphis: a widespread polymorphism with abnormal electrophoretic mobility of erythrocyte band 3 protein caused by substitution AAG-to-GAG (lys-to-glu) in codon 56. Blood 80:1592–1598
20. Quilty JA, Li J, Reithmeier RA (2002) Impaired trafficking of distal renal tubular acidosis mutants of the human kidney anion exchanger kAE1. Am J Physiol Renal Physiol 282:F810–F820

Pediatr Nephrol (2003) 18:257–260
DOI 10.1007/s00467-003-1067-7

ORIGINAL ARTICLE

Achra Sumboonnanonda · Prida Malasit
Voravarn S. Tanphaichitr · Sompong Ong-ajyooth
Siripan Petrarat · Arun Vongjirad

Renal tubular dysfunction in α-thalassemia

Received: 23 April 2002 / Revised: 29 October 2002 / Accepted: 30 October 2002 / Published online: 26 February 2003

Abstract Shortened red cell life span and excess iron cause functional and physiological abnormalities in various organ systems in thalassemia patients. In an earlier study, we showed that β-thalassemia patients have a high prevalence of renal tubular abnormalities. The severity correlated with the degree of anemia, being least severe in patients on hypertransfusion and iron chelation therapy, suggesting that the damage might be caused by the anemia and increased oxidation induced by excess iron deposits. This study was designed to define the renal abnormalities associated with α-thalassemia and to correlate the renal findings with clinical parameters. Thirty-four pediatric patients (mean age 8.2±2.8 years) with Hb H disease or Hb H/Hb CS were studied. Ten patients (group 1) were splenectomized, with a mean duration post splenectomy of 3.5±1.4 years; 24 patients (group 2) had intact spleens. The results were compared with 15 normal children. Significantly higher levels of urine *N*-acetyl-β-D-glycosaminidase, malondialdehyde (MDA), and β_2-microglobulin were found in both groups compared with normal children. An elevated urine protein/creatinine ratio was recorded in 60% of group 1 and 29% of group 2. Two patients (5.9%), 1 in each group, had generalized aminoaciduria. We found proximal tubular abnormalities in α-thalassemia patients. Increased oxidative stress, possibly iron induced, may play an important role, since urine MDA levels were significantly increased in both groups of patients.

Keywords α-Thalassemia · Renal tubular function · Malondialdehyde · Splenectomy

A. Sumboonnanonda (✉) · V. S. Tanphaichitr · S. Petrarat
A. Vongjirad
Department of Pediatrics, Faculty of Medicine,
Siriraj Hospital, Mahidol University,
Prannok Road, Bangkok 10700, Thailand
e-mail: siasb@mahidol.ac.th
Tel.: +66-2-4113010, Fax: +66-2-4121371

P. Malasit
Medical Molecular Biology Unit,
Office for Research and Development,
Siriraj Hospital, Mahidol University,
Prannok Road, Bangkok 10700, Thailand

S. Ong-ajyooth
Department of Biochemistry,
Siriraj Hospital, Mahidol University,
Prannok Road, Bangkok 10700, Thailand

Introduction

α-Thalassemia results from the loss of one or both of the duplicated α genes from chromosome 16. Carriers of the deletional form of α-thalassemia, genotype (–/αα) or (–α/αα), are clinically normal with only mild hypochromic, microcytic anemia. Compound heterozygotes, genotype (–/–α) and commonly called Hb H disease, usually have a moderately severe anemia. The prevalence of genotypes (–/αα) and (–α/αα) in Bangkok is 3.5% and 16%, respectively. Clinical phenotypes of Hb H disease can also be caused by non-deletion types of α-thalassemia. The most common non-deletion type of α-thalassemia in Thailand is known as Hb H disease with Hemoglobin Constant Spring (Hb H/Hb CS), genotype (–/αCSα) [1]. α-Thalassemia can be divided into four clinical subsets: Hb Bart's hydrops fetalis in which all the patients die in utero or soon after birth, Hb H disease with moderately severe anemia in most patients, Hb H/Hb CS with more severe anemia but good response to splenectomy, and Hb A-E-Bart's disease and Hb E-F-Bart's disease, which are rare and have similar clinical phenotype to Hb H [2, 3].

Recently, we demonstrated proximal tubular dysfunction in patients with homozygous β-thalassemia and β-thalassemia/Hb E disease. The cause of this dysfunction is not known, but anemia and iron overload may be important [3]. Excess free iron is known to be a catalyst of lipid peroxidation, which damages cells. In our previous study children with β-thalassemia had increased urinary malondialdehyde (MDA), indicating that lipid peroxidation did occur. Children on a hypertransfusion protocol with deferoxamine had less severe renal tubular dysfunction. This suggests that renal damage may be

reversible with iron chelation therapy [3]. According to this hypothesis, α–thalassemia patients with repeated episodes of hemolysis and increased iron deposition, although with a milder degree of anemia, will also be prone to renal dysfunction. About 5% of Thai children with α–thalassemia have splenectomy to reduce the degree of anemia and improve growth rate. Anemia and growth improve markedly, especially in Hb H /Hb CS patients, as early as 1 year after splenectomy (W. Tasaneeyapan, V.S. Tanphaichitr unpublished observation). Compared with β–thalassemia, α–thalassemia patients have less severe anemia, with less iron deposition [2]. Moreover, within the α–thalassemia group, patients with HbH/HbCS have more severe anemia than those with classic HbH disease [4]. Splenectomy is still an accepted treatment in α–thalassemia, especially HbH/HbCS patients with severe anemia, usually resulting in markedly increased hemoglobin (Hb) levels without the need for further blood transfusion. The less severe anemia in α–thalassemia and the availability of different groups of patients (with and without splenectomy) have provided an opportunity to compare the prevalence and the degree of renal tubular defects amongst different groups of patients. This study was designed to detect the prevalence of renal tubular dysfunction in α–thalassemia patients with intact spleens and after splenectomy and to correlate the renal findings with clinical parameters.

Materials and methods

Thirty-four pediatric patients between 3 and 15 years with α–thalassemia (Hb H disease or Hb H/Hb CS) attending the Department of Pediatrics, Siriraj Hospital were recruited with informed consent from their parents.

All patients had no acute febrile illness, acute hemolysis, or significant bacteriuria. Estimated glomerular filtration rate (GFR) was calculated according to Schwartz's formula [5]. The diagnosis of Hb H disease and Hb H/Hb CS was performed by standard techniques [6]. Height and weight standard deviation scores (SDS) were calculated according to Tanner et al. [7]. Patients were divided into two groups, group 1 had been splenectomized for at least 2 years and group 2 were patients with intact spleens.

Patients were instructed to fast overnight before attending the clinic in the morning, with no food or drink until their second void. Blood samples were collected from each patient for Hb and hematocrit, urea nitrogen, creatinine, and electrolytes. Fresh second–morning urine samples were collected; a portion was immediately aliquoted and frozen until further analysis. The remaining urine sample was tested for osmolality (by Osmomat 030 cryoscopic osmometer, Gonotec, Berlin, Germany), protein, and sugar (by Labstix, Bayer Diagnostics), and examined microscopically. *N*–Acetyl–β–D–glucosaminidase (NAG) (by a spectrophotometric method) [8], creatinine (Jaffe reaction, autoanalyzer), and amino acids (by paper chromatography) [9] were also measured. Urine MDA levels were measured by a spectrophotometric technique [10]. Urinary protein levels were assayed by a modified Bradford method (Bio–Rad Laboratories, Richmond Calif., USA) [11]. Urine β_2–microglobulin levels were assayed by enzyme-linked immunosorbent assay [12]. Fresh morning urine samples from 15 healthy children of the same age group were used as controls.

This study was approved by the Ethics Committee on Human Rights Related to Research Involving Human Subjects, Faculty of Medicine Siriraj Hospital, Mahidol University, Bangkok, Thailand.

Statistical methods

All calculations were carried out using SPSS statistic package. Comparison between groups was performed using unpaired two–tailed Student's *t*–test. Pearson correlation test was performed between tubular dysfunction and serum ferritin, Hb, and urine MDA levels. A *P* value of less than 0.05 was regarded as significant.

Results

Thirty–four patients, comprising patients with 14 Hb H disease and 20 with Hb H/ HbCS, were included in this

Table 1 Summary of demographic and biochemical data of two groups of patients and controls (*SDS* standard deviation score, *GFR* glomerular filtration rate, *NAG N*–acetyl–β–D–glucosaminidase, *MDA* malondialdehyde)[a, c]

	Group 1 n=10	Group 2 n=24	Controls n=15
Age (years)	9.7±2.4	7.6±2.7	9.8±3.3
Height (SDS)	−1.5±0.7	−1.1±0.9	
Weight (SDS)	−1.6±0.6	−1.1±1.0	
Hemoglobin (g/dl)	9.3±0.8	8.8±1.1	
Serum ferritin (ng/ml)	306.0±185.0	130.7±111.3***	
Serum potassium (mmol/l)	5.1±0.4	4.6±0.3	
Estimated GFR[b] (ml/min per 1.73 m^2)	109.1±19.3	104.0±18.5	
Urine osmolarity (mosmol/kg)	639.3±238.2	733.0±230.2	836.6±273.7
Urine urea nitrogen (mg/dl)	536.5±230.4**	616.7±256.9**	1,034.0±393.4
Urine protein (mg)/creatinine (mg)	0.97±1.69*	0.22±0.35	0.07±0.01
Urine NAG (unit)/g creatinine	27.5±44.4*	26.5±18.2*	3.5±1.7
Urine MDA (nmol)/mg creatinine	4.8±1.1**	3.9±1.8**	0.5±0.2
Urine β_2-microglobulin (μg)/mg creatinine	114.8±37.2*	137.1±92.9*	11.3±9.2

*P<0.05, **P<0.001 patients versus controls using unpaired two–tailed Student's *t*–test

***P<0.05 group 1 versus group 2 using unpaired two–tailed Student's *t*–test

[a] Values are mean±standard deviation

[b] As calculated by Schwartz's formula 0.55xheight (cm)/plasma creatinine (mg/dl)

[c] Group 1 consists of patients who had splenectomy for at least 2 years; group 2 are patients with intact spleens

study. Mean age was 8.2±2.8 years (range 3.4–13 years). Nine patients (90%) in group 1 and 11 patients (45.8%) in group 2 were Hb H/ HbCS patients. Table 1 summarizes the demographic data of patients and controls. No patient had hypertension. The mean time from splenectomy in group 1 patients was 3.5±1.4 years.

Blood urea nitrogen and serum creatinine levels were all within normal limits. Using Schwartz's formula [5] all patients had normal GFR. Serum electrolytes were normal, except for a marginally high mean serum potassium level in group 1. Six patients in group 1 and 1 patient in group 2 had serum potassium levels higher than 5 mmol/l, but only 1 patient in group 1 had a serum potassium level higher than 5.5 mmol/l.

Two patients (5.9%) had generalized aminoaciduria, 1 in each group. About half of the patients in both groups had fasting morning urine osmolality less than 700 mosmol/kg, no statistical difference was found between either group or control. The urine urea nitrogen was lower than in controls in both groups. Urine protein and sugar by Labstix were negative in all. None of the patients had microscopic hematuria. An elevated urine protein/creatinine ratio was recorded in 60% of group 1 and 29% of group 2.

Urine NAG, MDA, and β_2-microglobulin levels were increased in the patients, but no difference was found between the two groups. Urine protein was markedly increased in group 1. Using two-tailed Pearson test, significant correlations ($P<0.01$) were found between urinary NAG and MDA, β_2-microglobulin and MDA, β_2-microglobulin and NAG, and urine osmolality and MDA. Correlation was also found between serum ferritin and urine protein ($P<0.01$), but no other urine parameters. No correlation was found between Hb levels and any of the urine parameters (data not shown).

Discussion

We report proximal tubular dysfunction in children with α-thalassemia. The key abnormalities included increased levels of urine NAG, MDA, and β_2-microglobulin. Proteinuria, as detected by urinary protein/creatinine ratio, was increased in both groups of patients. Dipstick tests, which were used to detect proteinuria at the bedside, on the other hand, gave negative results. This could be explained by the fact that the dipstick test is known to detect mostly urinary albumin, as commonly found in glomerular diseases. In these cases the proteinuria was mainly due to low molecular weight tubular proteins, which could have caused the negative dipstick results. Increased urine NAG [13, 14] and β_2-microglobulin [13, 15, 16] are highly specific for proximal tubular disease in children as well as in adults. NAG is a high molecular weight lysosomal enzyme released from damaged tubular cells that has been used successfully as a marker of tubular dysfunction in various diseases [13, 14, 15, 16, 17, 18]. β_2-Microglobulin, a low molecular weight protein, is a sensitive and reliable marker of tubular dysfunction [15, 16, 17, 18]. The cause of renal tubular dysfunction in these patients is not known. Recently, we and others reported proximal tubular defects in children with β-thalassemia and postulated that anemia and iron deposition may be key factors [3, 19, 20]. In thalassemia, the imbalance in synthesis of Hb leads to excess unpaired globin chain and a high intracellular content of non-Hb iron. The unstable Hb subunits are known to generate free oxygen radical species, starting a chain of oxidative events, leading to disintegration to denatured globin chains, heme, and iron, which bind to different membrane proteins, altering the normal structure and function. The excess free iron is known to be a catalyst of lipid peroxidation via the Fenton reaction [21, 22, 23]. In both the β-thalassemia patients described previously and the α-thalassemia patients described in this study, proximal tubular dysfunction was associated with increased MDA levels. This suggests that there is a common mechanism of renal tubular injury [3].

Since most patients in Thailand cannot afford the high cost of iron chelation and regular blood transfusion, splenectomy has been the treatment of choice. Marked improvement of serum Hb, weight, and height (standard deviation scores) was observed after splenectomy. In our study, the group of splenectomized patients had slightly higher Hb levels, but other hematological parameters were similar. Both groups had similar levels of tubular dysfunction. Our previous study in β-thalassemia patients described less renal tubular dysfunction in a group receiving hypertransfusion and iron chelation. The α-thalassemia patients in this study were clinically less severe than the β-thalassemia patients in our previous study, as evidenced by the lower degree of growth failure and anemia, and lower serum ferritin levels. However, the degree and pattern of renal abnormalities are similar [3]. Moreover, group 2 patients with only marginally increased serum ferritin levels still have the same degree of renal dysfunction. We do not know why the degree of renal dysfunction is similar in patients with different iron metabolism, including those who had had good response to therapy (iron chelation, frequent transfusion, and/or splenectomy). It could be that the tubular damage is irreversible. Further study, in particular long-term follow-up in thalassemia patients before and after efficient iron chelation and hypertransfusion, is needed to clarify our observations.

Acknowledgement This study was funded by the Siriraj Grant for Research Development and Medical Education, Siriraj Hospital, Thailand (grant no. 75–348–292). P. Malasit is a recipient of the Senior Scholar Grant from the Thailand Research Fund. The Medical Molecular Biology Laboratory also operates as the Medical Biotechnology Unit funded by the National Center for Genetic Engineering (BIOTEC) of the National Science and Technology Development Agency (NSTDA), Thailand.

References

1. Winichagoon P, Thonglairuam V, Fucharoen S, Tanphaichitr VS, Wasi P (1988) Alpha-thalassemia in Thailand. Hemoglobin 12:485–498
2. Orkin SH, Nathan DG (1998) The thalassemias. In: Nathan DG, Orkin SH (eds) Nathan and Oski's hematology of infancy and childhood, 5th edn. Saunders, Philadelphia, pp 811–886
3. Sumboonnanonda A, Malasit P, Tanphaichitr VS, Ong-ajyooth S, Sunthornchart S, Pattanakitsakul S, Petrarat S, Assateerawatt A, Vongjirad A (1998) Renal tubular function in β-thalassemia. Pediatr Nephrol 12:280–283
4. Fucharoen S, Winichagoon P, Pootrakul P, Piankijgum A, Wasi P (1988) Differences between two types of Hb H disease, alpha-thalassemia$_1$/alpha-thalassemia$_2$ and alpha-thalassemia$_1$/Hb Constant Spring. Birth Defects 23:309–315
5. Schwartz GJ, Haycock GB, Edelmann CM Jr, Spitzer A (1976) A simple estimate of glomerular filtration rate in children derived from body length and plasma creatinine. Pediatrics 58:259–263
6. Tanphaichitr VS, Mahasandana C, Suvatte V, Yodthong S, Pung-amritt P, Seeloem J (1995) Prevalence of hemoglobin E, alpha-thalassemia and glucose-6-phosphate dehydrogenase deficiency in 1,000 cord blood studies in Bangkok. Southeast Asian J Med Public Health 26 [Suppl 1]:271–274
7. Tanner JM, Whitehouse RH, Cameron N, Marshall WA, Healy MJR, Goldstein H (1990) Assessment of skeletal maturity and prediction of adult height (TW2 method), 2nd edn. Alden, Oxford
8. Moor JC, Moris JE (1982) A simple automated colorimetric method for determination of *N*-acetyl-β-D-glucosaminidase. Ann Clin Biochem 19:157–159
9. Efran ML, Young O, Moser HW, MacCready RA (1964) A simple chromatography screening test for the detection of disorder of amino acid metabolism. N Engl J Med 270:1378–1380
10. Knight JA, Smith SE, Kinder VE, Pieper RK (1988) Urinary lipoperoxides quantified by liquid chromatography and determination of reference values for adults. Clin Chem 34: 1107–1110
11. Lim CW, Chisnall WN, Stokes YM, Debnam PM, Crooke MJ (1990) Effects of low and high relative molecular protein mass on four methods for total protein determination in urine. Pathology 22:89–92
12. Hemmingsen I, Skaarup P (1985) β_2-Microglobulin in urine and serum determined by ELISA technique. Scand J Clin Invest 45:367–371
13. Price RG (1982) Urinary enzymes, nephrotoxicity and renal disease. Toxicology 23:99–134
14. Kunin CM, Chesney RW, Craig WA, England AC, De Angelis C (1978) Enzymuria as a marker of renal injury and disease: studies of *N*-acetyl-β-glucosaminidase in the general population and in patients with renal disease. Pediatrics 62:751–760.
15. Guder WG, Hofmann W (1992) Markers for the diagnosis and monitoring of renal tubular lesions. Clin Nephrol 38 [Suppl 1]:S3–S7
16. Portman RJ, Kissane JM, Robson AM (1986) Use of β_2 microglobulin to diagnose tubulo-interstitial renal lesions in children. Kidney Int 30:91–98
17. Tomlinson PA (1992) Low molecular weight proteins in children with renal disease. Pediatr Nephrol 6:565–571
18. Piscator M (1989) Markers of tubular dysfunction. Toxicol Lett 46:197–204
19. Michelakakis H, Dimitriou E, Georgakis H, Karabatsos F, Fragodimitri C, Saraphidou J, Premetis E, Karagiorga-Lagana M (1997) Iron overload and urinary lysosomal enzyme levels in beta-thalassemia major. Eur J Pediatr 156:602–604
20. Aldudak B, Karabay Bayazit A, Noyan A, özel A, Anarat A, Sasmaz I, KilinÇ Y, Gali E, Anarat R, Dikmen N (2000) Renal function in pediatric patients with β-thalassemia major. Pediatr Nephrol 15:109–112
21. Shinar E, Rachmilewitz EA (1990) Oxidative denaturation of red blood cells in thalassemia. Semin Hematol 27:70–82
22. Hebble RP (1985) Auto-oxidation and a membrane-associated "Fenton reagent": a possible explanation for development of membrane lesions in sickle erythrocytes. Clin Haematol 14: 129–140
23. Boyce NW, Holdsworth SR (1986) Hydroxyl radical mediation of immune renal injury by desferroxamine. Kidney Int 30:813–817

Haemophilia (2003), 9, 179–186

Genotype and phenotype of haemophilia A in Thai patients

P. YENCHITSOMANUS,* V. AKKARAPATUMWONG,† P. PUNG-AMRITT,‡ S. INTORASOOT,† P. THANOOTARAKUL,* S. ORANWIROON,* G. VEERAKUL‡ and C. MAHASANDANA‡

**Divisions of Medical Molecular Biology and Molecular Genetics, Department of Research and Development, Faculty of Medicine Siriraj Hospital, and Medical Biotechnology Unit, National Center for Biotechnology and Genetic Engineering (BIOTEC), National Science and Technology Development Agency (NSTDA), Bangkok; †Institute of Molecular Biology and Genetics, Mahidol University, Salaya Campus, Nakorn Pathom; ‡Division of Hematology, Department of Pediatrics, Faculty of Medicine Siriraj Hospital, Mahidol University, Bangkok, Thailand*

Summary. To study genotype and phenotype correlation of haemophilia A in Thai patients, molecular defects of the factor VIII (*FVIII*) gene were examined and their correlation with clinical phenotypes were evaluated. The molecular pathologies of *FVIII* in Thai patients were found to be heterogeneous. The most common mutation was *FVIII* intron 22 inversion accounting for about 30% of the severe cases while gene deletion was rare. Sixteen point mutations were identified, comprising two nonsense mutations (R-5X and R1966X), five missense mutations (T233I, D542Y, G1850V, W2229S and G2325C), five nucleotide deletions (1145delT, 1187–8delACAC, 1191–4delA, 1458delGA and 1534delA), three nucleotide insertions (1439–41insA, 1934insTA and 2245insACTA) and one splicing defect (IVS15+1G>T). Nine mutations (T233I, D542Y, 1145delT, 1458delGA, 1534delA, 1934insTA, W2229S, 2245insACTA and G2325C) were novel, firstly identified in Thai patients. The genotypes were found to correlate with clinical phenotypes in a majority of cases. However, in five patients the molecular defects did not correlate with clinical severity and FVIII:C level. Cellular and molecular mechanisms were proposed to be responsible in amelioration of clinical severity caused by deleterious mutations. Carrier detection by direct mutation analysis was also demonstrated.

Keywords: factor VIII, *FVIII* gene, haemophilia A, mutation, Thai

Introduction

Factor VIII (*FVIII*) mutations causing haemophilia A (MIM *306700; F8C) are heterogeneous [1,2] (see also http://europium.csc.mrc.ac.uk). Gene inversion results from intrachromosomal inversion between homologous sequence in intron 22 (*int22h-1*) of *FVIII* and one of its two telomeric inverted copies (*int22h-2* and *int22h-3*) [3–5] is most frequent, identified in about 45% of the severe haemophilia A cases. Recently, a new type of *FVIII* gene-inversion with breaking site in intron 1 accounting for about 5% of severe cases of haemophilia A was reported [6]. In addition, a spectrum of other *FVIII* pathological defects described is characterized by an extensive heterogeneity with a predominance of private mutations and a relatively high rate of *de novo* sequence alterations [2].

To understand genotype and phenotype correlation and to develop methods for direct mutation analysis, we analysed *FVIII* in Thai patients with haemophilia A. Here, we report a collective data from our studies during the past several years. Although generally genotypes in a majority of the cases of haemophilia A in Thai correlate well with clinical phenotypes, a group of five patients with deleterious *FVIII* mutations had moderate clinical severity. Cellular and molecular mechanisms were proposed to account for the amelioration of the disease severity in these patients. In addition to carrier detection by linkage analysis regularly performed in families with haemophilia A under our care, direct mutation analysis has been applied to the families with identified *FVIII* mutations. As examples, the direct mutation analyses in

Correspondence: Pa-thai Yenchitsomanus, Division of Medical Molecular Biology, Department of Research and Development, Faculty of Medicine Siriraj Hospital, Mahidol University, Bangkok 10700, Thailand. Tel./fax: +662 4184793; e-mail: grpye@mahidol.ac.th

Accepted after revision 21 January 2003

three families with haemophilia A were also demonstrated.

Materials and methods

Subjects and blood samples

The subjects included in this study were patients with haemophilia A and their families who attended the Hematology Clinics of the Department of Pediatrics, Faculty of Medicine Siriraj Hospital, Mahidol University, Bangkok. The diagnosis of haemophilia A was based on clinical, haematological and coagulation findings. FVIII activity (FVIII:C) was determined by one-stage clotting assay [7]. Commercial plasma with 0% and 100% FVIII:C were used as controls in the clotting assay. A standard curve was constructed from the control plasmas with different FVIII:Cs for estimation of FVIII:C in the patients' plasma.

Variable numbers of patients were studied by different molecular methods (described below), which were conducted as separate projects at different times during a period of several years. About 15 mL of blood samples were collected with informed consent for mRNA and genomic DNA preparations. Total RNA was extracted from isolated lymphocytes by using Trizol^{TM} reagent (Gibco BRL, Gaithersburg, MD, USA). Genomic DNA was prepared from the remaining white blood cells by the standard phenol–chloroform extraction procedure. DNA linkage was analysed by using both intragenic and extragenic polymorphic DNA markers in the *FVIII* region [8], which included *Bcl* I-RFLP in intron 18 [9], microsatellites (CA repeats) in introns 13 and 22 [10,11] and extragenic St14 (DXS 52) VNTR [12]. Haplotypes in the *FVIII* region were constructed by using Cyrillic 2 program (Cherwell Scientific Publishing).

Analysis of FVIII deletion

FVIII deletion was analysed by multiplex PCR method; the details of this analysis have been described previously [13].

Analysis of FVIII intron 22 inversion

FVIII intron 22 inversion was examined by Southern-blot hybridization [3]. Genomic DNA samples were digested with *Bcl* I, electrophoresed on agarose gel, transferred to a nylon membrane, hybridized with α^{32} P dCTP-labelled p482.6 probe (ATCC, catalogue no. 57203) and subjected to autoradiography. The result was examined and interpreted as previously described [3].

Analysis of FVIII point mutations

FVIII coding and essential sequences isolated by long-range reverse transcriptase-PCR (RT-PCR) and PCR were used for analysis of point mutations by single strand conformation polymorphism (SSCP) and nucleotide sequencing as described previously [14]. Full-length *FVIII*-cDNA (9 kb) was synthesized from total RNA by Superscript II kit (Gibco BRL) using oligo(dT)$_{12-18}$ primer. The cDNA was further amplified by long-range PCR using a pair of primers flanking the *FVIII* open reading frame. The coding sequences between exons 1 and 13, and between exons 15 and 26 were isolated into four fragments by nested amplifications from the product of long-range PCR by using four pairs of primers as described [15]. The sequences of putative promoter, exon 14, and the polyadenylation signal region of *FVIII* were amplified from genomic DNA [15].

FVIII mutations were screened by a non-radioactive SSCP analysis [14]. All the amplified fragments, except for the polyadenylation signal region, were digested with multiple restriction enzymes in order to generate fragments with suitable sizes for the SSCP analysis. The fragments showing abnormal electrophoretic mobility on SSCP gel compared to normal control fragments were subjected to nucleotide sequencing by either a manual method or an automated sequencer (ABI 377, PE Applied Biosystems).

Amino acid sequences of human, murine and pig factor VIII; human, murine and bovine factor V; and human and rat ceruloplasmin were translated from mRNA or cDNA sequences retrieved from GenBank and EMBL databases (accession numbers: M14113, L05573, U49517, M16967, U52925, M81441, M13699 and L33869, respectively) for analysis of conserved motifs by Clustral X, multiple sequence alignment program [16].

Evaluation of genotype and phenotype correlation

The correlation between molecular defects identified and clinical phenotype of haemophilia A in the patients was evaluated. Severity of the molecular defects was considered from their types of mutations and effects on *FVIII* expression and FVIII protein structure and function. The criteria for grading clinical phenotypes were based on clinical manifestations, bleeding frequency and plasma FVIII:C activity. For quality control, FVIII:C activities were normally measured in the presence of positive (100% FVIII:C) and negative (0% FVIII:C) control plasmas. In case of doubt, the FVIII:C assay would be repeated

once or more using plasmas from the same patient. The FVIII:C activities of <1%, 2–5% and 6–30% were generally associated with severe, moderate and mild disease, respectively. The patient with mild haemophilia A had only occasional post-traumatic bleeding while the patient with moderate disease would have post-traumatic and occasional spontaneous bleeding episodes. The patient with severe disease had frequent spontaneous bleeding episodes, which usually required FVIII replacements.

Carrier detection by mutation analysis

Different techniques, including PCR-SSCP, heteroduplex analysis (HA), and allele specific amplification (ASA), were performed for analysis of *FVIII* mutations inherited in the affected families for the purpose of carrier detection. Details of the procedures and parts of the results have been described in our previous works [17,18].

Results

Altogether, 70 families containing 78 patients with haemophilia A were studied. Of these 70 families, two were families with mild, 16 with moderate and 52 with severe disease. All 70 families were screened for *FVIII* gene deletion by multiplex PCR but 59 were examined for *FVIII* intron 22 inversion by Southern-blot hybridization. The patients with mild haemophilia A and some with moderate and severe disease were not studied for *FVIII* intron 22 inversion. Twenty-seven families were analysed for point mutations by RT-PCR and SSCP method; 23 of 27 families had been excluded for the *FVIII* intron 22 inversion but three were not examined for this inversion.

FVIII gene deletion was found in only one of 70 families with haemophilia A when screened with multiplex PCR that simultaneously amplified sequences of seven exons [13]. The patient with this deletion had severe haemophilia A. The deletion spanned 2.2 kb DNA region extending from exon 26 to the 3′ non-coding sequence of *FVIII* [13]. *FVIII* intron 22 inversion was observed in 16 of 59 (27%) families with moderate and severe haemophilia A. Of these, 47 families had severe haemophilia A and 12 families had moderate disease. Considering only the families with severe disease, the *FVIII* intron 22 inversion was found in 14 of 47 families (29.8%). The *FVIII* intron 22 inversion type I (distal) was found in 14 families (87.5%) while type II was seen in two families (12.5%). Surprisingly, gene inversion (type I) was also detected in two patients with moderate disease, with FVIII:C of 3.7% and 3.0%. A *de novo FVIII* intron 22 inversion type I might be present in one family where it was observed only in the affected child but not in the mother. However, a maternity testing has not yet been carried out to confirm their biological relationship.

Point mutations of *FVIII* were analysed by RT-PCR and SSCP followed by nucleotide sequencing in the families with haemophilia A that did not have *FVIII* gene deletion or intron 22 inversion. A total of 16 mutations were identified in 16 out of 27 families studied (Table 1). In the remaining 11 families, mutations have not been found; this might be because of the sensitivity of the screening PCR-SSCP method used. The sensitivity of detection by this method was about 60%. The mutations that were identified comprised two nonsense mutations (R-5X and R1966X), five missense mutations (T233, D542Y, G1850V, W2229S and G2325C), five nucleotide deletions (1145delT, 1187–8delACAC, 1191–4delA, 1458delGA and 1534delA), three nucleotide insertions (1439–41insA, 1934insTA and 2245insACTA) and one splicing defect (IVS15+1G>T). One nonsense, R-5X, mutation was found to be associated with a moderate haemophilia A phenotype with a repeatable FVIII:C of 2.8% while the patient's mother did not carry this alteration, indicating a *de novo* mutation. Two frameshift (1191–4delA and 1439–41insA) mutations, instead of causing severe haemophilia A, resulted in moderate clinical phenotype with FVIII:C of 4.2% and 2.8%. All missense mutations occurred in conserved amino acid sequences. Nine mutations including T233, D542Y, 1145delT, 1458delGA, 1534delA, 1934insTA, W2229S, 2245insACTA and G2325C were novel and had never been observed in other populations but were firstly identified in Thai patients. We have submitted some of these mutations to the HAMSTeRS database. As the number of patients analysed by each method was not equal, the overall efficiency of the mutation detection techniques could not be estimated accurately; perhaps, it was lower than 50%.

After *FVIII* mutations were identified, carrier detection by direct mutation analysis was performed by suitable techniques. As examples, three techniques (PCR-SSCP, HA and ASA) were conducted for direct mutation analyses in three families (family numbers 21, 72 and 14) with different types of mutations (W2229S, 1187–8delACAC and T233I, respectively). The results are shown in Fig. 1. In families 21 and 72 (Fig. 1a,b), three female carriers each were detected and/or confirmed; in family 14 (Fig. 1c), two female carriers and one non-carrier were identified.

Table 1. Mutations of *FVIII* in 17 Thai families with haemophilia A (*FVIII* intron 22 inversion was not included).

Family number	Type of mutation	Mutation	Exon	Codon*	Domain	Clinical severity	FVIII:C (%)
3	Nonsense	CGA → TGA(R-5X)	1	−5	Signal†	Moderate	2.8
14	Missense	ACA → ATA (T233I)	6	233	A1	Moderate	2.5
29	Missense	GAT → TAT (D542Y)	11	542	A2	Severe	<1
7	Frameshift	1-bp deletion (T)	14	1145	B	Severe	<1
72	Frameshift	4-bp deletion (ACAC)	14	1187–8	B	Severe	<1
20	Frameshift	1-bp deletion (A)	14	1191–4	B	Moderate	4.2
15	Frameshift	1-bp insertion (A)	14	1439–41	B	Moderate	2.8
33	Frameshift	2-bp deletion (GA)	14	1458	B	Severe	<1
13	Frameshift	1-bp deletion (A)	14	1534	B	Severe	<1
8	Splicing defect	IVS15+1G>T	(15–16)	(1721–1788)	A3	Severe	<1
49	Missense	GGC → GTC(G1850V)	17	1850	A3	Severe	<1
70	Frameshift	2-bp insertion (TA)	18	1934	A3	Severe	<1
11	Nonsense	CGA → TGA(R1966X)	18	1966	A3	Severe	<1
21	Missense	TGG → TCG (W2229S)	25	2229	C2	Moderate	4.0
27	Frameshift	4-bp insertion (ACTA)	25	2245	C2	Severe	<1
28	Missense	GGC → TGC(G2325C)	26	2325	C2	Moderate	3.0
53	Deletion	>2.2 kb deletion	26-3′ end	(2281–2332)	C2	Severe	<1

*Codons are numbered as described [14].
†Signal peptide.

Discussion

Mutations of *FVIII* in Thai patients with haemophilia A were analysed in order to understand molecular defects, evaluate genotype and phenotype correlation and develop methods for direct mutation analysis. The *FVIII* mutations identified in the Thai patients included a partial (>2.2 kb) gene deletion in one patient, intron 22 inversion in 16 patients and various types of point mutations in 16 patients. *FVIII* gene deletion in the Thai patients was rare, similar to that found in other ethnic groups [1,19]. The *FVIII* intron 22 inversion, the most common mutation in the patients with severe haemophilia A accounting for 45% of the cases [20–23], was observed in about 30% of the Thai patients with severe disease. The lower percentage of this mutation in the Thai patients might be because of its variation in different ethnic groups or perhaps relatively greater clinical severity causing mortality, which led to reduction in frequency of the defective allele. The new type of *FVIII* gene inversion with breaking site in intron 1, which accounts for 5% of severe haemophilia A [6], has not been determined in Thai patients. It is interesting to analyse the *FVIII* intron 1 inversion in our patients in the near future.

The correlation between genotype and phenotype in the Thai patients with haemophilia A was evaluated. It was found that in a majority of patients molecular defects of *FVIII* correlated well with the clinical phenotypes and FVIII:C level. The patients with the *FVIII* gene deletion (one case), intron 22 inversion (14 cases), nonsense mutation (one case), frameshift mutation (six cases) and splicing defect (one case) presented with severe clinical phenotypes (e.g. frequent spontaneous bleeding episodes) with FVIII:C <1%. These mutations caused serious effects to the gene, totally disrupted gene expression and thus resulted in a complete FVIII deficiency.

The patients with missense mutations might cause either severe (two cases) or moderate (three cases) clinical phenotype (Table 1), depending on types of amino acid substitutions, their positions and roles in the protein structure and function. In the group with severe clinical phenotype, two missense mutations (D542Y and G1850V) were substitutions of hydrophilic negatively charged and non-hydrophobic amino acids by hydrophobic amino acids in the highly conserved regions of A2 and A3 domains of the FVIII protein, respectively.

In the group with moderate clinical phenotype, one missense (T233I) was a substitution of polar hydrophilic amino acid by hydrophobic amino acid in domain A1. Although it was a non-conservative amino acid change, the region where T223 locates is less conserved, connected to a region of non-conserved amino acid sequence in the FVIII protein. One missense mutation (W2229S) was a substitution of an aromatic hydrophobic-neutral amino acid by a polar hydrophilic-neutral amino acid and the other (G2325C) was a substitution of aliphatic-neutral amino acid by polar hydrophobic-neutral amino

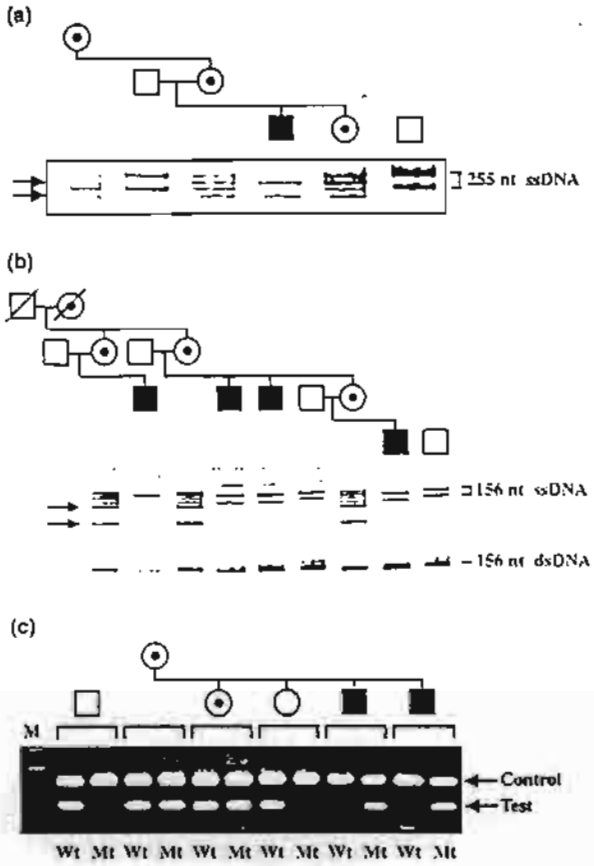

Fig. 1. Carrier detection by direct mutation analysis of *FVIII* in three Thai families with haemophilia A (family numbers 21, 72 and 14) carrying three different mutations (W2229S, 1187-8del-ACAC and T2331, respectively) by three techniques: (a) SSCP, (b) HA and (c) ASA. Arrows in 'a' and 'b' indicate mobility shifts of single-stranded DNAs and heteroduplex DNAs, respectively. In 'c', each DNA sample was separately amplified by wild-type (Wt) and mutant (Mt) primers paring with a common primer, as well as a pair of internal control primers. Female carrier showed positive amplifications by both pairs of primers, while normal female or affected male showed a positive amplification for wild-type or mutant primers, respectively. The symbols used are as follows:, □ = normal male;, ■ = affected male; ⊙ = carrier, ⌀ = dead male, ⌀ = dead carrier.

acid. Both substitutions were in the C2 domain of the protein. Although W2229S might result in change of hydrophobicity, this might not be strictly crucial as it was located within a less conserved sequence, flanked by several charged amino acids. Although G2325C created additional cysteine, with potential to disrupt normal disulphide bonding, a normal cysteine (C2326) was also located next to this substitution. Thus, if the disulphide bonding was formed, one of the two cysteines, either C2325 or C2326, might be used. However, the two adjacent cysteines might not exactly behave the same since the G2325C substitution caused a reduction of FVIII:C activity although it was not totally lost. These three amino acid substitutions probably occurred in the positions that were less critical than those of the first two substitutions.

However, there were five patients whose molecular defects of *FVIII* did not correlate with the clinical phenotype and FVIII:C level. Instead of having a severe clinical manifestation with complete absence of the FVIII activity, two patients with *FVIII* intron 22 inversion, one with nonsense (R-5X) mutation and two with frameshift (1191–4delA and 1439–41insA) mutations had a moderate severity, without frequent spontaneous bleeding episodes, with FVIII:C of 3.7%, 3.0%, 2.8%, 4.2% and 2.8%, respectively. The FVIII:C assays in these patients were repeated twice or more and the quality of the assays was well controlled. Four patients were sporadic cases, except for one with frameshift (1439–41insA) mutation.

These mutations were deleterious and would completely inactivate the gene. The FVIII protein and activity should not be present in these patients. The possible explanation for moderate severity with considerably high FVIII:C in the first three cases, two with the *FVIII* intron 22 inversion and one with nonsense (R-5X) mutation, would be that these patients carried *de novo* mutations with somatic mosaicism when the mutations occurred post-zygotically [19,24,25]. The FVIII protein would possibly be synthesized from the cells bearing normal *FVIII* allele. Although there was no evidence for a *de novo* mutation in the two patients with *FVIII* intron 22 inversion since their families were not available for the studies, there was a clear evidence supporting a *de novo* alteration in the patient with nonsense (R-5X) mutation [14,17] that the mutation was not observed in the patient's mother who inherited the same *FVIII* haplotype to the patient [17]. Thus, the present of FVIII:C activity might be because of post-zygotic somatic mosaicism in this patient. In addition, a *de novo FVIII* intron 22 inversion with usual severity was possibly also present in one family in this study although this still requires a confirmation for the biological relationship. Post-zygotic *de novo FVIII* intron 22 inversion as the cause of somatic mosaicism in a female carrier has been documented [26]. A relatively high frequency of *de novo* sequence alterations and somatic mosaicism in haemophilia A [19,27] makes it most likely to be a cellular mechanism ameliorating severity of the disease caused by these harmful mutations in Thai patients.

Two patients with frameshift (1191–4delA and 1439–41insA) mutations would create premature termination at codons 1198 and 1442, respectively, resulting in FVIII protein truncations, which would cause a severe clinical phenotype. However, these frameshift mutations were observed in the two patients with moderate clinical phenotype with FVIII:C of 4.2% and 2.8% and absence of frequent spontaneous bleedings. The deletion and insertion of 'A' nucleotide in these two frameshift mutations occurred in the sequences within the runs of 9 As (at codons 1191–4) and 8 As (at codons 1439–41) in exon 14 of *FVIII*, respectively [28]. There are many cases with an 'A' deletion or insertion in the run of 9 As at codons 1191–4, and with an 'A' insertion in the run of 8 As at codons 1439–41 listed in the Hemophilia A Database (http://europium.csc.mrc.ac.uk). Many cases with these mutations were associated with severe haemophilia A but the FVIII:C activity was not recorded in several cases. However, there were several cases with these mutations that had the FVIII:C activities between 2 and 5%. In addition, there was at least four cases with these mutations that had moderate clinical phenotype. Thus, it is certain that there were cases carrying these mutations with higher FVIII:C activities than that of other severe cases and some of these patients also presented moderate clinical phenotype. The deletion and insertion in these runs of polyA nucleotides were likely to cause moderate clinical phenotype in the patients of the present study due to a partial correction of translational reading frame because of errors during *FVII* expression. A partial correction of a severe molecular defect, a deletion of 'T' nucleotide at codon 1441 (1441delT) within an A8TA2 sequence in exon 14 of *FVIII*, due to errors during *FVIII* expression has been reported previously [29]. This nucleotide deletion was characterized in Japanese patients with mild to moderately severe haemophilia A. The deletion of 'T' nucleotide at codon 1441 (1441delT) in the A8TA2 sequence resulted in the consecutive running of 10 As, and a significant number of in-frame mRNA transcripts was produced in the patient. The authors concluded that the errors in DNA replication or RNA transcription/translation resulted in a partial restoration of the correct reading frame and in amelioration of the severe clinical phenotype. The same molecular mechanism is thus likely to also occur in the two Thai patients with haemophilia A, who had the frameshift (1191–4delA and 1439–41insA) mutations with the moderate clinical phenotype. Thus, the reduction in severity of disease in the patients carrying deleterious mutations may naturally involve either cellular or molecular mechanisms.

Linkage analysis has been used for haemophilia A carrier detection [30,31]. In our recent work [17], we have demonstrated that direct mutation analysis was also feasible for determination of haemophilia A carrier status. Carrier detection by direct mutation analysis was successful in almost all families with known *FVIII* mutations and as additional examples this was demonstrated in three families (Fig. 1). The PCR-SSCP and HA techniques are efficient for detection of the mutations that change, respectively, single- and double-stranded DNA molecules. Nucleotide substitutions in some types and positions would be detected by PCR-SSCP while nucleotide deletions/insertions are more likely to be detected by both PCR-SSCP and HA. ASA is a more universal technique applicable to all types of point mutations when the primers are well designed and PCR conditions are rightly optimized. These three techniques can readily be performed in a general molecular genetic laboratory, requiring unsophisticated equipment. In an advanced laboratory, more efficient, automated analytical techniques such as denaturing high-pressure liquid chromatography [32] and DNA sequencing [33,34] would be the methods of choice.

Acknowledgements

This work was supported by a research grant from the National Center for Genetic Engineering and Biotechnology (BIOTEC), National Science and Technology Development Agency (NSTDA), Bangkok, Thailand. The authors would like to thank for the kind support from Dr Prida Malasit, the Deputy Dean of Research, and the Director of Division of Medical Molecular Biology, Department of Research and Development, Faculty of Medicine Siriraj Hospital, Mahidol University, and the Director of Medical Biotechnology Unit, BIOTEC, NSTDA, and to Professor Sakol Panyim, the Director of Institute of Molecular Biology and Genetics, Mahidol Universtiy. The two supporters are also the recipients of Senior Scholar Award of Thailand Research Fund (TRF).

References

1 Antonarakis SE, Kazazian HH, Tuddenham EGD. Molecular etiology of factor VIII deficiency in hemophilia A. *Hum Mutat* 1995; 5: 1–22.

2 Kemball-Cook G, Tuddenham EGD, Wacey AI. The factor VIII structure and mutation resource site:

HAMSTeRS version 4. *Nucleic Acids Res* 1998; 26: 216–9.
3 Lakich D, Kazazian HH Jr., Antonarakis SE, Gitschier J. Inversions disrupting the factor VIII gene are a common cause of severe haemophilia A. *Nat Genet* 1993; 5: 236–41.
4 Naylor JA, Green PM, Rizza CR, Giannelli F. Analysis of factor VIII mRNA reveals defects in everyone of 28 haemophilia A patients. *Hum Mol Genet* 1993; 2: 11–7.
5 Naylor JA, Buck D, Green P, Williamson H, Bentley D, Giannelli F. Investigation of the factor VIII intron 22 repeated region (int22h) and the associated inversion junctions. *Hum Mol Genet* 1995; 4: 1217–24.
6 Bagnall RD, Waseem N, Green PM, Giannelli F. Recurrent inversion breaking intron 1 of the factor VIII gene is a frequent cause of severe hemophilia A. *Blood* 2002; 99: 168–74.
7 Proctor PR, Rappaport SI. The partial thromboplastin time with kaolin. A simple screening test for first stage plasma clotting factor deficiencies. *Am J Clin Pathol* 1961; 36: 212.
8 Mahasandana C, Pung-amritt P, Treesucon A *et al.* Carrier detection by DNA linkage analysis in eighty Thai hemophilia A families. *J Med Assoc Thai* 2002; 85 (Suppl. 2): S513–21.
9 Kogan SC, Gitschier J. Genetic prediction of haemophilia A. In: Innis MA, Gelfand DH, Sninsky JJ, White TJ, eds. *PCR Protocols: a Guide to Methods and Applications*. San Diego: Academic Press, 1990: 288–99.
10 Lalloz MR, McVey JH, Pattinson JK, Tuddenham EG. Haemophilia A diagnosis by analysis of a hypervariable dinucleotide repeat within the factor VIII gene. *Lancet* 1991; 338: 207–11.
11 Lalloz MR, Schwaab R, McVey JH, Michaelides K, Tuddenham EG. Haemophilia A diagnosis by simultaneous analysis of two variable dinucleotide tandem repeats within the factor VIII gene. *Br J Haematol* 1994; 86: 804–9.
12 Richards B, Heilig R, Oberle I, Storjohann L, Horn GT. Rapid PCR analysis of the St14 (DXS52) VNTR. *Nucleic Acids Res* 1991; 19: 1994.
13 Pung-amritt P, Treesucon A, Petrarat S, Veerakul G, Mahasandana C, Yenchitsomanus PT. Factor VIII gene deletion in a Thai hemophilia A patient. *Asian Pac J Mol Biol Biotech* 1998; 6: 115–20.
14 Akkarapatumwong V, Oranwiroon S, Pung-amritt P *et al.* Mutations of the factor VIII gene in Thai hemophilia A patients. *Hum Mutat* 2000; 15: 117–8.
15 Naylor JA, Green PM, Montandon AJ, Rizza CR, Giannelli F. Detection of three novel mutations in two haemophilia A patients by rapid screening of whole essential region of factor VIII gene. *Lancet* 1991; 337: 635–9.
16 Thompson JD, Gibson TJ, Plewniak F, Jeanmougin F, Higgins DG. The CLUSTAL X windows interface: flexible strategies for multiple sequence alignment aided by quality analysis tools. *Nucleic Acids Res* 1997; 25: 4876–82.
17 Oranwiroon S, Akkarapatumwong V, Pung-amritt P *et al.* Determination of haemophilia A carrier status by mutation analysis. *Haemophilia* 2001; 7: 20–5.
18 Yenchitsomanus P, Thanootarakul P, Akkarapatumwong *et al.* Mutation causing exon 15 skipping and partial exon 16 deletion in factor VIII transcript, and a method for direct mutation detection. *Haemophilia* 2001; 7: 335–8.
19 Becker J, Schwaab R, Moller-Taube A *et al.* Characterization of the factor VIII defect in 147 patients with sporadic hemophilia A: family studies indicate a mutation type-dependent sex ratio of mutation frequencies. *Am J Hum Genet* 1996; 58: 65–70.
20 Rossiter JP, Young M, Kimberland ML *et al.* Factor VIII gene inversions causing severe hemophilia A originate almost exclusively in male germ cells. *Hum Mol Genet* 1994; 3: 1035–9.
21 Jenkins PV, Collins PW, Goldman E *et al.* Analysis of intron 22 inversions of the factor VIII gene in severe hemophilia A: implications for genetic counseling. *Blood* 1994; 84: 2197–201.
22 Windsor S, Taylor SA, Lillicrap D. Direct detection of a common inversion mutation in the genetic diagnosis of severe hemophilia A. *Blood* 1994; 84: 2202–5.
23 Antonarakis SE, Rossiter JP, Young M *et al.* Factor VIII gene inversions in severe hemophilia A: results of an international consortium study. *Blood* 1995; 86: 2206–12.
24 Levinson B, Lehesjoki AE, de la Chapelle A, Gitschier J. Molecular analysis of hemophilia A mutations in the Finnish population. *Am J Hum Genet* 1990; 46: 53–62.
25 Bröcker-Vriends AH, Briet E, Dreesen JC *et al.* Somatic origin of inherited haemophilia A. *Hum Genet* 1990; 85: 288–92.
26 Oldenburg J, Rost S, El-Maarri O *et al.* De novo factor VIII gene intron 22 inversion in a female carrier presents as a somatic mosaicism. *Blood* 2000; 96: 2905–6.
27 Leuer M, Oldenburg J, Lavergne JM *et al.* Somatic mosaicism in hemophilia A: a fairly common event. *Am J Hum Genet* 2001; 69: 75–87.
28 Akkarapatumwong V, Intorasoot S, Oranwiroon S *et al.* Frameshift mutations with severe and moderate clinical phenotypes in Thai hemophilia A patients. *Hum Mutat* 2000; 16: 530–1.
29 Young M, Inaba H, Hoyer LW, Higuchi M, Kazazian HH Jr, Antonarakis SE. Partial correction of a severe molecular defect in hemophilia A because of errors during expression of the factor VIII gene. *Am J Hum Genet* 1997; 60: 565–73.
30 Peake IR, Lillicrap DP, Boulyjenkov V *et al.* Haemophilia: strategies for carrier detection and prenatal diagnosis. *Bull World Health Organ* 1933; 71: 429–58.
31 Goodeve AC. Advances in carrier detection in haemophilia. *Haemophilia* 1998; 4: 358–64.

32 Oldenburg J, Ivaskevicius V, Rost S *et al.* Evaluation of DHPLC in the analysis of hemophilia A. *J Biochem Biophys Methods* 2001; 47: 39–51.

33 Vidal F, Farssac E, Altisent C, Puig L, Gallardo D. Rapid hemophilia A molecular diagnosis by a simple DNA sequencing procedure: identification of 14 novel mutations. *Thromb Haemost* 2001; 85: 580–3.

34 Citron M, Godmilow L, Ganguly T, Ganguly A. High throughput mutation screening of the factor VIII gene (F8C) in hemophilia A: 37 novel mutations and genotype-phenotype correlation. *Hum Mutat* 2002; 20: 267–74.

Journal of Human Genetics
10.1007/s10038-003-0059-6

Original Article

Anion exchanger 1 mutations associated with distal renal tubular acidosis in the Thai population

Pa-thai Yenchitsomanus[1, 2] ✉, Nunghathai Sawasdee[1], Atchara Paemanee[1, 2], Thitima Keskanokwong[1], Somkiat Vasuvattakul[3], Sasitorn Bejrachandra[4], Warunee Kunachiwa[5], Supan Fucharoen[6], Prapaporn Jittphakdee[7], Wanwimon Yindee[7] and Charupon Promwong[7]

(1) Division of Medical Molecular Biology, Department of Research and Development, Faculty of Medicine Siriraj Hospital, Mahidol University, 10700 Bangkok, Thailand

(2) Medical Biotechnology Unit, National Center for Biotechnology and Genetic Engineering (BIOTEC), National Science and Technology Development Agency (NSTDA), Bangkok, Thailand

(3) Division of Nephrology, Department of Medicine, Faculty of Medicine Siriraj Hospital, Mahidol University, Bangkok, Thailand

(4) Department of Transfusion Medicine, Faculty of Medicine Siriraj Hospital, Mahidol University, Bangkok, Thailand

(5) Department of Clinical Immunology, Faculty of Associated Medical Sciences, Chiang Mai University, Chiang Mai, Thailand

(6) Department of Clinical Chemistry, Faculty of Associated Medical Sciences, Khon Kaen University, Khon Kaen, Thailand

(7) Department of Pathology, Faculty of Medicine, Prince of Songkla University, Songkla, Thailand

✉ **Pa-thai Yenchitsomanus**
Email: grpye@mahidol.ac.th
Phone: +66-2-4184793
Fax: +66-2-4184793

Received: 5 June 2003 **Accepted:** 3 July 2003

Abstract We have previously demonstrated that compound heterozygous (SAO/G701D) and homozygous (G701D/G70D) mutations of the *anion exchanger 1* (*AE1*) gene, encoding erythroid and kidney AE1 proteins, cause autosomal recessive distal renal tubular acidosis (AR dRTA) in Thai patients. It is thus of interest to examine the prevalence of these mutations in the Thai population. The SAO and G701D mutations were examined in 844 individuals from north, northeast, central, and south Thailand. Other reported mutations including R602H, ΔV850, and A858D were also examined in some groups of subjects. The SAO mutation was common in the southern Thai population; its heterozygote frequency was 7/206 and estimated allele frequency 1.70%. However, this mutation was not observed in populations of three other regions of Thailand. In contrast, the G701D mutation was not found in the southern population but was observed in the northern, northeastern, and central populations, with heterozygote frequencies of 1/216, 3/205, and 1/217, and estimated allele frequencies of 0.23%, 0.73%, and 0.23%, respectively. The higher allele frequency of the

G701D mutation in the northeastern Thai population corresponds to our previous finding that all Thai patients with AR dRTA attributable to homozygous G701D mutation originate from this population. This suggests that the G701D allele might arise in northeastern Thailand. The presence of patients with compound heterozygous SAO/G701D in southern Thailand and Malaysia and their apparently absence in northeastern Thailand indicate that the G701D allele may have migrated to the southern peninsular region where SAO is common, resulting in pathogenic allelic interaction.

Keywords Anion exchanger 1 (AE1) - Band 3 protein - Southeast Asian ovalocytosis (SAO) - Distal renal tubular acidosis - Thai

Introduction

The human *anion exchanger 1* (*AE1* or *SLC4A1*; MIM 109270) gene, located on chromosome 17q21 (Lux et al. *1989*), encodes AE1 or band 3 protein in erythrocytes and α-intercalated cells of kidney (Sahr et al. *1994*). Erythroid AE1 (eAE1) contains 911 amino acids, whereas kidney AE1 (kAE1) lacks 65 amino acids at its N-terminus (Kollert-Jons et al. *1993*) because of the use of different promoters (Sahr et al. *1994*). The promoter for eAE1 is upstream of exon 1 and that for kAE1 is within intron 3 of the gene. AE1 is an integral membrane glycoprotein containing a long cytoplasmic N-terminus (~400 amino acids), 12–13 transmembrane domains, and a short cytoplasmic C-terminus (~35 amino acids). In erythrocytes, eAE1 forms dimers, tetramers, or higher oligomers on the cell membrane; in addition to having an anion (Cl^-/HCO^-_3) exchange function, these eAE1 oligomers serve as anchor proteins of the cytoskeleton network, binding to ankyrin, bands 4.1 and 4.2, and cytoplasmic proteins (Tanner *1993*, *1997*). In the α-intercalated cells, kAE1 is located at the basolateral membrane (Kollert-Jons et al. *1993*) and functions in anion (Cl^-/HCO^-_3) exchange.

Because of the expression of AE1 in two different cells with distinct functions, AE1 mutations show pleiotrophic effects resulting in two distinct and seemingly unrelated phenotypes: hereditary spherocytosis (or other forms of erythrocyte abnormalities) and distal renal tubular acidosis (dRTA). AE1 mutations have been found to account for approximately 20% of spherocytosis and almost all ovalocytosis in southeast Asia (Tanner *1997*; Tse and Lux *1999*; Bruce and Tanner *1996*). Southeast Asian ovalocytosis (SAO), a well-known erythrocyte disorder that is widespread in the southeast Asian regions, is caused by a deletion of 27 bp in codons 400–408 in exon 11 (Ex11Δ27) of *AE1* leading to an in-frame lack of 9 amino acids in the protein (Jarolim et al. *1991*), which is inactive for anion transport. AE1 mutations also result in dRTA, because the defect in AE1 affects anion (Cl^-/HCO^-_3) exchange at the basolateral membrane of the α-intercalated cells in the distal nephron of the kidney (Rodriguez-Soriano *2000*; Batlle et al. *2001*; Alper *2002*). The accumulation of bicarbonate (HCO_3^-) within these cells may lead to the reduction of carbonic acid (H_2CO_3) dissociation and hydrogen (H^+) ion secretion at the apical membrane of the cells and, finally, to acidosis.

During the past few years, abnormalities of *AE1* associated with dRTA have been extensively investigated, and its mutations have been found in several kindreds with autosomal dominant (AD) dRTA (Bruce et al. *1997*; Jarolim et al. *1998*; Karet et al. *1998*). The characterization of *AE1* in AD dRTA has identified multiple families (Bruce et al. *1997*; Jarolim et al. *1998*; Karet et al. *1998*) with missense mutations in codon 589 (R589H, R589S, R589C), one

family (Bruce et al. *1997*) with an S613F mutation, and another family (Karet et al. *1998*) with an 11-amino-acid deletion at the carboxy terminus (R901X). Functional analysis of R589 mutations, however, has revealed only a modest reduction in AE1-mediated $^{36}Cl^-$ transport when expressed in *Xenopus* oocytes, whereas the S613F mutation is associated with the upregulation of anion transport. The mechanism by which mutant AE1 causes AD dRTA may involve impaired trafficking of the protein to cell surface and a dominant negative effect attributable to the formation of heterodimers between mutant and normal proteins (Quilty et al. *2002a*, *2002b*).

A novel *AE1* missense mutation linked to autosomal recessive (AR) dRTA and xerocytic hemolytic anemia in which red cell anion transport is normal has been reported in a Thai family (Tanphaichitr et al. *1998*). The two affected individuals, siblings of the same family, are homozygous for the functionally defective mutation, G701D (band 3 Bangkok I). The *AE1* G701D mutation results in inactive anion transport caused by impaired protein trafficking as shown by expression studies in *Xenopus* oocytes. Co-expression of *AE1* G701D with the erythroid AE1 chaperonin, glycophorin A (GPA), rescues both AE1-mediated Cl^- transport and AE1 surface expression in oocytes.

Co-existence of SAO and dRTA is not normally found in the same individual. However, the two conditions can co-exist as the result of compound heterozygosity between SAO and other *AE1* mutations. Our group has recently described a novel compound heterozygosity of *AE1* mutations causing AR dRTA in patients with SAO (Vasuvattakul et al. *1999*). Two clinically affected individuals from two unrelated families from southern Thailand had one *AE1* allele with an SAO mutation and the other allele with the missense G701D mutation (SAO/G701D). The patients with this compound heterozygosity presented with ovalocytic red cells and metabolic acidosis with failure to thrive and hypokalemia. However, they had no sign of hemolytic anemia. SAO/G701D and other genotypes including SAO/ΔV850, SAO/A858D, ΔV850/ΔV850, and ΔV850/A858D have also been observed in Malaysian and Papua New Guinean patients with dRTA (Bruce et al. *2000*).

We have recently identified an additional seven patients with AR dRTA from five families exhibiting the homozygous *AE1* G701D mutation in Thailand (Yenchitsomanus et al. *2002*). None of the patients had xerocytic hemolytic anemia, which was found in two patients with the homozygous AE1 G701D mutation previously documented (Tanphaichitr et al. *1998*). This different finding may be attributable to the patients that we studied also not being homozygous for hemoglobin E, as were both patients in the previous work (Tanphaichitr et al. *1998*). A new patient with AR dRTA resulting from the same genotype as that of another family has recently been identified (unpublished). It is of great interest that all Thai patients with AR dRTA attributable to homozygous *AE1* G701D mutation originate from northeastern Thailand, and those that result from compound heterozygous SAO/G701D mutations inhabit southern Thailand (Vasuvattakul et al. *1999*) and Malaysia (Bruce et al. *2000*), a southern neighboring country of Thailand. This has led to the suggestion that the *AE1* G701D mutation might be of ancient origin (Yenchitsomanus et al. *2002*), and that it might have evolved in this region of southeast Asia, especially in Thailand. To investigate the prevalence of the SAO and G701D mutations, their migration, and their interaction, we have therefore analyzed these two mutations in the Thai population.

Materials and methods

The subjects were healthy individuals who were school and university students and blood-donor volunteers anonymously recruited with informed consent. The persons who were not

native of relevant regions were excluded. Altogether, 844 subjects from four geographic areas of Thailand (Fig. 1), including 216 individuals from Chiang Mai (north), 205 from Khon Kaen (northeast), 217 from Bangkok (central), and 206 from Songkla (south) were studied. Blood samples (5–10 ml) were collected from these subjects. DNAs were prepared from leukocytes by the standard method of proteinase K digestion, phenol/chloroform extraction, and ethanol precipitation and used for analyses of *AE1* mutations.

Fig. 1. Map of Thailand showing the four geographic regions, viz., Chiang Mai (*North*), Khon Kaen (*Northeast*), Bangkok (*Central*), and Songkla (*South*), from which blood samples were collected for *AE1* analysis

Previously, we had identified and reported several cases with compound heterozygous (SAO/G701D) and homozygous (G701D/G701D) mutations of *AE1* (Vasuvattakul et al. *1999*; Yenchitsomanus et al. *2002*). The *AE1* mutations in the patients were initially screened by the polymerase chain reaction/single-stranded conformation polymorphism (PCR-SSCP) technique and characterized by nucleotide sequencing. We had also developed simple methods for detection of the SAO (Vasuvattakul et al. *1999*) and G701D (Yenchitsomanus et al. *2002*) mutations. These methods were therefore employed in the present study. In addition, the DNA samples with known SAO and G701D mutations were used as controls for the *AE1* analysis. The SAO (or Ex11Δ27) mutation was analyzed by amplification in exon 11 region of *AE1* by PCR. The sequences of forward and reverse primers used were: 5'-CCTCACCTCCTCCAGCTACTCC-3' and 5'-CAGAAGTTGGGGCTGAGACAGAG-3', respectively. PCR was performed as previously described (Vasuvattakul et al. *1999*). The PCR products were detected by agarose-gel electrophoresis, stained with ethidium bromide, examined on a UV transilluminator, and recorded by photography. The amplified DNA fragment of normal exon 11 was 318 bp in length, whereas that of SAO was 291 bp. The sample with the heterozygous SAO mutation showed fragments from the normal exon 11 (318 bp) and the deleted exon 11 (291 bp).

The G701D mutation was analyzed by amplification in exon 17 region of *AE1* by PCR and

digestion with restriction enzyme *Hpa*II before detection by agarose-gel electrophoresis as described above. The sequences of forward and reverse primers used were: 5'-TGGGCTCAACTATATGAACC-3' and 5'-TTGATACCTTTTTGAAGGGG-3', respectively. The amplified product was 321 bp in length. In the absence of the G701D mutation, the amplified product could be digested with *Hpa*II, producing two fragments of 254 bp and 67 bp in length. In the presence of the G701D mutation, the enzyme could not cleave the amplified product, because the restriction site was abolished, and the product remained 321 bp long. The sample with heterozygous the G701D mutation showed three fragments of 321 bp, 254 bp, and 67 bp.

Since other genotypes with compound heterozygosities, including SAO/R602H (Prapon Wilairat *2000*), SAO/ΔV850, SAO/A858D, ΔV850/ΔV850, and ΔV850/A858D (Bruce et al. *2000*), were identified, by dRTA, in the patients from southern Thailand, Malaysia and Papua New Guinea, the R602H, ΔV850, and A858D mutations were also examined in the southern Thai population in the present study. The methods used were allele-specific amplification (ASA) for R602H, SSCP for ΔV850, and PCR followed by *Bgl*I digestion for A858D.

The allele frequency of each mutation was calculated from the number of individuals carrying the mutation in the subject group from four geographic regions. The occurrences of homozygosity of SAO and G701D were also estimated from their allele frequencies.

Results

The results of *AE1* analyses for the SAO mutation by PCR and electrophoresis and for the G701D mutation by PCR followed by *Hpa*II digestion and electrophoresis are shown in Fig. 2. The analysis of the SAO and G701D mutations in DNA samples from 844 subjects demonstrated that the two mutations were present in the heterozygous condition in seven and five individuals, respectively (Table 1). All seven SAO heterozygotes were found in the southern Thai population; none was observed in the studied populations from other regions of Thailand. Of five G701D heterozygotes, one was found in the northern, three in the northeastern, and one in the central populations. The G701D mutation was not detected in the southern population. The allele frequency of SAO in the southern population was 0.0170, whereas the allele frequencies of G701D in the northern, northeastern, and central populations were 0.0023, 0.0073, and 0.0023, respectively. Although the SAO mutation was found to be common in the southern Thai population, the G701D mutation had a higher allele frequency in the northeastern Thai population than in the populations of other regions.

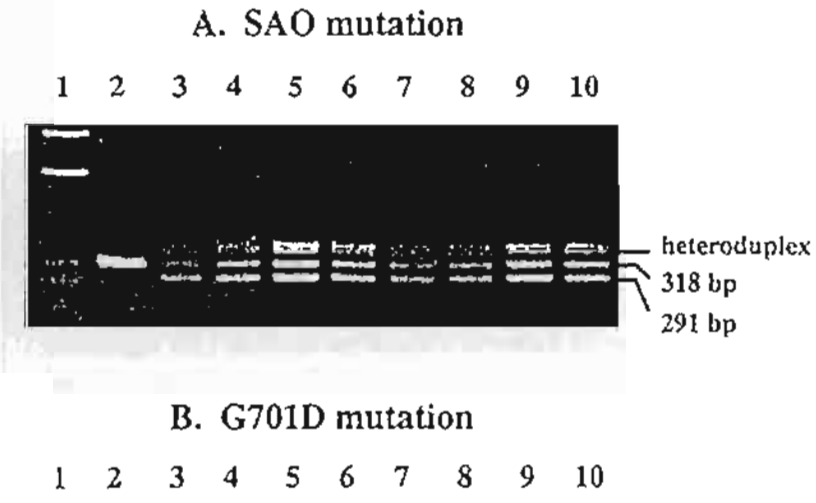

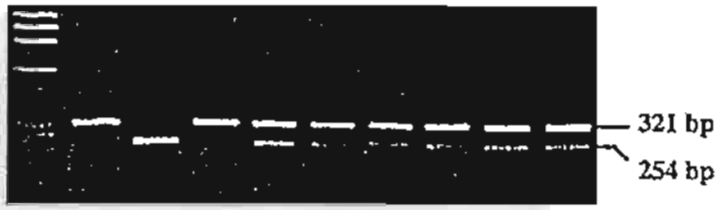

Fig. 2A, B. Analyses of *AE1* SAO and G701D mutations. **A** The SAO mutation was analyzed by amplification in the exon 11 region of *AE1* by PCR and agarose-gel electrophoresis. *Lane 1* Standard DNA markers, PhiX174/*Hae*III, *lane 2* a normal control sample, showing a fragment of 318 bp, *lane 3* sample from an individual with a known heterozygous SAO mutation, showing two fragments of 318 bp and 291 bp and two bands of heteroduplex DNA, *lanes 4–10* samples from seven subjects with heterozygous SAO mutations, showing the same pattern as that in *lane 3*. **B** The G701D mutation was analyzed by amplification in the exon 17 region of *AE1* with PCR, followed by restriction enzyme-*Hpa*II digestion and agarose-gel electrophoresis. *Lane 1* Standard DNA markers, PhiX174/*Hae*III, *lane 2* undigested normal control sample, showing a fragment of 321 bp, *lane 3 Hpa*II-digested normal control sample, showing a fragment of 254 bp but no fragment of 67 bp, *lane 4 Hpa*II-digested sample from an individual with a known homozygous G701D mutation, showing only an undigested fragment of 321 bp, *lane 5 Hpa*II-digested control sample from an individual with a known heterozygous G701D mutation, showing both undigested and digested fragments of 321 bp and 254 bp, respectively, *lanes 6–10 Hpa*II-digested samples from five subjects with heterozygous G701D mutation studied, showing the same pattern as that in *lane 5*

Table 1. *AE1* SAO and G701D mutations in populations from four geographic regions of Thailand

Region	Number of subjects	*AE1* mutation			
		SAO		G701D	
		Number of heterozygotes	Allele frequency	Number of heterozygotes	Allele frequency
North	216	0	0	1	0.0023
Northeast	205	0	0	3	0.0073
Central	217	0	0	1	0.0023
South	206	7	0.0170	0	0
Total	844	7	0.0041	5	0.0030

From their allele frequencies, the occurrence of SAO homozygote was estimated to be 1 per 3,300 individuals in the southern Thai population and that of G701D homozygotes in northern, northeastern, and central Thai populations to be 1 per 200,000, 1 per 20,000, and 1 per 200,000, respectively.

The analyses of *AE1* R602H, ΔV850, and A858D mutations in 206 subjects of the southern Thai population showed the absence of these three mutations in the subjects examined.

Discussion

Although *AE1* defects are known to result in erythrocyte disorders, a great deal of attention has recently been paid to the analyses of *AE1* mutations in the patients with dRTA, since mutations of this gene have also been found to be involved in the pathogenesis of dRTA. The *AE1* abnormality thus shows a pleiotrophic effect, causing seemingly unrelated defects in two different cell types. However, the two disorders may co-exist in some individuals. Baehner

and colleagues (*1968*) first recognized the association between erythrocyte abnormality and dRTA in affected children in a Filipino family, but Wrong and co-workers (*1996*) were the first to suspect a common molecular basis for SAO and dRTA. The finding that compound heterozygosity between the SAO and G701D mutations caused the combined defects of SAO and dRTA was originally reported by our group (Vasuvattakul et al. *1999*). This was confirmed and extended to other types of compound heterozygosity (Bruce et al. *2000*). Recent studies in Thailand (Tanphaichitr et al. *1998*; Vasuvattakul et al. *1999*; Yenchitsomanus et al. *2002*) and in other countries of southeast Asia and Melanesia (Bruce et al. *2000*; Wrong et al. *2002*) clearly indicate that a group of particular *AE1* mutations could cause AR dRTA, these mutations being different from the *AE1* mutations found to be associated with AD dRTA (Bruce et al. *1997*; Jarolim et al. *1998*; Karet et al. *1998*). The molecular mechanism by which different *AE1* mutations give rise to either AR or AD dRTA remains to be elucidated.

Since several cases of AR dRTA caused by compound heterozygous (SAO/G701D) and homozygous (G701D/G70D) mutations of *AE1* have been found in Thailand (Tanphaichitr et al. *1998*; Vasuvattakul et al. *1997*; Yenchitsomanus et al. *2002*), it is of great interest to study the prevalence of the mutant (SAO and G701D) alleles in the Thai population. The results of mutation analyses in the present study show that these two mutations are present in considerable frequencies in the populations from different geographic regions. SAO is common in the southern Thai population but it has not been observed in the populations from three other regions. A previous study has shown that SAO is not present in many ethnic groups in Thailand (Kimura et al. *1998*); it has also not been found in a small number of subjects (43 individuals) in an ethnic group from southern Thailand. In another study on SAO in the southern Thai population, 44 of 1,556 individuals were reported to be SAO heterozygotes (allele frequency: 0.0141; Nopparatana et al. *1996*). The allele frequency of SAO in our study (0.0170) is slightly different from that found in the previous work. This may be attributable to variation in sampling. The high frequencies of SAO in southeast Asian and Melanesian populations may be related to its selective survival advantage against malaria infection; individuals with SAO are less susceptible to cerebral malaria (Allen et al. *1999*). SAO homozygosity in southern Thai population would be expected, from its allele frequency, to be about 1 per 3,300 individuals. However, SAO homozygotes have never been observed, suggesting that it is a lethal condition (Liu et al. *1994*; Mgone et al. *1996*). The abnormality in the SAO homozygote may involve severe abnormalities of both erythrocyte and kidney. The high prevalence of the SAO allele in some regions of southeast Asia and Melanesia where malaria is endemic, despite its homozygous condition probably being lethal, indicates that a balanced polymorphism might occur in such regions.

In contrast, the G701D mutation has been detected in northern, northeastern, and central Thai populations but is not found in southern Thai subjects. It is not known whether this allele confers an advantage against malaria infection. The allele frequency of the G701D mutation in the northeastern population (0.0073) was higher than that in the northern and central populations (0.0023). The estimated occurrence rates of G701D homozygosity in the northeastern, northern, and central Thai populations are 1 per 20,000, 1 per 200,000, and 1 per 200,000, respectively. In total, there should be several hundred cases of dRTA attributable to the homozygous G701D mutation. However, the actual incidence rates of this condition seem to be very low. Only a few cases have been observed. One explanation is possibly that this disease is not noticed and that many children with this disease die at an early age.

The higher allele frequency of the G701D mutation in the northeastern population was in agreement with our observation that all Thai patients with AR dRTA resulting from the homozygous G701D mutation were northeastern. Thus, the G701D mutation might anciently originate in this population and might later have spread to other regions. If this is the case, the

presence of compound heterozygous SAO/G701D in the southern Thai (Vasuvattakul et al. *1999*) and Malaysian (Bruce et al. *2000*) patients with AR dRTA and its apparent absence in northeastern Thai patients indicate that the G701D allele might have migrated to the southern peninsular region. The SAO allele, on the other hand, has not spread from southern Thailand to central, north, and northeast Thailand because the southern Thai people might not have migrated to other parts of the country. The southern region is a highly fertile land and rich in natural resources, when compared with other parts of Thailand, especially the northeastern region. This has been an important factor in maintaining the population in the region. The situation might change as people migrate for social, economic, and educational reasons. Thus, the SAO allele constitutes a genetic background of the southern Thai population, providing an increased chance for the occurrence of dRTA. The introduction of a new allele, such as G701D, from the migration of the population from the northeastern and other regions to the southern area will result in their pathogenic allelic interaction.

Acknowledgements This work was supported by a grant from the National Center for Biotechnology and Genetic Engineering (BIOTEC grant no. BT-B-07-MG-B4-4501) and the National Science and Technology Development Agency (NSTDA), Bangkok, Thailand. We are grateful to Dr. Prida Malasit, the Director of Division of Medical Molecular Biology, the Director of Medical Biotechnology Unit, and the recipient of Senior Research Scholar Award of Thailand Research Fund (TRF), for kind and continuous support.

References

Allen SJ, O'Donnell A, Alexander ND, Mgone CS, Peto TE, Clegg JB, Alpers MP, Wheatherall DJ (1999) Prevention of cerebral malaria in children in Papua New Guinea by southeast Asian ovalocytosis band 3. Am J Trop Med Hyg 60:1056–1060
ChemPort PubMed

Alper SL (2002) Genetic diseases of acid-base transporters. Annu Rev Physiol 64:899–923
crossref ChemPort PubMed

Baehner RL, Cilchrist GS, Anderson EJ (1968) Hereditary elliptocytosis and primary renal tubular acidosis in a single family. Am J Dis Child 115:414-419
ChemPort PubMed

Batlle D, Ghanekar H, Jain S, Mitra A (2001) Hereditary distal renal tubular acidosis: new understandings. Annu Rev Med 52:471–484
crossref ChemPort PubMed

Bruce LJ, Tanner MJ (1996) Structure-function relationships of band 3 variants. Cell Mol Biol 42:975–984

Bruce LJ, Cope DL, Jones GK, Schofield AE, Burley M, Povey S, Unwin RJ, Wrong O, Tanner MJA (1997) Familial distal renal tubular acidosis is associated with mutations in the red cell anion exchanger (band 3, *AE1*) gene. J Clin Invest 100:1693–1701
ChemPort PubMed

Bruce LJ, Wrong O, Toye AM, Young MT, Ogle G, Ismail Z, Sinha AK, McMaster P, Hwaihwanje I, Nash GB, Hart S, Lavu E, Palmer R, Othman A, Unwin RJ, Tanner MJ (2000) Band 3 mutations, renal tubular acidosis and south-east Asian ovalocytosis in Malaysia and Papua New Guinea: loss of up to 95% band 3 transport in red cells. Biochem J 350:41–51
crossref ChemPort PubMed

Jarolim P, Palek J, Amato D, Hassan K, Sapak P, Nurse GT, Rubin HL, Zhai S, Sahr KE, Liu S-C (1991) Deletion in erythrocyte band 3 gene in malaria-resistant southeast Asian ovalocytosis. Proc Natl Acad Sci USA 88:11022–11026
ChemPort PubMed

Jarolim P, Shayakul C, Prabakaran D, Jiang L, Stuart-Tilley A, Rubin HL, Simova S, Zavadil J, Herrin JT, Brouillette J, Somers MJG, Seemanova E, Brugnara C, Guay-Woodford LM, Alper SL (1998) Autosomal dominant distal renal tubular acidosis is associated in three families with heterozygosity for the R589H mutation in the AE1 (band 3) Cl^-/HCO_3^- exchanger. J Biol Chem 273:6380–6388
crossref ChemPort PubMed

Karet FE, Gainza FJ, Gyory AZ, Unwin Rj, Wrong O, Tanner MJ, Nayir A, Alpay H, Santos F, Hulton SA, Bakkaloglu A, Ozen S, Cunningham MJ, Di Pietro A, Walker WG, Lifton RP (1998) Mutations in the chloride-bicarbonate exchanger gene AE1 cause autosomal dominant but not autosomal recessive distal renal acidosis. Proc Natl Acad Sci USA 95:6337–6342
crossref ChemPort PubMed

Kimura M, Shimizu Y, Ishida WS, Soemantri A, Tiwawech D, Romphruk A, Duangchan P, Ishida T (1998) Twenty-seven base pair deletion in erythrocyte band 3 protein gene responsible for southeast Asian ovalocytosis is not common among southeast Asians. Hum Biol 70:993–1000
ChemPort PubMed

Kollert-Jons A, Wagner S, Hubner S, Appelhans H, Drenckhahn D (1993) Anion exchanger 1 in human kidney and oncocytoma differs from erythroid AE1 in its NH_2 terminus. Am J Physiol 265:F813–F821
ChemPort PubMed

Liu S-C, Jarolim P, Rubin HL, Palek J, Amato D, Hassan K, Zaik M, Sapak P (1994) The homozygous state for the band 3 protein mutation in southeast Asian ovalocytosis may be lethal. Blood 84:3590–3591
ChemPort PubMed

Lux SE, John KM, Kopito RR, Lodish HF (1989) Cloning and characterization of band 3, the human erythrocyte anion-exchange protein (AE1). Proc Natl Acad Sci USA 86:9089–9093
ChemPort PubMed

Mgone CS, Koki G, Paniu MM, Kono J, Bhatia KK, Genton B, Alexander NDE, Alpers MP (1996) Occurrence of the erythrocyte band 3 (AE1) gene deletion in relation to malaria endemicity in Papua New Guinea. Trans R Soc Trop Med Hyg 90:228–231
ChemPort PubMed

Nopparatana C, Nopparatana C, Kanjanaopas S, Saechan V, Matsuo M (1996) Southeast Asian ovalocytosis (SAO) in the south of Thailand (abstract). PSU-ICMR Symposium, 25–26 July 1996, Songkhla, Thailand

Prapon Wilairat X (2000) Compound heterozygosity of SAO/R602H. FAOPS Newsletter 9:3–8

Quilty JA, Li J, Reithmeier RA (2002a) Impaired trafficking of distal renal tubular acidosis mutants of the human kidney anion exchanger kAE1. Am J Physiol Renal Physiol 282:F810–F820
ChemPort PubMed

Quilty JA, Cordat E, Reithmeier RA (2002b) Impaired trafficking of human kidney anion exchanger (kAE1) caused by hetero-oligomer formation with a truncated mutant associated with distal renal tubular acidosis. Biochem J 368:895–903
crossref ChemPort PubMed

Rodriguez-Soriano J (2000) New insights into the pathogenesis of renal tubular acidosis—from functional to molecular studies. Pediatr Nephrol 14:1121–1136
[SpringerLink] ChemPort PubMed

Sahr KE, Taylor WM, Daniels BP, Rubin HL, Jarolim P (1994) The structure and organization of the human erythroid anion exchanger (AE1) gene. Genomics 24:491–501
crossref ChemPort PubMed

Tanner MJ (1993) Molecular and cellular biology of the erythrocyte anion exchanger (AE1). Semin Hematol 30:34–57
ChemPort

Tanner MJ (1997) The structure and function of band 3 (AE1): recent developments. Mol Membr Biol 14:155-165
ChemPort PubMed

Tanphaichitr VS, Sumboonnaonda A, Ideguchi JH, Shayakul C, Brugnara C, Takao M, Veerakul G, Alper SL (1998) Novel AE1 mutations in recessive distal renal tubular acidosis: loss-of-function is rescued by glycophorin A. J Clin Invest 102:2173–2179
ChemPort PubMed

Tse WT, Lux SE (1999) Red blood cell membrane disorders. Br J Haematol 104:2–13
ChemPort PubMed

Vasuvattakul S, Yenchitsomanus P, Vachuanichsanong P, Thuwajit P, Kaitwatcharachai C, Laosombat V, Malasit P, Wilairat P, Nimmannit S (1999) Autosomal recessive distal renal tubular acidosis associated with southeast Asian ovalocytosis. Kidney Int 56:1674–1682
crossref ChemPort PubMed

Wrong O, Unwin RJ, Cohen E, Tanner M, Thakker R (1996) Unravelling of the molecular mechanism of kidney stones. Lancet 348:1561–1565
crossref PubMed

Wrong O, Bruce L, Unwin RJ, Toye AM, Tanner MJA (2002) Band 3 mutations, distal renal tubular acidosis, and southeast Asian ovalocytosis. Kidney Int 62:10-19
crossref ChemPort PubMed

Yenchitsomanus P, Vasuvattakul S, Kirdpon S, Wasanawatana S, Susaengrat W, Sreethiphayawan S, Chuawatana D, Mingkum S, Sawasdee N, Thuwajit P, Wilairat P, Malasit P, Nimmannit S (2002) Autosomal recessive distal renal tubular acidosis caused by G701D mutation of anion exchanger 1 gene. Am J Kidney Dis 40:21-29
crossref ChemPort PubMed